Kognisyonun Ritimleri

RHYTHMS OF COGNITION

Using transcranial alternating current stimulation to modulate neural oscillations with measurable impact on memory performance

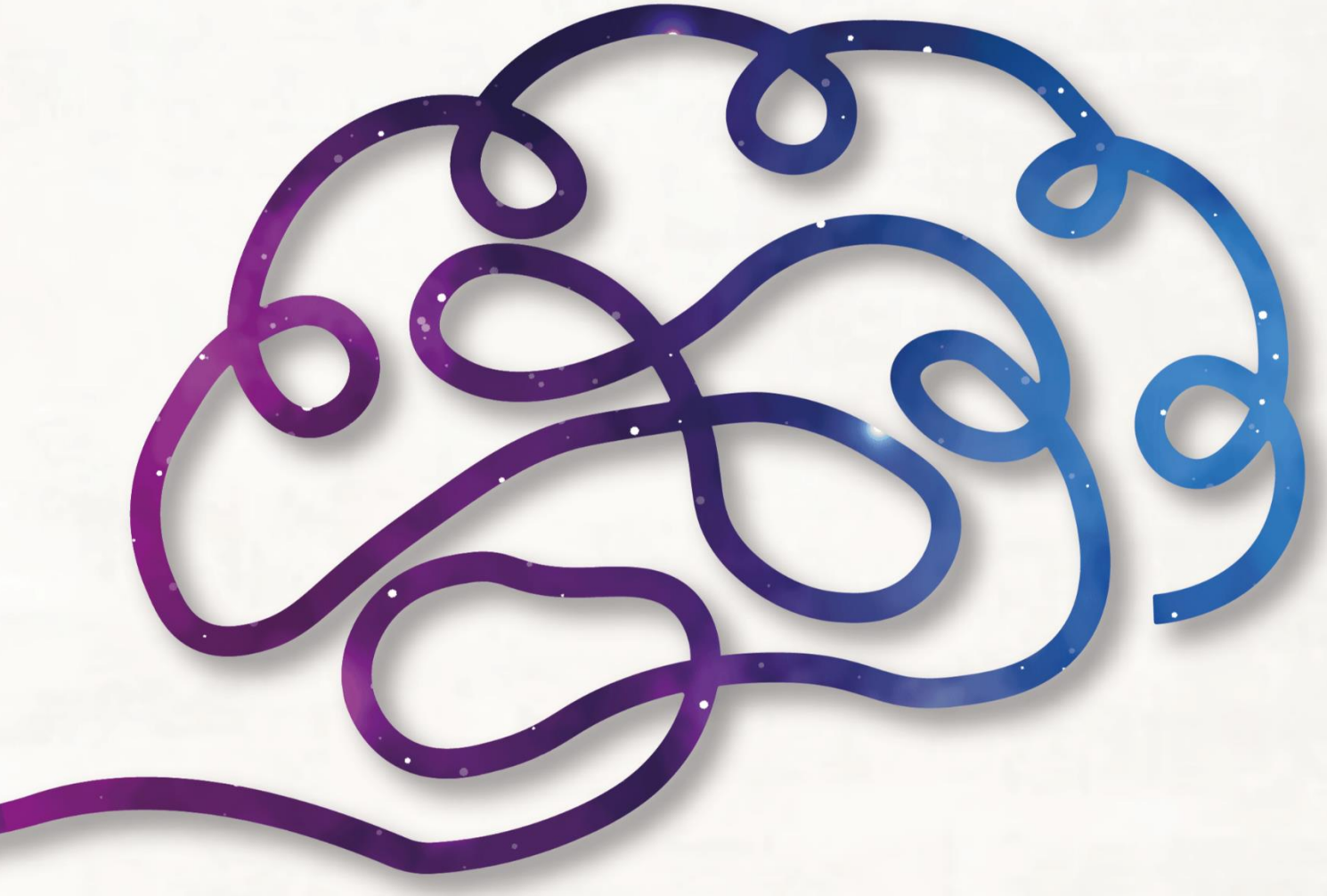

- Empirical Chapters -

TUBA AKTÜRK

Empirical Chapters of the thesis

Rhythms of cognition

Using transcranial alternating current stimulation to modulate neural oscillations with measurable impact on memory performances

Tuba Aktürk

2022

Kognisyonun ritimleri

Bellek performansları üzerinde ölçülebilir etki ile nöral osilasyonları modüle etmek için transkraniyal alternatif akim uyarımının kullanılması

Rhythms of cognition

Using transcranial alternating current stimulation to modulate neural oscillations with measurable impact on memory performances

DISSERTATION

to obtain the degree of Doctor at the Maastricht University and Istanbul Medipol University,

on the authority of the Rector Magnifici,

Prof.dr. Pamela Habibović and Rector Prof. dr. Ömer Ceran

in accordance with the decision of the Board of Deans,

to be defended in public

on Tuesday 13th of December 2022, at 13:00 hours

by

Tuba Aktürk

Supervisors (Danışmanlar):

Prof. Dr. Alexander T. Sack

Prof. Dr. Bahar Güntekin, Istanbul Medipol University, Turkey

Assessment Committee (Değerlendirme Komitesi):

Prof. Dr. Yasin Temel (chair)

Prof. Dr. Fuat Balcı, University of Manitoba, Canada & Koc University, Turkey

Prof. Dr. Onur Güntürkün, Ruhr-Universität Bochum, Germany

Dr. Yusuf Çakmak

Oscillatory delta and theta frequencies differentially support multiple items encoding to optimize memory performance during the digit span task

Tuba Aktürk, Tom A. de Graaf, Furkan Erdal, Alexander T. Sack, Bahar Güntekin

Corresponding manuscript: Aktürk, T., de Graaf, T. A., Erdal, F., Sack, A. T., & Güntekin, B. (2022). Oscillatory delta and theta frequencies differentially support multiple items encoding to optimize memory performance during the digit span task. NeuroImage, 119650. https://doi.org/10.1016/j.neuroimage.2022.119650

Abstract

The human brain has limited storage capacity often challenging the encoding and recall of a long series of multiple items. Different encoding strategies are therefore employed to optimize performance in memory processes such as chunking where particular items are 'grouped' to reduce the number of items to store artificially. Additionally, related to the position of an item within a series, there is a tendency to remember the first and last items on the list better than the middle ones, which calls the "serial position effect". Although relatively well-established in behavioral research, the neuronal mechanisms underlying such encoding strategies and memory effects remain poorly understood.

Here, we used event-related EEG oscillation analyses to unravel the neuronal substrates of serial encoding strategies and effects during the behaviorally controlled execution of the digit span task. We recorded EEG in forty-four healthy young-adult participants during a backward digit span (ds) task with two difficulty levels (i.e., 3-ds and 5-ds). Participants were asked to recall the digits in reverse order after the presentation of each set. We analyzed the pattern of event-related delta and theta oscillatory power in the time-frequency domain over fronto-central and parieto-occipital areas during the item (digit) list encoding, focusing on how these oscillatory responses changed with each subsequent digit being encoded in the series.

Results showed that the development of event-related delta power evoked by digits in each series matched the 'serial position curve', with higher delta power being present during the first, and especially last, digits as compared to digits presented in the middle of a set, for both difficulty levels. Event-related theta power, in contrast, rather resembled a neural correlate of a chunking pattern where, during the 5-ds encoding, a clear change in event-related theta occurred around the third/fourth positions, with decreasing power values for later digits. This suggests that different oscillatory mechanisms linked to different frequency bands may code for the different encoding strategies and effects in serial item presentation. Furthermore, recall-EEG correlations suggested that participants with higher fronto-central delta responses during digit encoding showed also higher recall scores.

The here presented findings contribute to our understanding of the neural oscillatory mechanisms underlying multiple item encoding, directly informing recent efforts towards memory enhancement through targeted oscillation-based neuromodulation.

Key Words: brain oscillation, working memory, serial position effect, chunking, encoding, number perception

Graphical Abstract

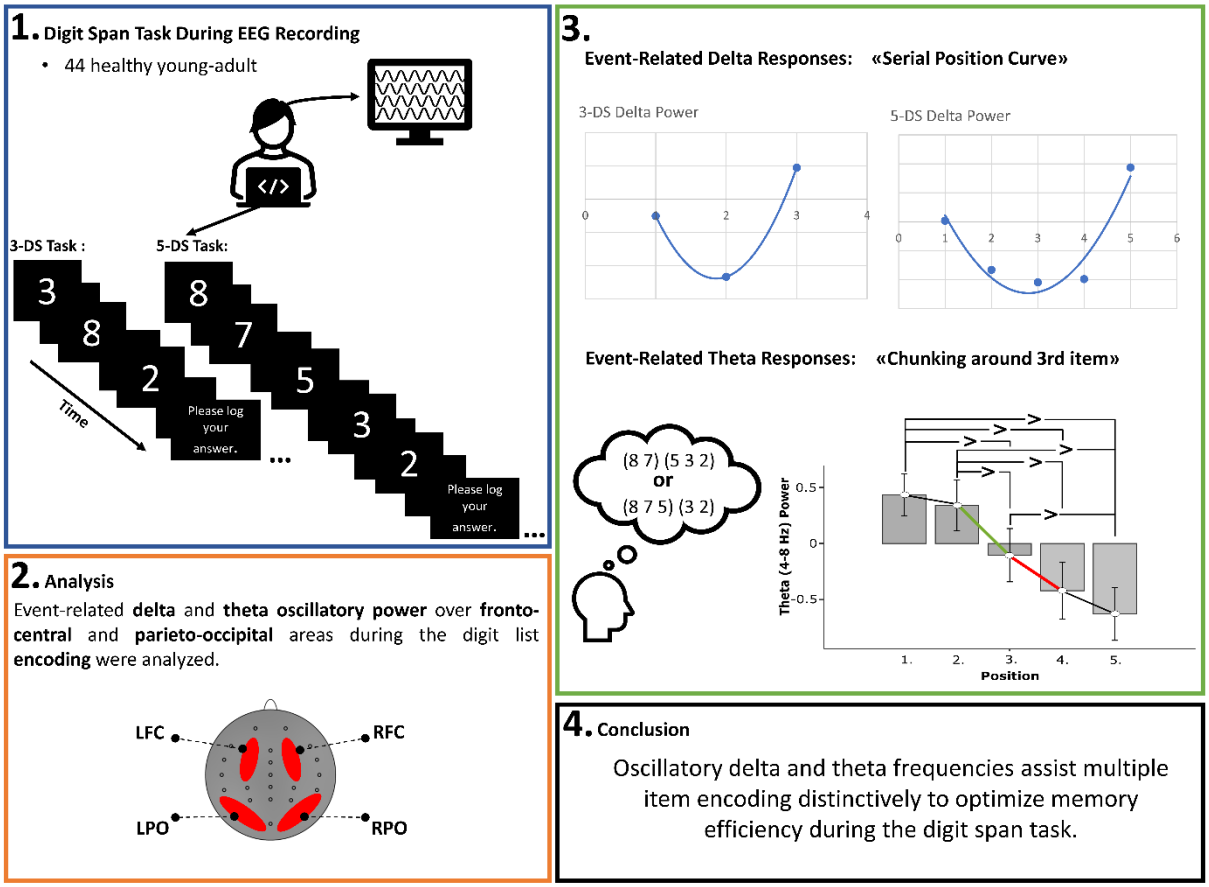

Highlights

- Slow oscillatory responses differentially contribute to the digit span task performance.
- Delta responses matched nicely the suggested “serial position curve” model.
- Theta responses reflect the probably chunked items.
- Anterior delta responses during encoding positively correlated with the recall scores.
- Digit encoding elicited higher right parietal EEG responses.

1. Introduction

Despite the human brain's remarkable complexity and computational resources, it has a restricted capacity when it comes to working memory (Constantinidis & Klingberg, 2016; Cowan, 2001; Marois & Ivanoff, 2005). The human brain has limited storage capacity directly related to how information is encoded and represented in the brain. The mere position of an element within a series and/or the overall number of items to be stored affect these capacity limits and the chance of successful recall (Constantinidis & Klingberg, 2016; Murre & Dros, 2015). Furthermore, the number of items to be held and their position within a sequence of items determine how to best encode such lists to optimize memory storage (Saito et al., 2008; Thalmann et al., 2019). A well-established example of how the position of an item in a list can affect the memory processes is the "serial position effect" (SPE) (Feigenbaum & Simon, 1962; Murdock, 1962; Murre & Dros, 2015). The SPE describes the propensity to remember the first and last items on a list more efficiently than the middle ones. In addition to such memory effects of serial position, there is also an encoding strategy to optimize memory performance. This encoding strategy is known as “chunking” (Ericsson et al., 1980; Shiffrin & Nosofsky, 1994), a strategy where distinct items are ‘grouped’ to artificially reduce the number of items in a list in order to retain more of them. Chunking may be a common approach for encoding episodic information, and it is an effective way to reduce the buildup of error inherent in long sequences by reducing the amount of information to be recalled (Buzsáki & Moser, 2013; Cowan, 2001, 2005, 2010; Wickelgren, 1999).

Despite well-established behavioral demonstrations of such memory effects and encoding strategies from a research tradition that began more than a century ago (i.e., Ebbinghaus, 1885; Jevons, 1871), their underlying neural mechanisms remain less fully understood. There are a limited number of event-related electroencephalography (EEG) studies focusing on the above-mentioned encoding processes. In EEG literature, several studies studied “chunking" in the scope of language processing (Bonhage et al., 2017; Gilbert et al., 2014, 2015). According to these studies, delta-theta oscillatory responses (Bonhage et al., 2017), as well as N400 and P300 components (Gilbert et al., 2014), may reflect chunking-related encoding during language processing. Additionally, Nogueira et al (2015) showed increased late positive slow waves during the encoding of the words when the items were chunked (Nogueira et al., 2015) compared to a control condition. On the other hand, the serial position

effect was reflected mostly by the late positive event-related potentials (ERP), with the effect depending on stimulus modality (Azizian & Polich, 2007; Patterson et al., 1991). To our knowledge, there are only a few studies investigating neural oscillations underlying the SPE directly (Jensen & Lisman, 1998; Sederberg et al., 2006). While Jensen & Lisman (1998) focused on the role of theta oscillations in the serial position effect, Sederberg et al. (2006) showed that the posterior gamma (at early serial positions) and widespread slow oscillatory responses (for later serial positions) may reflect the serial position effect. These relatively few event-related EEG studies nonetheless clearly demonstrate that the EEG is a tool and method that has been used successfully before to investigate the processes of chunking and SPE in memory research.

Although these limited numbers of pioneering studies in which the effect of item position and item number on encoding processes were studied with the event-related EEG method, results were not consistent, and we found little recent work explicitly addressing these mechanisms. Given the relevance of serial encoding for our everyday cognition (remembering a shopping list), this seems surprising. Intriguingly, noninvasive neuromodulation techniques have recently been used successfully to specifically target cognitively relevant brain oscillations to enhance memory performance (Grover et al., 2022; Aktürk et al., 2022). Therefore, an in-depth understanding of brain oscillations underlying encoding processes related to serial position effect and chunking might directly inform such developments towards cognitive neuroenhancement in healthy populations as well as benefit intervention in pathologies in which encoding is disrupted.

To this end, we here decided to focus on slow oscillatory EEG responses (i.e., delta and theta), since they are widely associated with cognitive processes such as attention and memory. Delta responses have mostly been associated with immediate memory mechanisms, decision-making, and attention allocation processes (Başar-Eroglu et al., 1992; Ergen et al., 2008; Harper et al., 2017; Polich & Kok, 1995; Sutton et al., 1965). For example, studies using the oddball paradigm report an amplitude increase at delta frequency when the participants perceive a target stimulus, necessitating the perception and attention processes (Başar-Eroglu et al., 1992; Demiralp et al., 1999; Ergen et al., 2008). Considering this link between delta responses and immediate memory and attention mechanisms, which are basic information-processing mechanisms in working memory, we might expect that the delta response will be affected by the serial positions of items in a list and therefore related to the serial position effect (Feigenbaum & Simon, 1962). Theta responses, on the other hand, are mostly associated with working memory capacity and thereby with the number of items that should be remembered,

as also shown by research on theta-gamma coupling (Goodman et al., 2018; Herweg et al., 2020; J. E. Lisman & Jensen, 2013; J. Lisman & Idiart, 1995). Theta oscillations take part in managing successive inputs by holding items within a single theta cycle (Buzsáki, 2005; Herweg et al., 2020). Therefore, one might hypothesize that "chunking" could be reflected by theta activity rather than delta.

Here, we analyzed the pattern of event-related delta and theta power in the time-frequency domain over bilateral fronto-central and parieto-occipital areas during the digit span backward working memory task. In this task, digits were presented to the participants sequentially in two different list lengths: 3 digit span (3-ds) and 5 digit span (5-ds), respectively. After each set of digits, the participants were asked to recall the digit sets in reverse order. In order to disentangle possible encoding mechanisms and memory effects reflected by delta-theta slow brain oscillations, the encoding phase of the task, during the item (digit) representation, was analyzed.

2. Materials and Methods

This study is part of a larger study investigating EEG-informed theta tACS after effects. Here, we used the pre-tACS EEG data of the participants that were recorded during the working memory task. These participants did not have tACS during or before they performed this task, and they were not prepared for tACS yet; therefore, the current EEG results and preparation are indistinguishable from an isolated EEG experiment. However, we think it is important to mention that prior to the digit span task, as a part of the larger tACS study design, a neuropsychological battery and visual and auditory memory tasks were administered to participants for approximately one hour (for details please see; Aktürk et al., 2022).

2.1 Participants

A total of 44 (33 females) right-handed, educated (mean years of education (SD): 16.3 (±2.7)), healthy young-adult (mean age (SD): 24.4 (±4.8)) subjects were included in the study. All participants had normal or corrected-to-normal vision and no specified hearing impairment. Participants with symptoms or history of psychiatric or neurological disorders and psychiatric or neurological medication usage were not included in the study.

Participants provided written informed consent, and there was no compensation for participation as indicated in the written informed consent. The study was approved by the Istanbul Medipol University Ethics Committee (No: 10840098-604.01.01-E.18575).

2.2 Experimental Design and Task Procedure

The digit span backward task was prepared and presented via E-prime software (Psychology Software Tools Inc., Pittsburgh, PA). This task mainly measures the working memory abilities of the subjects. Here, we presented the task in the two different difficulty levels, namely, the 3-digit span (3-ds) set and the 5-digit span set (5-ds) during the EEG recording. These levels were always presented in the same order (first: 3-digit span sets and then 5-digit span sets). A total of 30 different digit sets were presented during the task in each difficulty level. Digit sets were presented in the pseudorandom order across participants. During the encoding phase of the task, the digits appeared on the screen sequentially for each digit span set, namely 5 digits were presented for a 5-ds set and 3 digits were presented for a 3-ds set. Stimulation time per digit was 900 ms, and interstimulus interval was 600 ms between the digits in a set. The encoding phase was followed by the recall phase. Before the task, participants were instructed to pay attention to approaching stimuli (learning/encoding phase) and recall a set of digits in reverse order to log answers via a keyboard on the answer screen following each digit set (recall phase). The answer screen was presented 600 ms after the offset of the last digit in the set and disappeared after the participant entered and confirmed their answer by pressing "enter"; or the answer screen disappeared after a maximum of 7 seconds for 3 digits set; 15 seconds for 5 digits set. A 1-second black wait screen was presented after the answer screen. The design of the digit span backward paradigm is shown in Figure 1.

Each digit span set entered correctly to the answer screen for a presented digit span set was considered a "correct answer". Accordingly, for a participant, the total number of correct answers were calculated as a "recall score" for each difficulty level separately. The maximum recall score achievable is 30 as this is the amount of sets presented for each difficulty level.

To ensure that participants understood the tasks, right before the task, a short version of the 3-digit span task was given as the trial. The same procedure was applied in the actual task with the different stimuli from the actual task in the trial. During the trials, 3 different 3-ds sets were presented.

The digits were shown on a 47.5 x 26.8 cm size monitor with a refresh rate of 60 Hz that was placed 90 cm away from the participants. Digits were presented in the center of the screen. The approximate visual angle for the stimuli (each digit) measured 3 degrees horizontally and 3.3 degrees vertically.

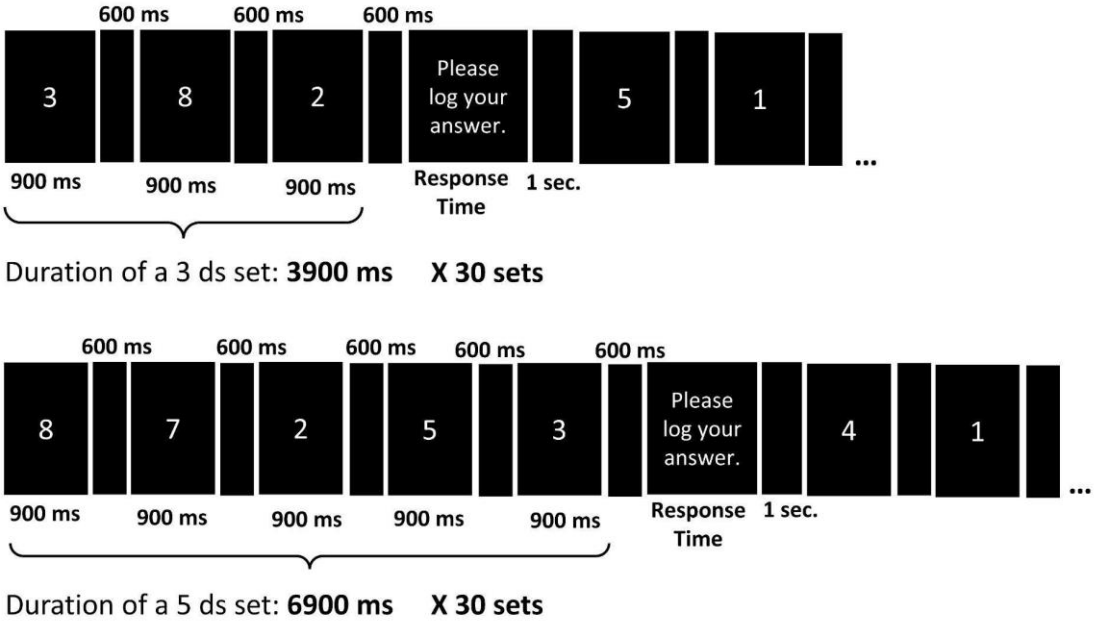

Figure 1. Task procedure. The representations of the applied digit span backward task during the EEG recordings (3ds set above and 5ds set below). ds: digit span, ms: millisecond, sec.: second

2.3 EEG Recording

EEG was recorded from Fp1, Fp2, F7 F3, Fz, F4, F8, Ft7, Fc3, Fcz, Fc4, Ft8, Cz, C3, C4, T7, T8, Tp7, Cp3, Cpz, Cp4, Tp8, P3, Pz, P4, P7, P8, O1, Oz and O2 electrodes with "BrainCap with Multitrodes" model cap (EasyCap GmbH, Germany) with 32 electrodes placed based on the international 10–20 system. Two linked earlobe electrodes (A1 + A2) served as references. The electrooculogram (EOG) was recorded at the left eye's medial upper and lateral orbital rim. The impedance of all electrodes was kept below approximately 10 kΩ. The EEG was amplified by means of a BrainAmp MR plus 32-channel DC system machine (Brain Product GmbH, Germany) with band limits of 0.01–250 Hz and digitized online with a sampling rate of 500 Hz. The participants were sitting in a dimly lit and shielded room during EEG recordings.

2.4 EEG Analysis

The preprocessing steps and further analyses of the event-related EEG data were performed in Brain Vision Analyzer software (BVA). For the event-related EEG data

preprocessing steps were as follows; I) data were filtered between 0.1 Hz to 60 Hz, II) independent component analysis was applied to remove eye-movement related artifacts, III) data were segmented into 5.5-second (1 second before and 4.5 seconds after the stimulus) and 8.5-second epochs (1 second before and 7.5 seconds after the stimulus) for 3-ds and 5-ds set tasks, respectively, IV) manual artifact rejection was performed over the segmented data. EEG data were not re-referenced since the online referencing scheme remained/unchanged (two linked earlobe electrodes (A1 + A2)) for the further EEG analyses.

While the importance of frontal and central areas is shown in the memory processes (i.e., Jensen & Tesche, 2002; Nogueira et al., 2015) the importance of parietal and occipital areas in number perception is known from the literature (i.e., Hesse et al., 2017; Rinsveld et al., 2020), as mentioned in the Introduction; therefore, here, anterior (fronto-central) and posterior (parieto-occipital) electrode pairs were chosen for the analysis. Accordingly, the further EEG analysis was run over two locations, namely 8 electrodes (fronto-central: F3, F4, C3, C4, parieto-occipital: P7, P8, O1, O2).

Over the preprocessed data, event-related analyses in the time-frequency domain were applied by the Gabor normalized complex Morlet Wavelet Transform (WT) with 4 cycle wavelet widths for the 1-15 Hz frequency range. The determined frequency range (1-15 Hz) was subdivided into 60 bins (the "frequency steps" parameter was set as "60"), scaled logarithmically (the “Logarithmic Steps” option was selected). The WT was calculated in each frequency bin. Analysis was performed for both 3-ds and 5-ds tasks separately (over 5.5 and 8.5 seconds length epochs, respectively).

In the event-related power analysis, as a normalization, the values were converted to the decibel (dB) scale. In this decibel normalization, pre-stimulus activity in the time window -500 ms to the -200 ms was used as the reference interval in time. The event-related power was calculated by averaging single trials to which WT was applied to reach total power (evoked+induced power).

Stimulation time per digit was 900 ms and ISI was 600 ms between digits presented in a set (see Method section for detail of the task design). And wavelet analysis was not applied for each digit separately but for a set of digits, which means we used 5.5 second time interval for the 3-ds set and 8.5 second time interval for the 5-ds. For obtaining event-related delta and theta responses values for each digit we averaged values within the “determined time” and frequency (Delta:1-3.5 Hz and theta: 4-8 Hz) window. The determined time window was 20-

700 ms for delta and 50-250 ms for theta, from digit onset to digit offset for each digit presented in a set. The sum values of the specified time and frequency window were divided by the total number of data points in the chosen time-frequency interval (point mean normalization), producing average values; and these values were used in the statistical analyses.

2.5 Statistical Analysis

Statistical analyses were performed with IBM SPSS Statistic 22 Software (IBM Corp., Armonk, N.Y., USA), R Statistical Software (Foundation for Statistical Computing, Vienna, Austria), and Jamovi (The jamovi project, 2021) software.

For the statistical analysis of the delta event-related power analysis, to test the serial position effect, the positions of the digit in a set were added as a within-subject factor as well as location and hemisphere factors. Therefore, three-way (2x2x3) repeated measures ANOVA was performed. The location (Fronto-Central, Parieto-Occipital), hemisphere (Right, Left), and position (First, Middle(s), Last) were the within-subjects factors in the design. In the 5-ds task, for the "middles" level of position factor, second, third, and fourth digits' delta responses were averaged.

For the statistical analysis of the theta event-related power analysis, repeated-measures ANOVA was run only to see the topographical distribution over the selected locations and hemispheres. Therefore, 2-by-2 repeated-measures ANOVA was performed. The location (Fronto-Central, Parieto-Occipital) and hemisphere (Right, Left) were the within-subjects factors in the design. Additionally, to evaluate the possible chunking strategy, as an encoding strategy reflected by theta responses, we employed the findchangepts algorithm used for change point detection in MATLAB (Killick et al., 2012; Lavielle, 2005). The algorithm finds where the abrupt change occurs across the signal. This function was here used to find the change points among up to four points (since the task has the 5 items in a set, leading to 4 changes) where the changes in root-mean-square level were most pronounced. Then, the Chi-Square test was used to statistically test the distribution of the detected change points across the possible four change points. This would reveal whether, across participants, there was statistically significant consistency at the moment in time where the change in event-rated power was most pronounced (null hypothesis; all change points equally likely, so no consistency). The change point detection function results allow us to see where the change happened; however, we cannot know the direction of the changes, and the change could have happened in both directions. Therefore, following the change point analysis, the repeated measure ANOVA with position (first, second,

third, fourth, last) factor was run to evaluate the direction of the power changes across the positions.

In order to reveal possible EEG-behavior interaction, a bivariate linear correlation (Pearson correlation, 2-tailed) analysis between behavioral scores and EEG data was used. As behavioral data, only 5-ds task scores were used in the correlation analysis since there was not enough variation in the 3-ds task scores due to its ease. As the EEG data, delta and theta mean power values of each response to the digits in a set were used separately over fronto-central and parieto-occipital areas.

The significance threshold was set at $p < 0.05$. Greenhouse Geisser corrected p values reported for the ANOVA analysis. For post-hoc comparisons, Holm adjusted p values were reported.

3. Results

3.1 Behavioral Results

In the digit span backward working memory task, a participant's total correct responses were determined as a "recall score" out of 30 points for each difficulty level independently (3-ds and 5-ds) since 30 sets were presented for each difficulty level. In order to see the effect of list length on task performance of individuals, a paired samples t-test was conducted. As expected, the results indicate that participants showed higher performance on 3-ds ($M = 27.7$, $SD = 2.05$) condition compared to the 5-ds ($M = 23.6$, $SD = 4.68$) ($t(36.0) = 5.26$, $p < .001$). Considering the study's participant population (educated, healthy, young-adult), it was quite expected that they would have a very high mean score for the 3-ds task.

3.2 EEG Results

3.2.1 Delta Power Results

We used complex Morlet Wavelet Transform to obtain event-related delta (1-3.5 Hz) oscillations in the time-frequency domain in response to each digit in the digit span backward working memory task. The position of the digits in a digit set was considered as a factor to assess the serial position effect on delta responses.

3.2.1.1 Three Digit Span Results

A 2 (Location: Fronto-Central, Parieto-Occipital) X 2 (Hemisphere: Right, Left) X 3 (Position: First, Middle, Last) repeated measures ANOVA results with a Greenhouse-Geisser correction indicated that there were main effects of digit Position ($F(1.40, 60.21) = 24.95$, *MSe*

= 6.79, $p < .001$, $\eta 2 = .37$) and electrode cluster (Location; ($F(1, 43) = 16.96$, $MSe = 4.17$, $p = .005$, $\eta 2 = .17$)) on event-related delta power. However, these main effects were dependent on the location and hemisphere, since there were significant location*position, hemisphere*position and location*hemisphere interactions. In the following paragraphs these interaction results were elaborated, respectively.

The ANOVA results indicated that there was an interaction between location and position factors ($F(1.76, 75.71) = 6.99$, $MSe = 1.22$, $p = .002$, $\eta 2 = .14$) (Fig. 2). We followed up this 2-way interaction by performing separate one-way repeated measure ANOVAs for the two locations (FC & PO) to see whether the expected position effect (u-shaped serial position curve) is location specific. Results showed that the position main effect was significant in both locations (in FC: ($F(1.45, 62.26) = 30.0$, MSe = 1.98, $p < .001$, $\eta 2 = .41$; in PO: ($F(1.51, 65.13) = 13.8$, MSe = 1.90, $p < .001$, $\eta 2 = .24$). Accordingly, in FC, pairwise comparisons showed that participants had lower power for the first digit position ($M = -.64$, $SD = .92$) than the last digit position ($M = .44$, $SD = 1.78$) ($t(86.0) = -4.23$, $p < 0.001$); and, they had lower power for the middle digit position ($M = -1.53$, $SD = 1.14$) than the first and last digit positions (first vs. middle, $t(86.0) = 3.50$, $p < .001$; last vs. middle, $t(86.0) = -7.73$, $p < .001$) (Fig. 2A, Fig. 5A). The similar pattern found in PO as well (first ($M = .13$, $SD = 1.01$) vs. middle ($M = -.80$, $SD = 1.46$), $t(86.0) = 3.65$, $p < .001$; last ($M = .51$, $SD = 2.09$) vs. middle, $t(86.0) = -5.11$, $p < .001$) except first-last digit difference ($t(86.0) = -1.45$, $p = .15$) (Fig. 2A, Fig. 5A).

The ANOVA results showed that there was also a significant interaction between position and hemisphere ($F(1.57, 67.30) = 7.43$, $MSe = 0.32$, $p = .003$, $\eta 2 = .15$). We followed up this 2-way interaction by performing separate one-way repeated measure ANOVAs for the two hemispheres (R & L) to see whether the expected position effect (u-shaped serial position curve) is hemisphere specific. Results showed that the position main effect was significant in both hemisphere (in L: ($F(1.31, 59.15) = 26.5$, MSe = 2.13, $p < .001$, $\eta 2 = .38$; in R: ($F(1.57, 67.39) = 21.0$, MSe = 1.42, $p < .001$, $\eta 2 = .33$). The post-hoc comparison analysis showed that in the left hemisphere, participants had a higher delta response for first ($M = -.32$, $SD = .86$) and last ($M = .56$, $SD = 1.86$) positions than the middle ($M = -1.27$, $SD = 1.18$) (first vs. middle, $t(86.0) = 3.78$, $p < .001$; last vs. middle, $t(86.0) = -7.28$, $p < .001$) and also had a higher delta response for the last position than the first ($t(86.0) = -3.50$, $p < .001$) (Fig. 5A). The same pattern was seen in the right hemisphere; participants had a higher delta response for the first ($M = -.19$, $SD = .81$) and last ($M = -.38$, $SD = 1.69$) positions than the middle ($M = -1.06$, $SD = 1.11$)

(first vs. middle, $t(86.0) = 3.89$, $p < .001$; last vs. middle, $t(86.0) = -6.43$, $p < .001$), and had a higher delta response for the last position than the first ($t(86.0) = -2.54$, $p = .013$) (Fig. 5A).

As can be seen from the follow-up analyses of the interactions, the pattern (serial position curve) seen in the position main effect is preserved despite significant interactions (Fig 2A) (see Supplementary Figure 1-7 for the individual level quadratic relationship model and distribution of the digit position-delta power values.).

In addition, the ANOVA results showed that there was an interaction between location and hemisphere ($F(1, 43) = 16.96$, $MSe = .32$, $p < .001$, $\eta 2 = .28$) (Fig. 2B). The post-hoc analysis demonstrated that participants had lower left PO ($M = -.18$, $SD = 1.27$) power compared to the right PO ($M = .074$, $SD = 1.28$) ($t(75.5) = 2.93$, $p = 0.019$) (Fig. 5A). Yet, there was no such hemispheric difference in the FC ($t(75.5) = -1.62$, $p = 0.17$).

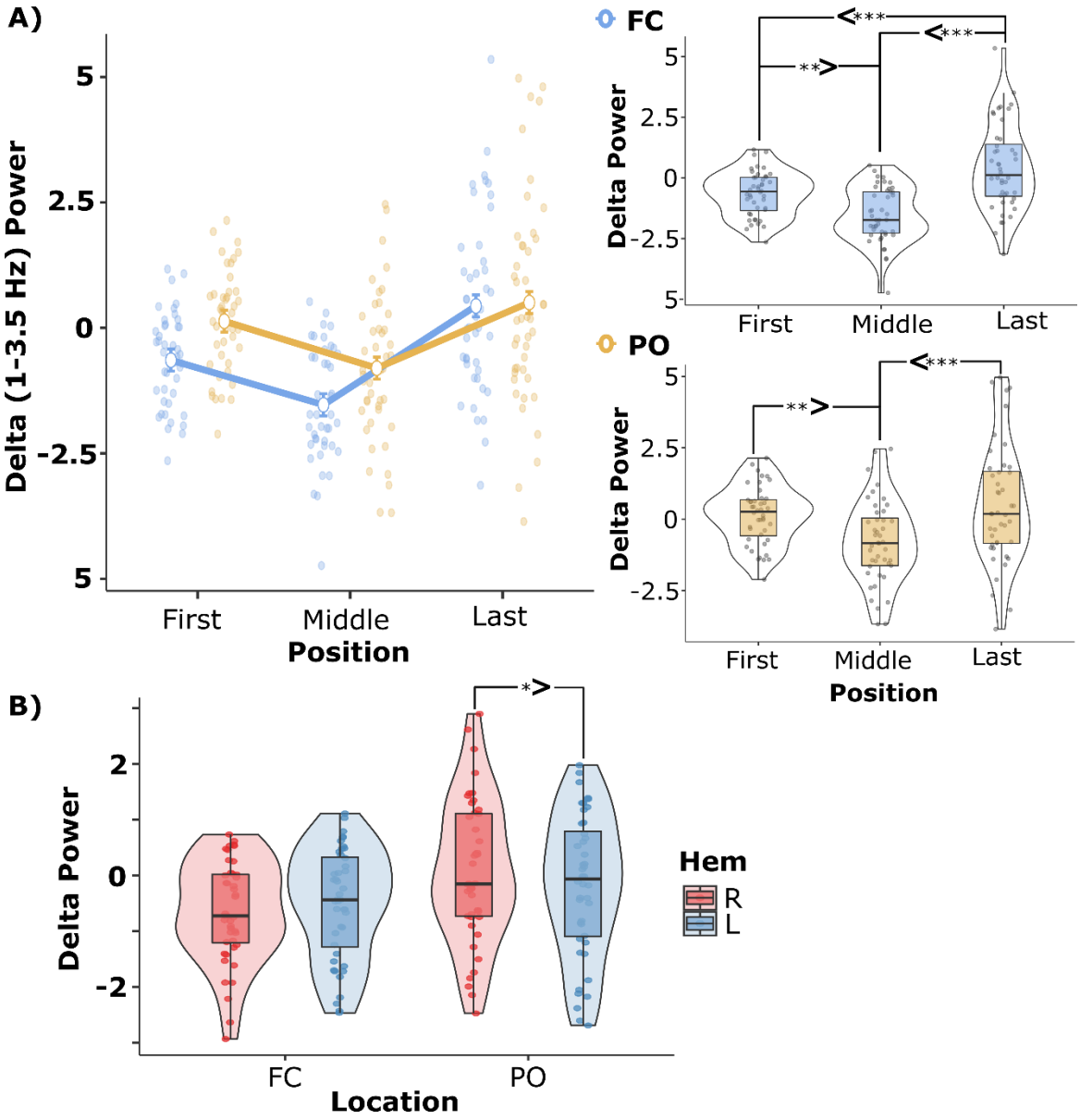

Figure 2. The location*position and location*hemisphere plots for delta responses (1-3.5 Hz) in 3-ds backward task. A) The left plot shows the significant location*position interaction (p = .002). The right plots show the position effect for each location. In the FC, participants had lower power for the first digit position than for the last digit position (p < 0.001); and, they had lower power for the middle digit position than for the first and last digit positions (first vs. middle, p = .004; last vs. middle, p < .001). In the PO, participants had lower power for the middle digit position than the first and the last positions (first vs. middle, p = .003; last vs. middle, p < .001), and there was no difference between the delta response given to the first and last digit (p = 0.59). **B)** The plot shows the significant location*hemisphere interaction (p < .001). Participants had lower left PO power compared to the right PO (p = 0.019). Yet, there was no such hemispheric difference in the FC (p = 0.17). Hem: hemisphere, R: right, L: left, FC: fronto-central, PO: parieto-occipital. The error bars on box plots denote the standard error of the mean**.** Asterisks indicate statistical significance (*: $p \leq .05$, **: $p \leq .01$, ***: $p \leq .001$). Dots represent the observed scores.

3.2.1.2 Five Digit Span Results

A 2 (Location: Fronto-Central, Parieto-Occipital) X 2 (Hemisphere: Right, Left) X 3 (Position: First, Middles, Last) repeated measures ANOVA results with a Greenhouse-Geisser correction revealed that there was a main effect of position (F(1.38, 56.72) = 22.90, MSe = 9.51, p < .001, $\eta 2$ = .36). However, this effect was dependent on the location and hemisphere factors since there is a significant location*hemisphere*position interaction (F(1.88, 77.27) = 4.53, MSe = 0.12, p = .02, $\eta 2$ = .10) (Fig. 3). We followed up this 3-way interaction by performing separate 2x2 ANOVAs for the two locations (FC & PO) to determine for which locations and hemispheres we can see the expected position effect (u-shaped serial position curve). Results showed that the hemisphere*position interaction was significant in the FC (F(1.44, 59.19) = 13.02, MSe = 0.22, p < .001, $\eta 2$ = .24). And when we followed up this 2-way interaction with the one-way repeated measures ANOVAs for each hemisphere (Left & Right), the position main effect was found significant for both hemispheres (left FC: F(1.39, 57.04) = 28.5, MSe = 3.52, p < .001, $\eta 2$ = .41; right FC: F(1.55, 63.51) = 20.7, MSe = 2.48, p < .001, $\eta 2$ = .34). Accordingly, pairwise comparisons showed that in left FC participants had higher power for the first (M = -.14, SD = 1.27) and last digits (M = 1.58, SD = 2.35) than middle (M = -.95, SD = 1.58) (first vs. middle, t(82.0) = 2.37, p = .02*;* middle vs. last, t(82.0) = -7.39, p < .001), and last digit elicited higher power than first (t(82.0) = -5.08, p < .001) (Fig. 3, Fig. 5B). Same pattern observed in right FC as well; participants had higher power for the first (M = -.26, SD

= 1.31) and last digits (*M* = 1.01, *SD* = 1.98) than middle (*M* = -.90, *SD* = 1.62) (first vs. middle, *t*(82.0) = 2.21, *p* = .04; middle vs. last, *t*(82.0) = -6.32, *p* < .001), and last digit had higher power than first (*t*(82.0) = -4.21, *p* < .001) (Fig. 3, Fig. 5B). When we look at the PO, we found that not the position*hemisphere interaction (*F*(1.88, 76.90) = 2.77, *MSe* = 0.17, *p* = .07, *η2* = .06) but the position main effect was significant (*F*(1.42, 58.20) = 17.45, *MSe* = 4.62, *p* < .001, *η2* = .30). The results of the post-hoc analysis for the main effect of position demonstrated that participants had higher power for the first (M = .23, SD = 1.04) and last (M = .58, SD = 2.00) digit position than the middle position (M = -.99, SD = 1.43) (first vs. middle, *t*(82.0) = 4.38, *p* < .001; middle vs. last, *t*(82.0) = -5.62, *p* < .001) (Fig. 3, Fig. 5B).

As for the delta 3-ds statistical results, we also here revealed that the pattern seen across digit positions is largely preserved despite significant interactions (see also Supplementary Figure 8-17 for the individual level quadratic relationship model and the distribution of the digit position-delta power values).

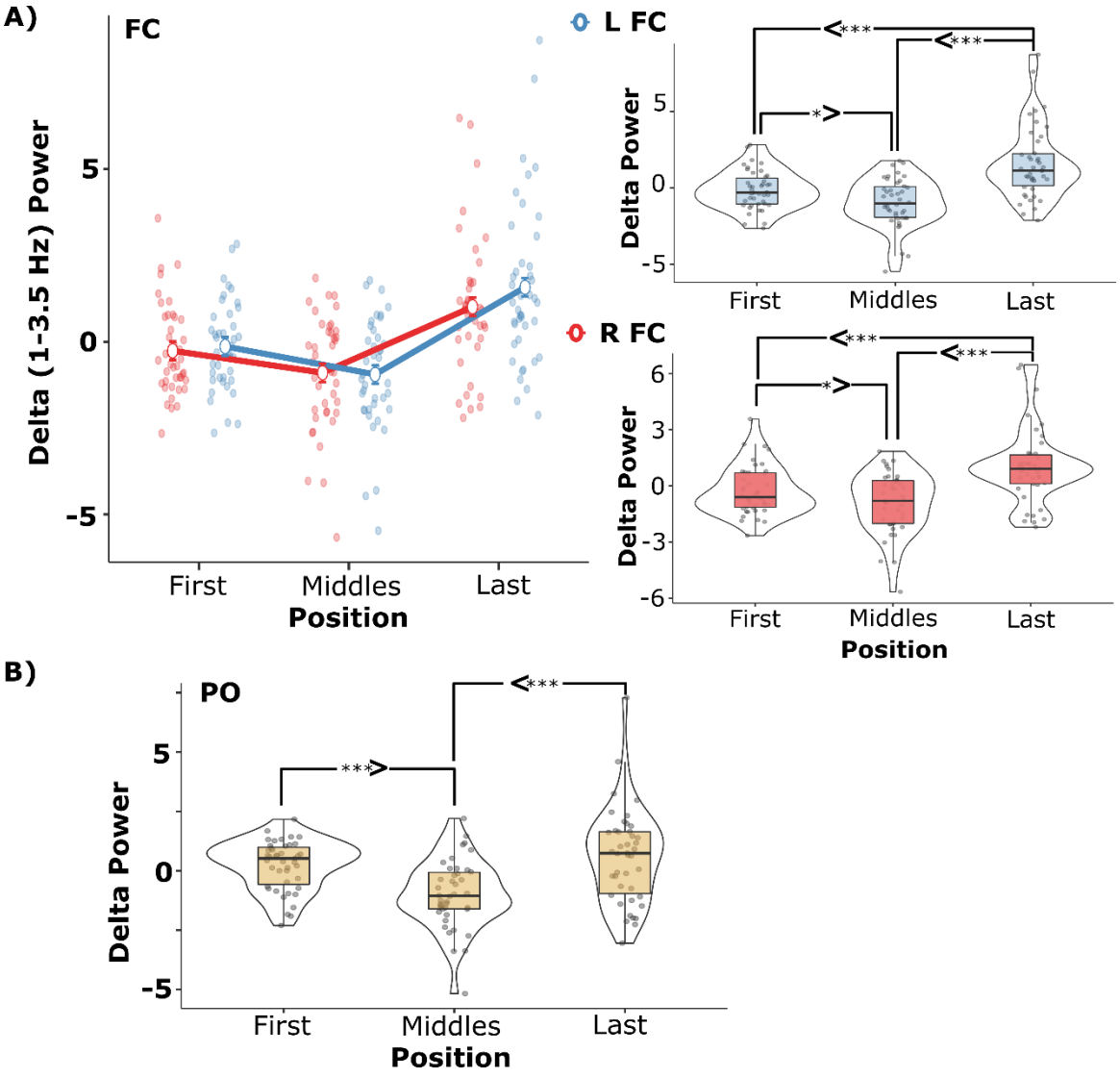

Figure 3. The plots of the hemisphere*position interaction in the FC (A) and the position effect in the PO (B) for delta responses (1-3.5 Hz) in the 5-ds backward task. A) The hemisphere*position interaction was significant in the FC ($p < .001$), and in the follow-up analyses position main effect was found significant for both hemispheres (left FC, $p < .001$; right FC, $p < .001$). Pairwise comparisons showed that in left FC, participants had higher power for the first and last digits than middle (first vs. middle, $p = .02$; middle vs. last, $p < .001$), and the last digit elicited higher power than the first ($p < .001$). The same pattern was observed in right FC as well; participants had higher power for the first and last digits than middle (first vs. middle, $p = .04$; middle vs. last, $p < .001$), and the last digit had higher power than the first ($p < .001$). **B)** In the PO, the position main effect was significant ($p < .001$). Pairwise comparisons showed that participants had higher power for the first and the last digit position than the middle position (first vs. middle, $p < .001$; middle vs. last, $p < .001$) L: left, R: right, FC: fronto-central, PO: parieto-occipital. The error bars on box plots denote the standard error of the mean**.** Asterisks indicate statistical significance (*: $p \leq .05$, **: $p \leq .01$, ***: $p \leq .001$). Dots represent the observed scores.

In addition, Linear Mixed-Effects Models analysis was performed to investigate the continuous quadratic distributions of "digit position" in both 3-ds and 5-ds delta power responses. The models indicated that there were quadratic relationships between delta power values and digit positions. The results of these models were significant for both, the averaged data (all locations & hemispheres) and for each location and hemisphere separately (all *ps* < .0001). We included the figures of distributions, model results, and analysis results in the Supplementary Materials.

3.2.2 Theta Power Results

We used the complex Morlet Wavelet Transform to obtain event-related theta (4-8 Hz) oscillations in the time-frequency domain, in response to each digit in the digit span backward working memory task. Both 5 and 3-ds tasks were investigated in terms of locations (FC & PO) and hemispheres (LH & RH) with 2-by-2 ANOVA. Furthermore, theta responses in the 5-ds task were evaluated for chunking strategy. For this purpose, changepoint (cp) detection analysis was applied to find where the most significant theta power change happened during 5-ds (between the possible four transitions) in the root-mean-square level. Then, a Chi-Square test was used to evaluate the uniformity or lack thereof of the cp distribution across the four possible change points (5 digits results in 4 transitions between digits and their event-related theta

responses and therefore 4 changepoints). Subsequently, repeated measures ANOVA were employed with the position factor to interpret the direction of the changes happening at the cp.

3.2.2.1 Three Digit Span Results

For investigating power changes of participants at theta frequency for three digit span conditions across the locations and hemispheres, we performed a 2 (Location: Fronto-Central, Parietal-Occipital) X 2 (Hemisphere: Right, Left) repeated measures ANOVA with a Greenhouse-Geisser correction. There was a main effect of the hemisphere ($F(1, 43) = 8.38$, $MSe = 0.69$, $p = .006$, $\eta 2 = .16$). The post-hoc analysis of this main effect demonstrated that participants had higher power at the right hemisphere ($M = .64$, $SD = 1.33$) than the left ($M = .28$, $SD = 1.26$) ($t(43.0) = 2.89$, $p = .006$) (Fig. 5A). In addition to these, the main effect of location was significant ($F(1, 43) = 30.79$, $MSe = 4.89$, $p < .001$, $\eta 2 = .42$). The pairwise comparison indicated that participants had higher power in the PO ($M = 1.38$, $SD = 2.05$) than FC ($M = -.46$, $SD = 1.13$) ($t(43.0) = -5.55$, $p < .001$) (Fig. 5A).

3.2.2.2 Five Digit Span Results

Another 2 (Location: Fronto-Central, Parieto-Occipital) X 2 (Hemisphere: Right, Left) repeated measures ANOVA with a Greenhouse-Geisser correction was performed for investigating power changes of participants at theta frequency for five digit span conditions. The results indicated that there were significant main effects of hemisphere ($F(1, 41) = 17.47$, $MSe = 0.35$, $p < .001$, $\eta 2 = .26$) and location ($F(1, 41) = 15.03$, $MSe = 3.52$, $p < .001$, $\eta 2 = .27$), however, there was also a significant location*hemisphere interaction ($F(1, 41) = 4.64$, $MSe = 0.39$, $p = .037$, $\eta 2 = .10$). Follow-up post-hoc analysis demonstrated that the right PO ($M = .76$, $SD = 2.09$) had higher power than the left ($M = .21$, $SD = 1.78$) ($t(81.7) = -4.18$, $p < .001$) while there was no such a hemispheric difference in the FC ($t(81.7) = -1.05$, $p = .30$).

To investigate the theta power results for the chunking strategy in the five digit span task performances of participants, we used the findchangepts algorithm in MATLAB. As we explained in the methods section, this algorithm finds where the theta power values change most strongly among the four transitions between the five digits. The results of this algorithm demonstrated that 22 (%52,4) participants had the biggest change at the third digit (meaning the transition between digits 2 and 3), and 20 (%47,6) participants had the biggest change at the fourth digit (meaning the transition between digits 3 and 4), while no participant showed the biggest change at digits 2 or 5, relative to the preceding digits. As may readily be seen, detected

change points were not uniformly distributed among the possible four transitions between the five digits ($X^2(3, N=42) = 42.19$, $p < 0.001$). In Figure 4, the detected strongest changes between digits were demonstrated on the averaged data.

These findings showed where the greatest changes occurred, but we cannot know the direction of the changes from this analysis; the change could have happened in both directions. For investigating the direction of the power changes, we performed a repeated-measures ANOVA with the position factor. The results showed that position had a main effect on the theta power value of participants ($F(2.75, 112.61) = 14.2$, $MSe = 0.92$, $p < .001$, $\eta 2 = .07$). Pairwise comparisons revealed that participants had higher power for the first digit ($M = .43$, $SD = 1.20$) than third ($M = -.10$, $SD = 1.53$) (first vs. third, $t(164) = 3.10$, $p = .01$), fourth ($M = -.42$, $SD = 1.63$) (first vs. fourth, $t(164) = 4.91$, $p < .001$), and fifth ($M = -.63$, $SD = 1.53$) (first vs. fifth, $t(164) = 6.10$, $p < .001$) digits. Theta power values were also higher for the second digit ($M = .34$, $SD = 1.45$) than third (second vs. third, $t(164) = 2.55$, $p = .05$), fourth (second vs. fourth, $t(164) = 4.37$, $p < .001$) and fifth digits (second vs. fifth, $t(164) = 5.56$, $p < .001$). The third digit had higher power than the fifth digit ($t(164) = 3.01$, $p = .02$). There were no other differences between positions ($ps > .21$). In other words, there were significant decreases in power values after the second and third digits (Fig. 4, Fig 5B). Together with these results, we understand the changes that were depicted by the findchangepts algorithm had a decreasing pattern.

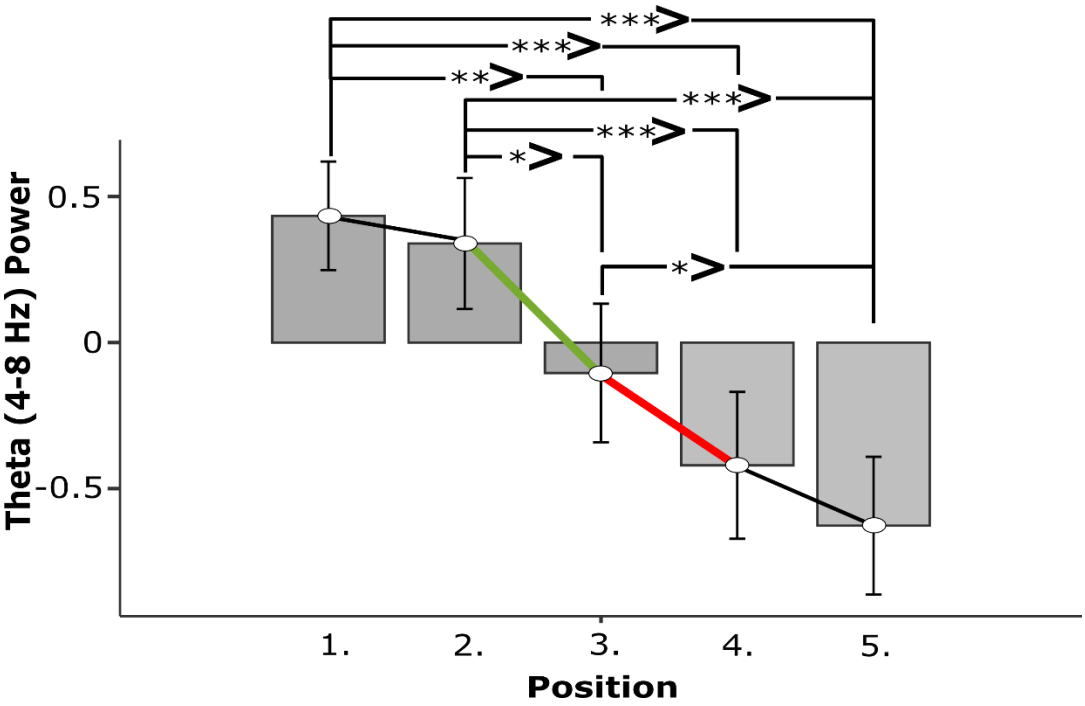

Figure 4. The event-related theta (4-8 Hz) power values for each digit positions in the 5-ds backward task. The vertical axis shows the average theta power for each digit across subjects. The green (in 22 participants) and red (in 20 participants) lines represent where the theta power values changed most strongly among the four transitions between the five digits. The error bars on bar plots denote the standard error of the mean**.** Asterisks indicate statistical significance (*: $p \leq .05$, **: $p \leq .01$, ***: $p \leq .001$).

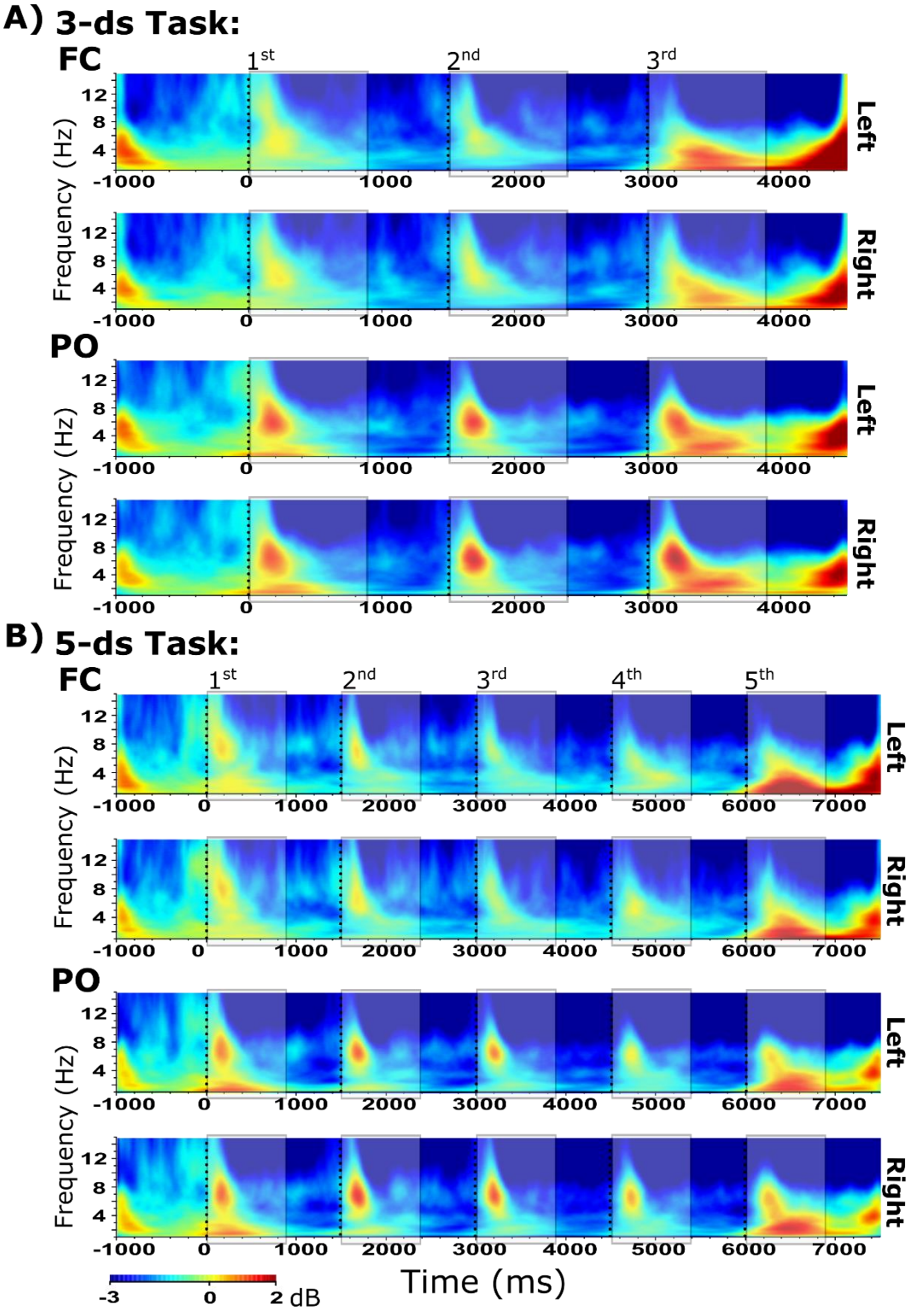

Figure 5. The grand average figures of event-related power analysis (1-15 Hz) in the time-frequency domain during the digit span backward task. A) The grand average figures of event-related power analysis in the time-frequency domain in response to digits in the 3-ds backward task. The fronto-central area (upper) and parieto-occipital (bottom) areas for both hemispheres were presented in the figures. **B)** The grand average figures of event-related power

analysis in the time-frequency domain in response to digits in the 5-ds backward task. The fronto-central area (upper) and parieto-occipital (bottom) areas for both hemispheres were presented in the figures. The X-axis represents time, and the Y-axis represents frequency; the point at which the first stimulus (digit) from the digit span set arrives is marked as a zero point on the X-axis. The point where each digit in a set comes from is indicated by black dashed vertical lines. And the 900 ms time interval that digits were presented in each set was marked with the gray transparent blocks on the plots. FC: fronto-central, PO: parieto-occipital, ds: digit span.

3.3 EEG-behavior interaction Results

Correlation analyses between behavioral data, namely, 5-ds recall scores, and EEG data were conducted with bivariate linear correlation (Pearson correlation, 2-tailed). As EEG data, delta and theta mean power values of each response to a set of digits were employed for the fronto-central and parieto-occipital regions, separately.

The subjects with increased fronto-central delta power during the item encoding had the higher recall scores (r = 0.396, p = 0.019) while no correlation was found between the parieto-occipital delta and recall scores (r = 0.144, p = 0.411) (Fig. 6A). There were no significant correlations between recall scores and theta responses in any locations as well (FC: r = 0.096, p = 0.584, PO: r = -0.062, p = 0.722) (Fig. 6B).

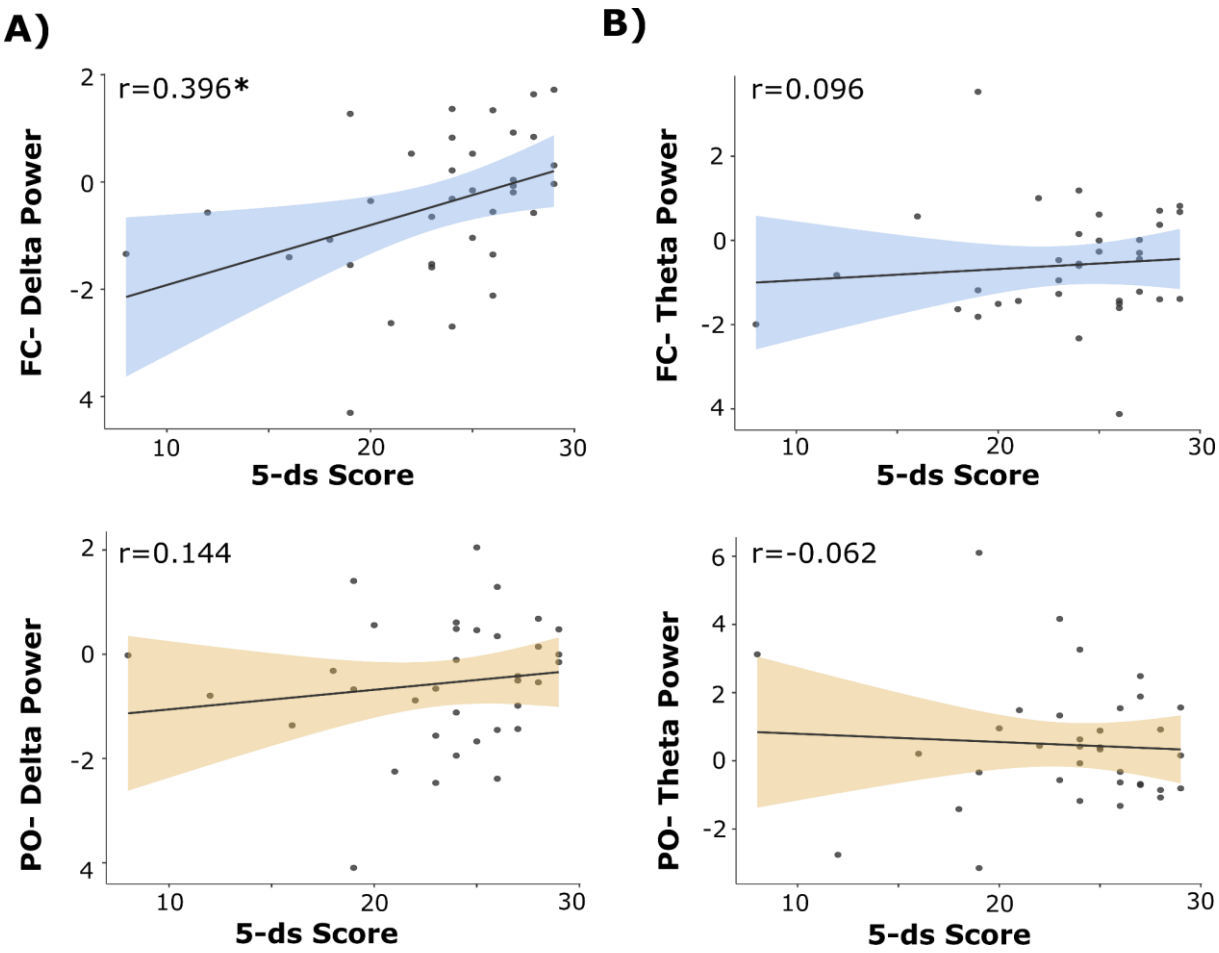

Figure 6. The scatter plots of the correlation analysis result. A) The scatter plots of the correlation between the task scores and delta responses (1-3.5 Hz) in the FC (upper) and PO (bottom) areas. **B)** The scatter plots of the correlation between the task scores and theta responses (4-8 Hz) in the FC (upper) and PO (bottom) areas. FC: fronto-central, PO: parieto-occipital, ds: digit span. Asterisks indicate statistical significance ($p < 0.05$). The shaded area denotes the standard error. Dots represent the observed scores.

4. Discussion

Here we mainly aimed to investigate how brain theta and delta oscillations reflect the item position and number of items (to be held) during the encoding process in the working memory digit span backward task. Specifically, we searched for the "serial position" and "chunking" effects on delta and theta responses over the fronto-central and parieto-occipital areas. As an oscillatory reflection of the serial position effect, we expected increased delta power at the first and last digit compared to the middle digit(s). Our results demonstrate the delta responses were higher for the first and last items than for the middle items in the digit list, which match nicely the suggested "serial position curve" model (Murdock, 1962; Murre &

Dros, 2015). Besides that, for theta frequency responses, as a sign of the chunking strategy, we expected altered oscillatory dynamics around the 3rd or 4th digit in light of our tendency to group items in three or four (Cowan, 2001, 2005, 2010). In line with the theories that emphasize memory chunks, change in the theta responses during the digit list encoding occurred during transitions to the third or fourth item; and the direction of change was downward, namely, theta responses to particularly the 3rd or 4th item decreased relative to preceding items. Furthermore, a positive correlation was found between frontal delta responses and task performance. This correlation was specific to location and frequency. Additionally, even though the primary aim of the current study was not to investigate number perception itself, the task used in the study naturally involved number processing as well. Therefore, according to previous literature on number processing studies (Hesse et al., 2017; Rinsveld et al., 2020), one might expect greater parieto-occipital (posterior) brain responses, and right hemisphere dominance, during number processing. Accordingly, results showed that the parieto-occipital areas had higher theta responses in the right hemisphere than the left, which supports previous studies (Hesse et al., 2017; Rinsveld et al., 2020) that showed the importance of the right parietal-occipital activation during number perception.

The serial position effect is a behavioral finding that experimental psychology studies on memory have widely demonstrated. Accordingly, the first (primacy effect) and last items (recency effect) in a list are recalled better than the middle ones. This is also called the serial position curve. This U-shaped curve shows the learning curve of the items in the list. Our study showed that delta oscillations reflect the suggested serial position effect with a higher delta power in response to the first and last items than the middle during the item list encoding. The most accepted model of the mechanism underlying the serial position effect is the dual-store processing model (Atkinson & Shiffrin, 1968; Talmi et al., 2005). In this model, the serial position effect relies on a distinction between short-term memory and long-term memory (Glanzer & Cunitz, 1966; Waugh & Norman, 1965). And per the concept, serial position effect occurs because the initial items on a list are retrieved from long-term memory, since the earliest items are rehearsed the most, thereby reinforcing their place in memory. The last items on the list, on the other hand, are still in short-term memory and hence can be retrieved without rehearsing. Atkinson, & Shiffrin (1968) suggest that the primacy effect in this model is also strictly related to the number of items in the list. Accordingly, if the list exceeds the "rehearsal buffer" then the presentation of new items forces a move of older items into long-term memory (Lehman & Malmberg, 2013). Another explanation of the serial position effect is based on

attentional processes (Azizian & Polich, 2007; Melton, 1963; Page & Norris, 1998; Sederberg et al., 2006). In the scope of this claim, people may pay greater attention to the first and last items in the list, which creates "anchor points" for better learning the rest of the information by reducing the demands on memory. And in our case, considering the serial position effect was seen in the delta responses even for the 3-ds task, which is within the suggested memory limits in terms of the number of items to be held, possibly not only dual-store mechanisms but also attention allocation mechanisms might be involved. Therefore, it can be thought that the serial position effect reflected by delta oscillations is more related to immediate memory and attention-related processes, which these roles of the delta have been shown in many previous studies (Başar-Eroglu et al., 1992; Ergen et al., 2008; Harper et al., 2017; Polich & Kok, 1995; Sutton et al., 1965). In addition to this "serial position curve" reflected in delta, the last digit had a higher delta response than the first digit, especially for the FC location. It may indicate that participants are aware, either consciously or unconsciously, that the task list (digit set) has ended, allowing the required brain processes to prepare for recalling the digits backward. This additional process that is not present in the other digit positions (knowing that the recall process will start right after it) may have caused the greater delta response for the last digit due to the load it created. This is also in line with Wilsch and Obleser's (2006) findings that show higher delta may be related to the stimuli encoding and subsequent reduction of memory load (Wilsch & Obleser, 2006). Overall, it seems, here, delta responses serve as the neural start and end markers of the encoding of a list.

According to Cowan (2001; 2005; 2010), the limit of the mental storage capacity is 3-4 (up to 5). Therefore, it is assumed that the created chunks consist of grouping 3-4 items. Additionally, Nogueira et al. (2015) showed increased late positive slow waves during encoding the successively presented words when the items were chunked compared to the control condition. Accordingly, we hypothesized that created chunks in mentioned strategy may be reflected by theta oscillations since theta is majorly associated with the item encoding in literature. And as we expected, in line with Cowan's suggested mental storage capacity (3-4 items) and Nogueira et al. (2015)'s ERP study, event-related theta oscillations showed a decreasing pattern starting with the 3rd or 4th item. Similarly, Agam & Sekuler (2007) showed that EEG response declined as more chunks had to be stored, and they discussed it as the "interactions between working memory and visual perception" (Agam & Sekuler, 2007). They suggested memory load influences how the brain reacts to visual inputs. Azizian & Polich (2007) also found decreased EEG responses with the incoming stimulus in the encoding task as

well, however, they associated the pattern found in EEG mostly with a decrease in attention with the approaching stimuli. According to them, the reason for the decrease in the EEG response to incoming stimulus was that each successive stimulus receives less attention than the previous one (Brown et al., 2000; Page & Norris, 1998). As a matter of fact, these two discussion points, namely, mental storage capacity limit and attentional decrease, also cannot be considered as purely separate processes. Considering capacity-limited attentional processes (Marois & Ivanoff, 2005) it is inevitable that exceeding this limit will lead to the creation of a way to better encoding, such as memory chunks. Therefore, it is very likely that these two bottlenecks (capacity-limited attentional processes and object encoding limit) are already interacting with each other and, accordingly, have led to the development of strategies. And yet, both limitations might be responsible for the created memory chunks during the item list encoding, which is reflected by the theta oscillations. Here we should also note that our results indicated that created chunks consist of 2 or 3 items, which is 1 item below the suggested memory limit (3 or 4). There may be two possible reasons why the chunks found here contain fewer items (2 or 3) than the suggested capacity limit (3 or 4): I) The total number of items was already low (5 digits were presented in a set), which may have caused the chunks to consist of fewer items. II) To optimize performance, it might have been more strategic to make smaller chunks because of the additional cognitive load as participants had to remember the sequences in "reverse" order for the digit span "backward" task.

Based on the studies in which increased slow oscillatory (< ~8 Hz) responses for the successfully encoded items in the anterior areas were shown (De Vries et al., 2018; Sederberg et al., 2006; Summerfield & Mangels, 2005; Weiss & Rappelsberger, 2000), accordingly, we expected a positive correlation between task scores and anterior EEG responses. Our results indicate that the anterior delta, but not theta, may relate to successful subsequent recall performance. However, in the literature, the most pronounced frequency that reflects the subsequent memory is theta oscillations, contrary to our findings (Friese et al., 2013; Herweg et al., 2020; Klimesch et al., 2004; Köster et al., 2018; Solomon et al., 2019; Staudigl & Hanslmayr, 2013). There are few studies in which similar subsequent memory effects have been shown for delta frequency (Sederberg et al., 2006; Weiss & Rappelsberger, 2000). According to these studies, delta power as response to the presented stimuli (visually and/or auditorily presented words) was higher for later successful recall. This frequency specific subsequent memory effect found in our study for delta frequency, but not for theta, might be specific to the task used in our study (digit-span backward), considering that most of the studies in the

literature showing theta subsequent memory effect used the object (pictural) encoding tasks mostly.

All in all, the results of this study may suggest that different frequencies might be responsible for different elements of serial encoding that have previously been demonstrated mostly in behavioral studies. For further research, our findings on EEG indicators of the memory processes could provide a deeper insight which may also lead to more goal-directed neuromodulation approaches, especially for the clinical populations who have difficulties in these memory processes and encoding strategies.

References

Agam, Y., & Sekuler, R. (2007). Interactions between working memory and visual perception: An ERP/EEG study. *NeuroImage*, *36*(3), 933–942. https://doi.org/10.1016/J.NEUROIMAGE.2007.04.014

Aktürk, T., de Graaf, T.A., Güntekin, B. Hanoğlu, L., Sack, A.T. (2022). Enhancing memory capacity by experimentally slowing theta frequency oscillations using combined EEG-tACS. *Scientific Reports*, 12, 14199. https://doi.org/10.1038/s41598-022-18665-z

Atkinson, R. C., & Shiffrin, R. M. (1968). Human Memory: A proposed system and its control processes BT - The Psychology of Learning and Motivation. *The Psychology of Learning and Motivation*, *2*(5), 89–195.

Azizian, A., & Polich, J. (2007). Evidence for attentional gradient in the serial position memory curve from event-related potentials. *Journal of Cognitive Neuroscience*, *19*(12), 2071–2081. https://doi.org/10.1162/jocn.2007.19.12.2071

Başar-Eroglu, C., Başar, E., Demiralp, T., & Schürmann, M. (1992). P300-response: possible psychophysiological correlates in delta and theta frequency channels. A review. *International journal of psychophysiology*, 13(2), 161-179. https://doi.org/10.1016/0167-8760(92)90055-G

Bonhage, C. E., Meyer, L., Gruber, T., Friederici, A. D., & Mueller, J. L. (2017). Oscillatory EEG dynamics underlying automatic chunking during sentence processing. *NeuroImage*, *152*, 647–657. https://doi.org/10.1016/J.NEUROIMAGE.2017.03.018

Brown, G. D. A., Hulme, C., & Preece, T. (2000). Oscillator-Based Memory for Serial Order. *Psychological Review*, *107*(1), 127–181. https://doi.org/10.1037/0033-295X.107.1.127

Buzsáki, G. (2005). Theta rhythm of navigation: Link between path integration and landmark navigation, episodic and semantic memory. In *Hippocampus* (Vol. 15, Issue 7, pp. 827–840). https://doi.org/10.1002/hipo.20113

Buzsáki, G., & Moser, E. I. (2013). Memory, navigation and theta rhythm in the hippocampal-entorhinal system. *Nature Neuroscience*, *16*(2), 130–138. https://doi.org/10.1038/nn.3304

Constantinidis, C., & Klingberg, T. (2016). The neuroscience of working memory capacity and

training. *Nature Reviews Neuroscience*, *17*(7), 438–449. https://doi.org/10.1038/NRN.2016.43

Cowan, N. (2001). The magical number 4 in short-term memory: A reconsideration of mental storage capacity. *Behavioral and Brain Sciences*, *24*(1), 87–114. https://doi.org/10.1017/S0140525X01003922

Cowan, N. (2005). Working Memory Capacity Working memory capacity. Psychology Press. https://doi.org/10.4324/9780203342398

Cowan, N. (2010). The magical mystery four: How is working memory capacity limited, and why? *Current Directions in Psychological Science*, *19*(1), 51–57. https://doi.org/10.1177/0963721409359277

De Vries, I. E. J., Van Driel, J., Karacaoglu, M., & Olivers, C. N. L. (2018). Priority Switches in Visual Working Memory are Supported by Frontal Delta and Posterior Alpha Interactions. *Cerebral Cortex*, *28*(11), 4090–4104. https://doi.org/10.1093/CERCOR/BHY223

Demiralp, T., Ademoglu, A., Schürmann, M., Basar-Eroglu, C., & Basar, E. (1999). Detection of P300 Waves in Single Trials by the Wavelet Transform (WT). *Brain and Language*, *66*(1), 108–128. https://doi.org/10.1006/BRLN.1998.2027

Ebbinghaus, H. (1885). Über das Gedächtnis: Untersuchungen Zur Experimentellen Psychologie. Duncker & Humblot.

Ergen, M., Marbach, S., Brand, A., Başar-Eroğlu, C., & Demiralp, T. (2008). P3 and delta band responses in visual oddball paradigm in schizophrenia. *Neuroscience Letters*, *440*(3), 304–308. https://doi.org/10.1016/j.neulet.2008.05.054

Ericsson, K. A., Chase, W. G., & Faloon, S. (1980). Acquisition of a memory skill. *Science*, *208*(4448), 1181–1182. https://doi.org/10.1126/SCIENCE.7375930

Feigenbaum, E. A., & Simon, H. A. (1962). A theory of the serial position effect. *British Journal of Psychology (London, England : 1953)*, *53*, 307–320. https://doi.org/10.1111/j.2044-8295.1962.tb00836.x

Friese, U., Köster, M., Hassler, U., Martens, U., Trujillo-Barreto, N., & Gruber, T. (2013).

Successful memory encoding is associated with increased cross-frequency coupling between frontal theta and posterior gamma oscillations in human scalp-recorded EEG. *NeuroImage*, *66*, 642–647. https://doi.org/10.1016/j.neuroimage.2012.11.002

Gilbert, A. C., Boucher, V. J., & Jemel, B. (2014). Perceptual chunking and its effect on memory in speech processing: ERP and behavioral evidence. *Frontiers in Psychology*, *5*(MAR), 1–9. https://doi.org/10.3389/fpsyg.2014.00220

Gilbert, A. C., Boucher, V. J., & Jemel, B. (2015). The perceptual chunking of speech: A demonstration using ERPs. *Brain Research*, *1603*, 101–113. https://doi.org/10.1016/J.BRAINRES.2015.01.032

Glanzer, M., & Cunitz, A. R. (1966). Two storage mechanisms in free recall. *Journal of Verbal Learning and Verbal Behavior*, *5*(4), 351–360. https://doi.org/10.1016/S0022-5371(66)80044-0

Goodman, M. S., Kumar, S., Zomorrodi, R., Ghazala, Z., Cheam, A. S. M., Barr, M. S., Daskalakis, Z. J., Blumberger, D. M., Fischer, C., Flint, A., Mah, L., Herrmann, N., Bowie, C. R., Mulsant, B. H., Rajji, T. K., Pollock, B. G., Lourenco, L., Butters, M., Gallagher, D., … Voineskos, A. N. (2018). Theta-Gamma coupling and working memory in Alzheimer's dementia and mild cognitive impairment. *Frontiers in Aging Neuroscience*, *10*(APR), 1–10. https://doi.org/10.3389/fnagi.2018.00101

Grover, S., Wen, W., Viswanathan, V., Gill, C. T., & Reinhart, R. M. (2022). Long-lasting, dissociable improvements in working memory and long-term memory in older adults with repetitive neuromodulation. *Nature Neuroscience*, 1-10. https://doi.org/10.1038/s41593-022-01132-3

Harper, J., Malone, S.M. & Iacono, W.G. (2017). Theta-and delta-band EEG network dynamics during a novelty oddball task. *Psychophysiology*, 54(11), 1590–1605. doi:10.1111/psyp.12906.

Herweg, N. A., Solomon, E. A., & Kahana, M. J. (2020). Theta Oscillations in Human Memory. *Trends in Cognitive Sciences*, *24*(3), 208–227. https://doi.org/10.1016/j.tics.2019.12.006

Hesse, P. N., Schmitt, C., Klingenhoefer, S., & Bremmer, F. (2017). Preattentive Processing of Numerical Visual Information. *Frontiers in Human Neuroscience*, *0*, 70.

https://doi.org/10.3389/FNHUM.2017.00070

Jensen, O., & Lisman, J. E. (1998). An oscillatory short-term memory buffer model can account for data on the Sternberg task. *Journal of Neuroscience*, *18*(24), 10688–10699. https://doi.org/10.1523/jneurosci.18-24-10688.1998

Jensen, O., & Tesche, C. D. (2002). Frontal theta activity in humans increases with memory load in a working memory task. *European Journal of Neuroscience*, *15*(8), 1395–1399. https://doi.org/10.1046/J.1460-9568.2002.01975.X

Jevons, W. S. (1871). The power of numerical discrimination. *Nature*, *3*(67), 281–282. https://doi.org/10.1038/003281A0

Killick, R., Fearnhead, P., Eckley, I.A., 2012. Optimal detection of changepoints with a linear computational cost. JASA 107 (500), 1590–1598. doi:10.1080/01621459.2012.737745.

Klimesch, W., Schack, B., Schabus, M., Doppelmayr, M., Gruber, W., & Sauseng, P. (2004). Phase-locked alpha and theta oscillations generate the P1-N1 complex and are related to memory performance. *Cognitive Brain Research*, *19*(3), 302–316. https://doi.org/10.1016/j.cogbrainres.2003.11.016

Köster, M., Finger, H., Graetz, S., Kater, M., & Gruber, T. (2018). Theta-gamma coupling binds visual perceptual features in an associative memory task. *Scientific Reports*, *8*(1), 1–9. https://doi.org/10.1038/s41598-018-35812-7

Lavielle, M. (2005). Using penalized contrasts for the change-point problem. *Signal Processing*, *85*(8), 1501–1510. https://doi.org/10.1016/j.sigpro.2005.01.012

Lehman, M., & Malmberg, K. J. (2013). A buffer model of memory encoding and temporal correlations in retrieval. *Psychological Review*, *120*(1), 155–189. https://doi.org/10.1037/A0030851

Lisman, J. E., & Jensen, O. (2013). The θ-γ neural code. *Neuron*, *77*(6), 1002–1016. https://doi.org/10.1016/j.neuron.2013.03.007

Lisman, J., & Idiart, M. (1995). Storage of 7 +/- 2 short-term memories in oscillatory subcycles. *Science*, *267*(5203), 1512–1515. https://doi.org/10.1126/science.7878473

Marois, R., & Ivanoff, J. (2005). Capacity limits of information processing in the brain. *Trends in Cognitive Sciences*, *9*(6), 296–305. https://doi.org/10.1016/j.tics.2005.04.010

Melton, A. W. (1963). Implications of short-term memory for a general theory of memory. *Journal of Verbal Learning and Verbal Behavior*, *2*(1), 1–21. https://doi.org/10.1016/S0022-5371(63)80063-8

Murdock, B. B. (1962). The serial position effect of free recall. *Journal of Experimental Psychology*, *64*(5), 482–488. https://doi.org/10.1037/h0045106

Murre, J. M. J., & Dros, J. (2015). Replication and Analysis of Ebbinghaus' Forgetting Curve. *PLOS ONE, 10*(7), e0120644. https://doi.org/10.1371/JOURNAL.PONE.0120644

Nogueira, A. M. L., Bueno, O. F. A., Manzano, G. M., Kohn, A. F., & Pompéia, S. (2015). Late positive slow waves as markers of chunking during encoding. *Frontiers in Psychology*, *6*. https://doi.org/10.3389/fpsyg.2015.01032

Page, M. P. A., & Norris, D. (1998). The Primacy Model: A New Model of Immediate Serial Recall. *Psychological Review*, *105*(4), 761–781. https://doi.org/10.1037/0033-295X.105.4.761-781

Patterson, J. V., Pratt, H., & Starr, A. (1991). Event-related potential correlates of the serial position effect in short-term memory. *Electroencephalography and Clinical Neurophysiology*, *78*(6), 424–437. https://doi.org/10.1016/0013-4694(91)90060-H

Polich, J., & Kok, A. (1995). Cognitive and biological determinants of P300: an integrative review. *Biological Psychology*, *41*(2), 103–146. https://doi.org/10.1016/0301-0511(95)05130-9

Rinsveld, A. Van, Guillaume, M., Kohler, P. J., Schiltz, C., Gevers, W., & Content, A. (2020). The neural signature of numerosity by separating numerical and continuous magnitude extraction in visual cortex with frequency-tagged EEG. *Proceedings of the National Academy of Sciences*, *117*(11), 5726–5732. https://doi.org/10.1073/PNAS.1917849117

Saito, S., Logie, R. H., Morita, A., & Law, A. (2008). Visual and phonological similarity effects in verbal immediate serial recall: A test with kanji materials. *Journal of Memory and Language*, *59*(1), 1–17. https://doi.org/10.1016/j.jml.2008.01.004

Sederberg, P. B., Gauthier, L. V., Terushkin, V., Miller, J. F., Barnathan, J. A., & Kahana, M. J. (2006). Oscillatory correlates of the primacy effect in episodic memory. *NeuroImage*, *32*(3), 1422–1431. https://doi.org/10.1016/j.neuroimage.2006.04.223

Shiffrin, R. M., & Nosofsky, R. M. (1994). Seven plus or minus two: A commentary on capacity limitations. *Psychological Review*, *101*(2), 357–361. https://doi.org/10.1037/0033-295X.101.2.357

Solomon, E. A., Stein, J. M., Das, S., Gorniak, R., Sperling, M. R., Worrell, G., Inman, C. S., Tan, R. J., Jobst, B. C., Rizzuto, D. S., & Kahana, M. J. (2019). Dynamic Theta Networks in the Human Medial Temporal Lobe Support Episodic Memory. *Current Biology*, *29*(7). https://doi.org/10.1016/j.cub.2019.02.020

Staudigl, T., & Hanslmayr, S. (2013). Theta Oscillations at Encoding Mediate the Context-Dependent Nature of Human Episodic Memory. *Current Biology*, *23*(12), 1101–1106. https://doi.org/10.1016/J.CUB.2013.04.074

Summerfield, C., & Mangels, J. A. (2005). Coherent theta-band EEG activity predicts item-context binding during encoding. *NeuroImage*, *24*(3), 692–703. https://doi.org/10.1016/J.NEUROIMAGE.2004.09.012

Sutton, S., Braren, M., Zubin, J., & John, E. R. (1965). Evoked-potential correlates of stimulus uncertainty. *Science*, *150*(3700), 1187–1188. https://doi.org/10.1126/SCIENCE.150.3700.1187

Talmi, D., Grady, C. L., Goshen-Gottstein, Y., & Moscovitch, M. (2005). Neuroimaging the serial position curve: A test of single-store versus dual-store models. *Psychological Science*, *16*(9), 716–723. https://doi.org/10.1111/j.1467-9280.2005.01601.x

Thalmann, M., Souza, A. S., & Oberauer, K. (2019). How does chunking help working memory? *Journal of Experimental Psychology: Learning, Memory, and Cognition*, 45(1). 37–55. https://doi.org/10.1037/xlm0000578

The jamovi project (2021). jamovi (Version 1.6) [Computer Software]. Retrieved from https://www.jamovi.org

Waugh, N. C., & Norman, D. A. (1965). Primary memory. *Psychological Review*, *72*(2), 89–

104. https://doi.org/10.1037/H0021797

Weiss, S., & Rappelsberger, P. (2000). Long-range EEG synchronization during word encoding correlates with successful memory performance. *Cognitive Brain Research*, *9*(3), 299–312. https://doi.org/10.1016/S0926-6410(00)00011-2

Wickelgren, W. A. (1999). Webs, cell assemblies, and chunking in neural nets: introduction. *Canadian Journal of Experimental Psychology = Revue Canadienne de Psychologie Expérimentale*, *53*(1), 118–131. https://doi.org/10.1037/H0087304

Wilsch, A., & Obleser, J. (2016). What works in auditory working memory? A neural oscillations perspective. *Brain research*, 1640, 193-207. https://doi.org/10.1016/j.brainres.2015.10.054

Supplementary Materials: Oscillatory delta and theta frequencies differentially support multiple items encoding to optimize memory performance during the digit span task

1. Delta Power Results

Linear Mixed-Effects Models analysis was performed in R by using lmr4 R package (Bates et al., 2015) to investigate the continuous quadratic distributions of "digit position" in both 3-ds and 5-ds delta power responses.

1.1 Three Digit Span Results

For investigating the delta power distribution of all subjects in 3 digit-span conditions, we performed linear mixed effect analysis. With the models, we investigated whether the distribution of delta power values is quadratic.

Examination of the summary output for the full model indicated that there is a quadratic relationship between *averaged delta* power (averaged for all locations and hemispheres) values and digit positions (β = 1.28, SE = 0.20, t = 6.34, $p < .0001$) (Supplementary Figure 1). A likelihood-ratio test indicated that the model for investigating the quadratic relationship provided a better fit for the data, $\chi 2$ (1) = 40.16, $p < .0001$.

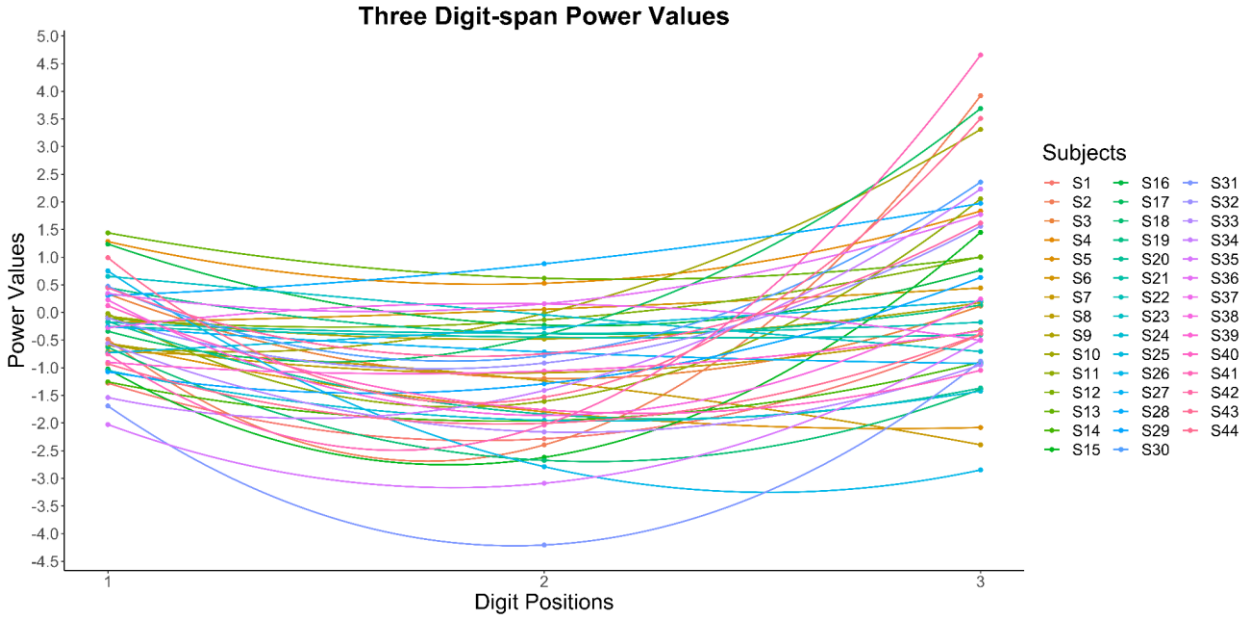

Supplementary Figure 1. Averaged delta (1-3.5 Hz) responses power value distribution across the digit positions in the 3-ds backward task for each subject.

Examination of the summary output for the full model indicated that there is a quadratic relationship between *fronto-central delta* power values and digit positions (β = 1.43, *SE* = 0.22, t = 6.48, $p < .0001$) (Supplementary Figure 2). A likelihood-ratio test indicated that the model for investigating the quadratic relationship provided a better fit for the data, $\chi 2$ (1) = 41.99, $p < .0001$.

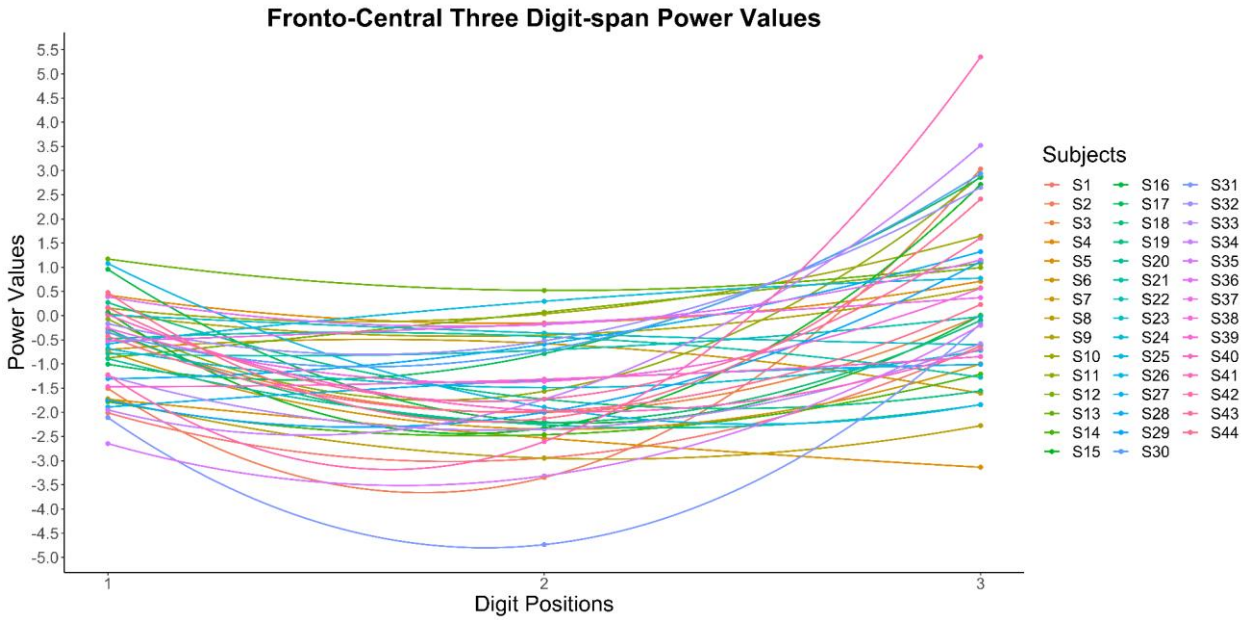

Supplementary Figure 2. Fronto-Central delta (1-3.5 Hz) responses power value distribution across the digit positions in the 3-ds backward task for each subject.

Examination of the summary output for the full model indicated that there is a quadratic relationship between *parieto-occipital delta* power values and digit positions (β = 1.12, *SE* = 0.22, t = 5.06, $p < .0001$) (Supplementary Figure 3). A likelihood-ratio test indicated that the model for investigating the quadratic relationship provided a better fit for the data, $\chi 2$ (1) = 25.56, $p < .0001$.

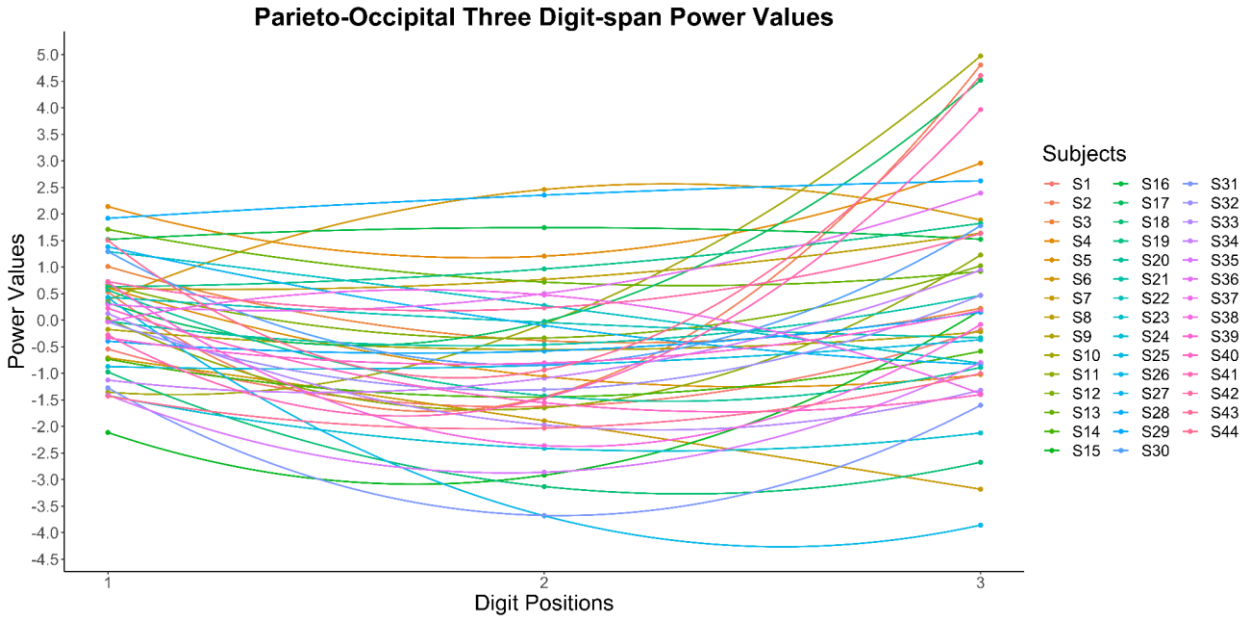

Supplementary Figure 3. Parieto-Occipital delta (1-3.5 Hz) responses power value distribution across the digit positions in the 3-ds backward task for each subject.

Examination of the summary output for the full model indicated that there is a quadratic relationship between *right fronto-central delta* power values and digit positions (β = 1.29, *SE* = 0.21, t = 6.02, $p < .0001$) (Supplementary Figure 4). A likelihood-ratio test indicated that the model for investigating the quadratic relationship provided a better fit for the data, $\chi 2$ (1) = 36.21, $p < .0001$.

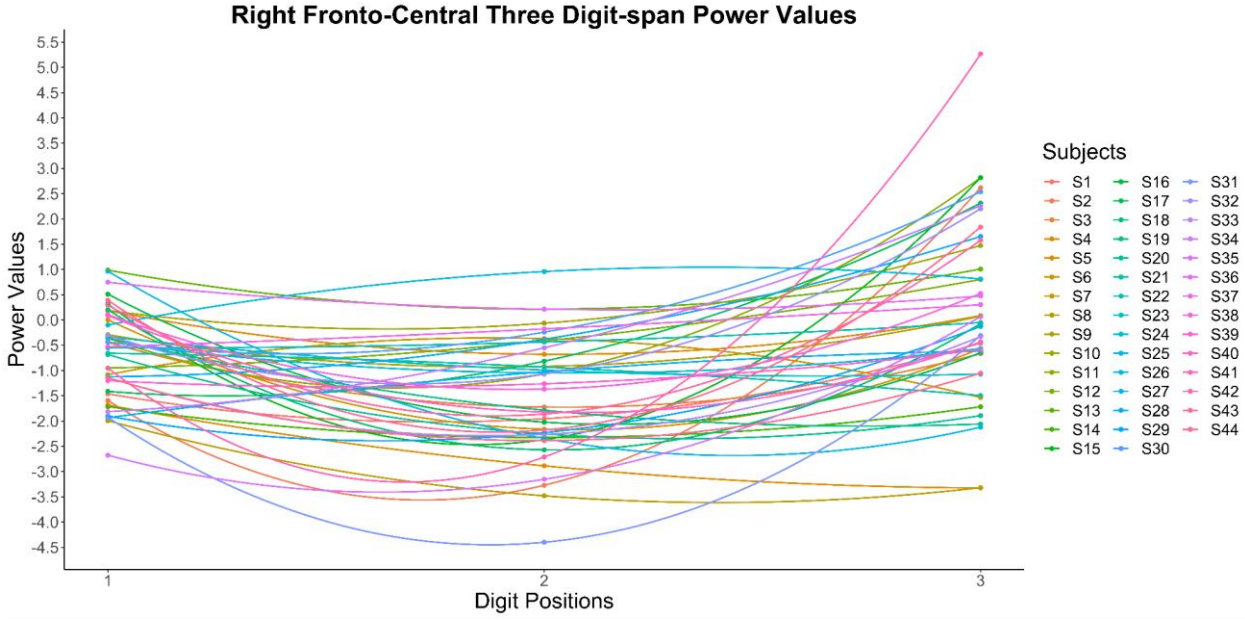

Supplementary Figure 4. Right Fronto-Central delta (1-3.5 Hz) responses power value distribution across the digit positions in the 3-ds backward task for each subject.

Examination of the summary output for the full model indicated that there is a quadratic relationship between *left fronto-central delta* power values and digit positions (β = 1.57, *SE* = 0.24, t = 6.52, $p < .0001$) (Supplementary Figure 5). A likelihood-ratio test indicated that the model for investigating the quadratic relationship provided a better fit for the data, $\chi 2$ (1) = 42.52, $p < .0001$.

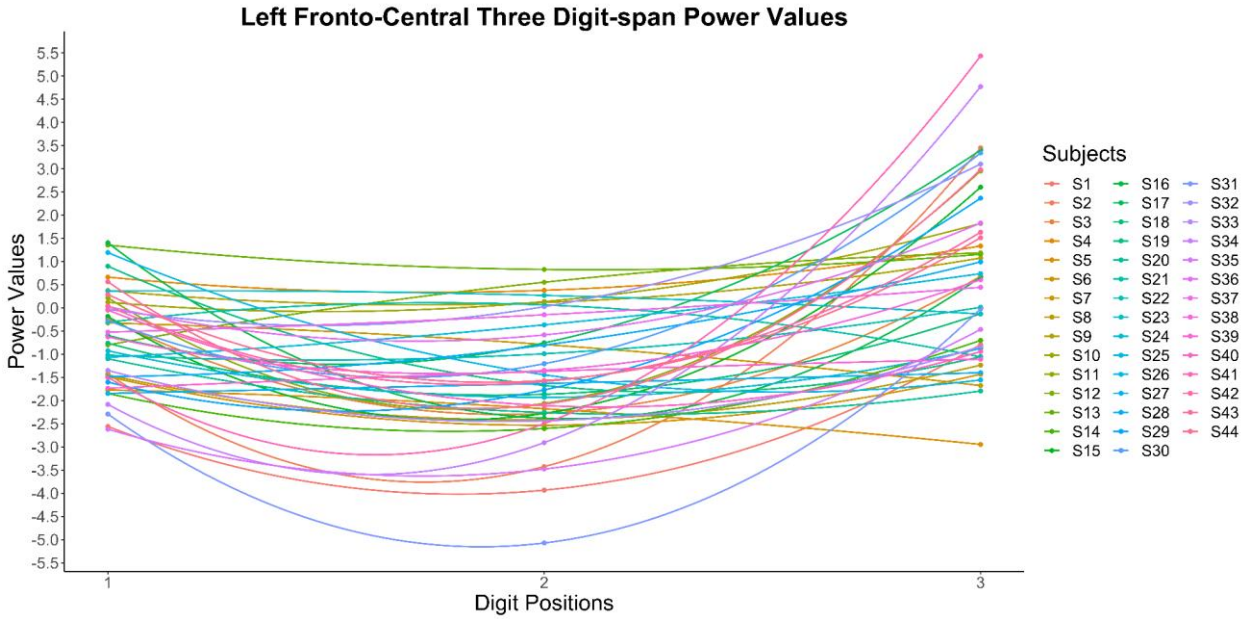

Supplementary Figure 5. Left Fronto-Central delta (1-3.5 Hz) responses power value distribution across the digit positions in the 3-ds backward task for each subject.

Examination of the summary output for the full model indicated that there is a quadratic relationship between *right parieto-occipital delta* power values and digit positions (β = 1.03, *SE* = 0.22, t = 4.67, $p < .0001$) (Supplementary Figure 6). A likelihood-ratio test indicated that the model for investigating the quadratic relationship provided a better fit for the data, $\chi 2$ (1) = 21.83, $p < .0001$.

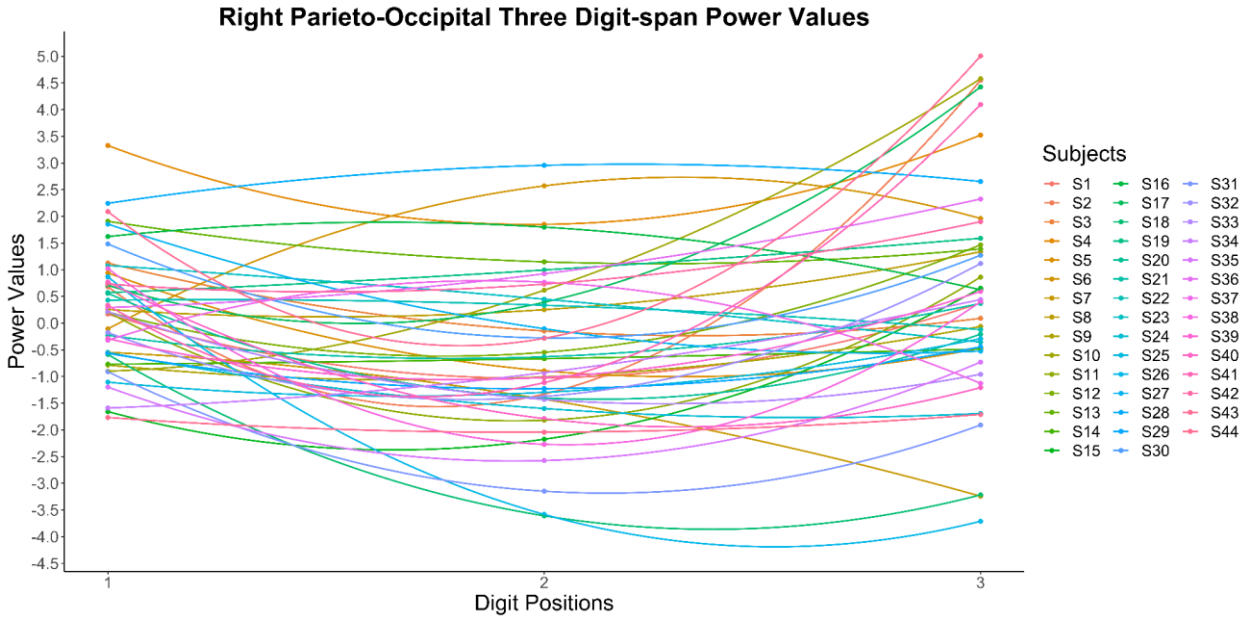

Supplementary Figure 6. Right Parieto-Occipital delta (1-3.5 Hz) responses power value distribution across the digit positions in the 3-ds backward task for each subject.

Examination of the summary output for the full model indicated that there is a quadratic relationship between *left parieto-occipital delta* power values and digit positions (β = 1.21, *SE* = 0.24, t = 5.10, $p < .0001$) (Supplementary Figure 7). A likelihood-ratio test indicated that the model for investigating the quadratic relationship provided a better fit for the data, $\chi 2$ (1) = 26.00, $p < .0001$.

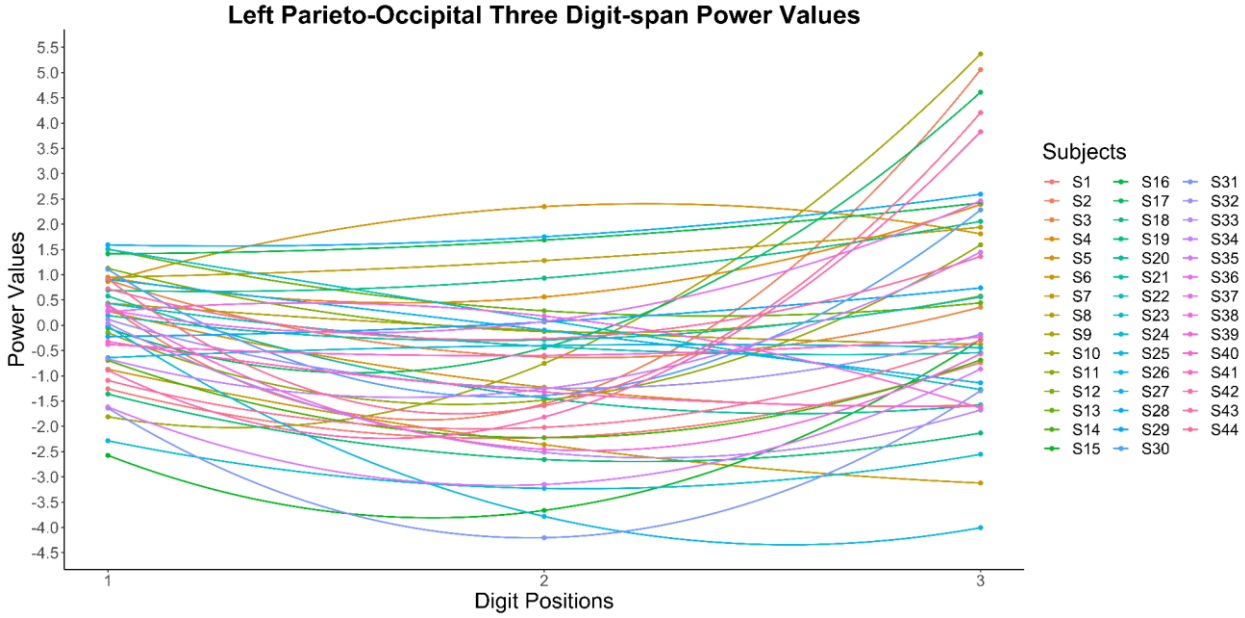

Supplementary Figure 7. Left Parieto-Occipital delta (1-3.5 Hz) responses power value distribution across the digit positions in the 3-ds backward task for each subject.

1.2 Five Digit Span Results

For investigating the delta power distribution of all subjects in 5 digit-span conditions, we performed linear mixed effect analysis. With the models, we investigated whether the distribution of delta power values is quadratic.

Examination of the summary output for the full model indicated that there is a quadratic relationship between *averaged delta* power values and digit positions (β = 0.42, *SE* = 0.05, *t* = 9.27, $p < .0001$) (Supplementary Figure 8). A likelihood-ratio test indicated that the model for investigating the quadratic relationship provided a better fit for the data, $\chi 2$ (1) = 85.95, $p < .0001$.

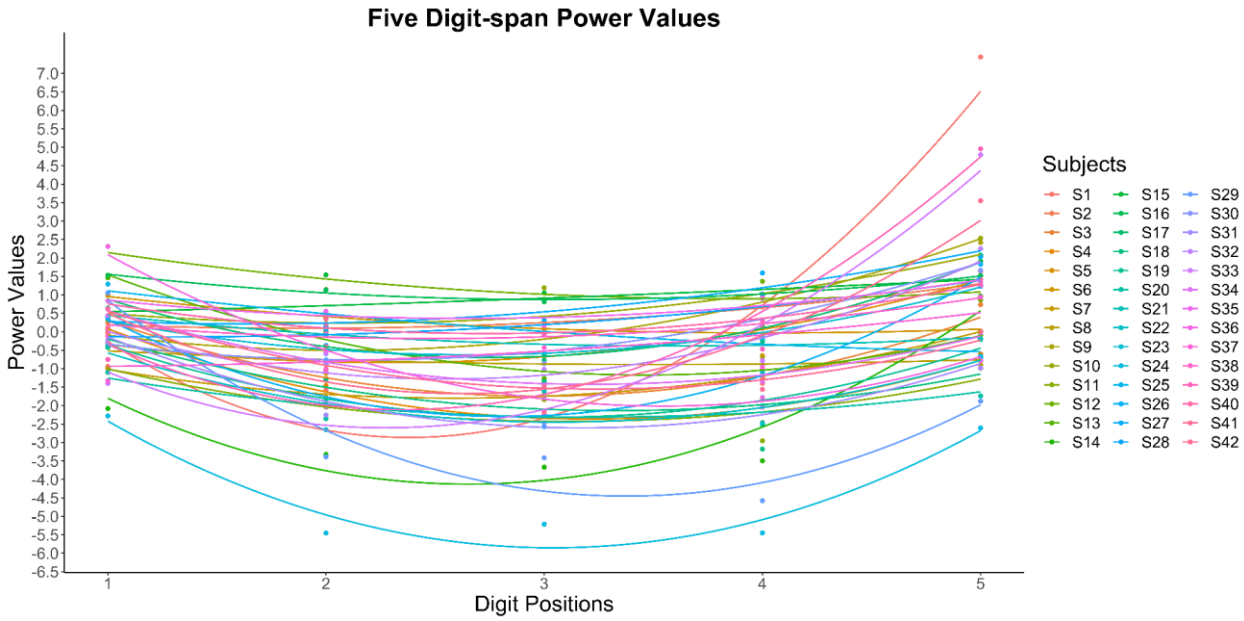

Supplementary Figure 8. Averaged delta (1-3.5 Hz) responses power value distribution across the digit positions in the 5-ds backward task for each subject.

Examination of the summary output for the full model indicated that there is a quadratic relationship between *fronto-central delta* power values and digit positions (β = 0.43, *SE* = 0.05, *t* = 8.24, $p < .0001$) (Supplementary Figure 9). A likelihood-ratio test indicated that the model for investigating the quadratic relationship provided a better fit for the data, $\chi 2$ (1) = 67.89, $p < .0001$.

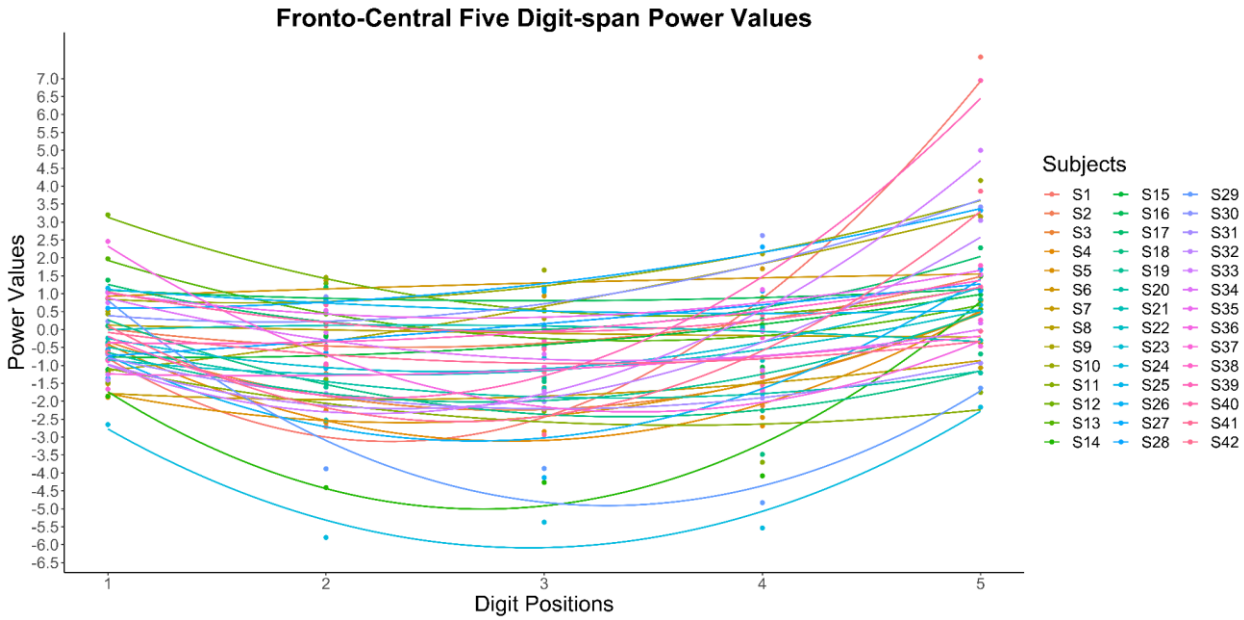

Supplementary Figure 9. Fronto-Central delta (1-3.5 Hz) responses power value distribution across the digit positions in the 5-ds backward task for each subject.

Examination of the summary output for the full model indicated that there is a quadratic relationship between *parieto-occipital delta* power values and digit positions (β = 0.40, *SE* = 0.05, t = 8.74, $p < .0001$) (Supplementary Figure 10). A likelihood-ratio test indicated that the model for investigating the quadratic relationship provided a better fit for the data, $\chi 2$ (1) = 76.45, $p < .0001$.

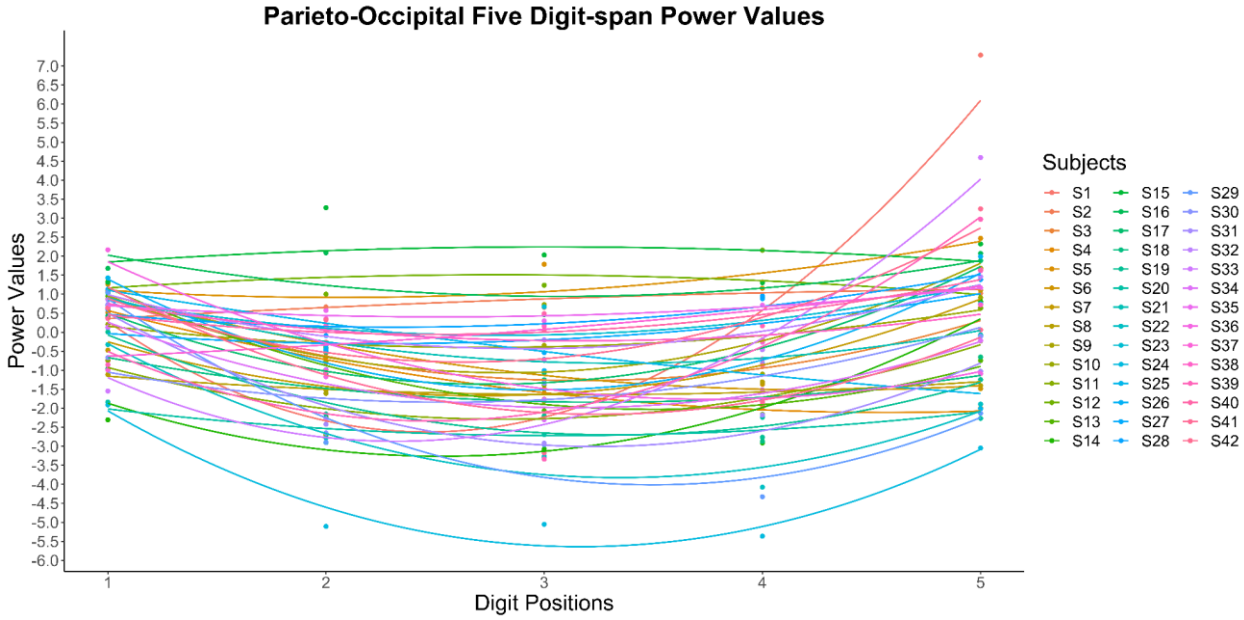

Supplementary Figure 10. Parieto-Occipital delta (1-3.5 Hz) responses power value distribution across the digit positions in the 5-ds backward task for each subject.

Examination of the summary output for the full model indicated that there is a quadratic relationship between *right fronto-central delta* power values and digit positions (β = 0.37, *SE* = 0.05, t = 7.31, $p < .0001$) (Supplementary Figure 11). A likelihood-ratio test indicated that the model for investigating the quadratic relationship provided a better fit for the data, $\chi 2$ (1) = 53.40, $p < .0001$.

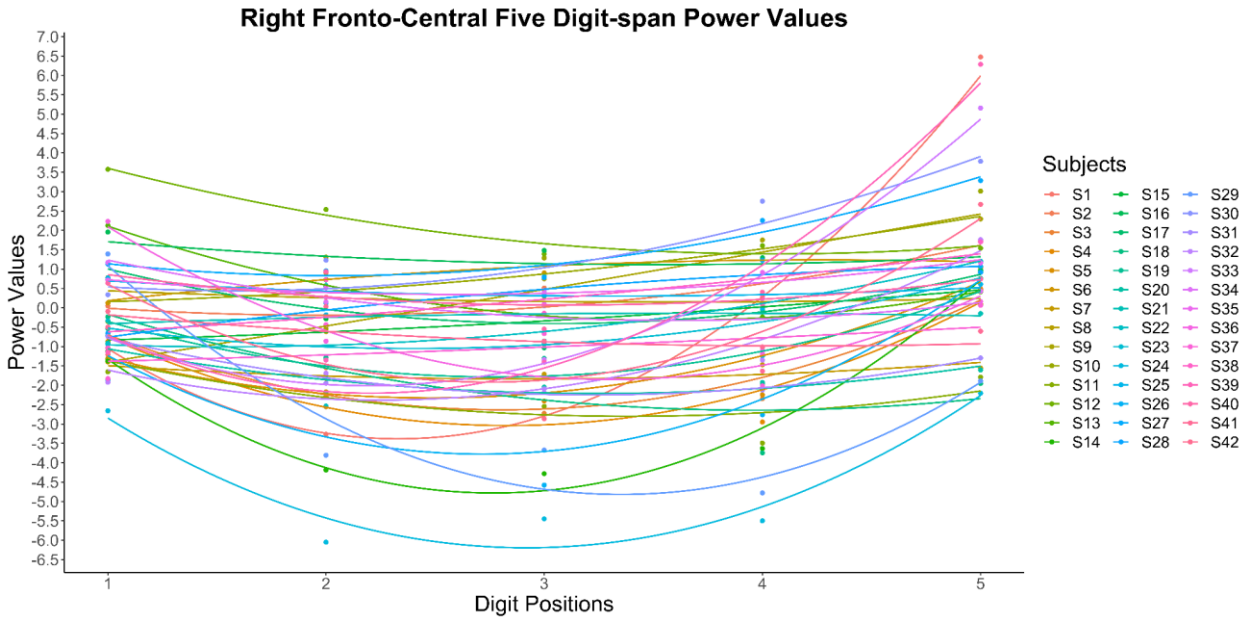

Supplementary Figure 11. Right Fronto-Central delta (1-3.5 Hz) responses power value distribution across the digit positions in the 5-ds backward task for each subject.

Examination of the summary output for the full model indicated that there is a quadratic relationship between *left fronto-central* delta power values and digit positions (β = 0.49, *SE* = 0.06, t = 8.72, $p < .0001$) (Supplementary Figure 12). A likelihood-ratio test indicated that the model for investigating the quadratic relationship provided a better fit for the data, $\chi 2$ (1) = 75.99, $p < .0001$.

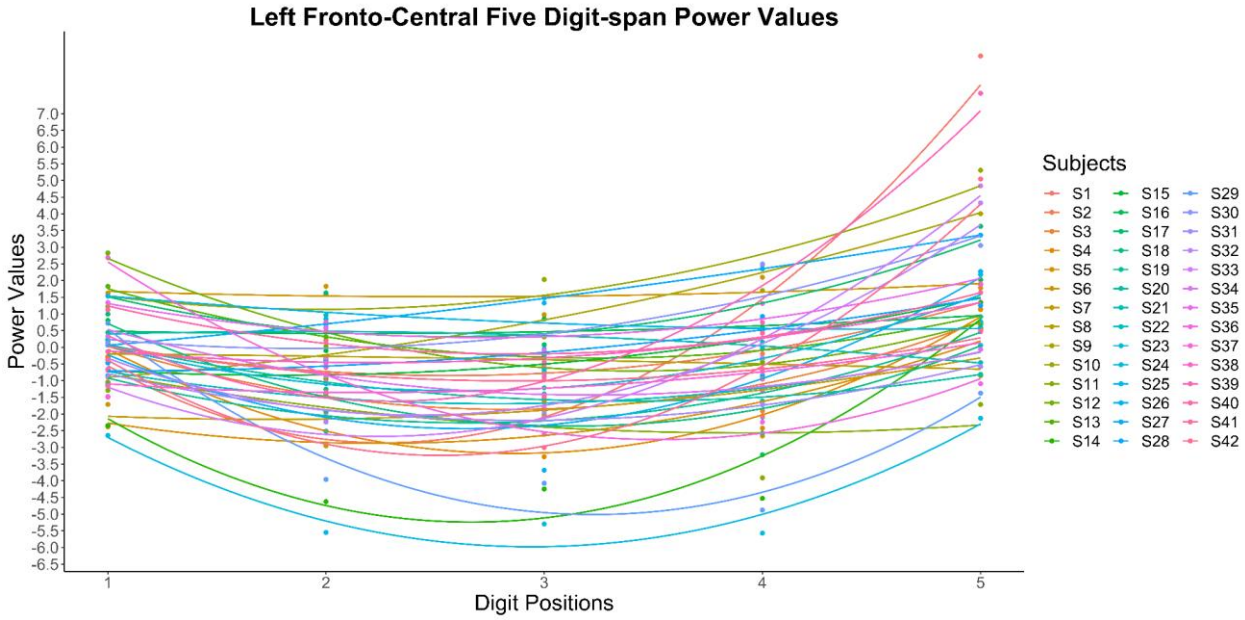

Supplementary Figure 12. Left Fronto-Central delta (1-3.5 Hz) responses power value distribution across the digit positions in the 5-ds backward task for each subject.

Examination of the summary output for the full model indicated that there is a quadratic relationship between *right parieto-occipital delta* power values and digit positions (β = 0.37, *SE* = 0.05, *t* = 7.98, $p < .0001$) (Supplementary Figure 13). A likelihood-ratio test indicated that the model for investigating the quadratic relationship provided a better fit for the data, $\chi 2$ (1) = 63.68, $p < .0001$.

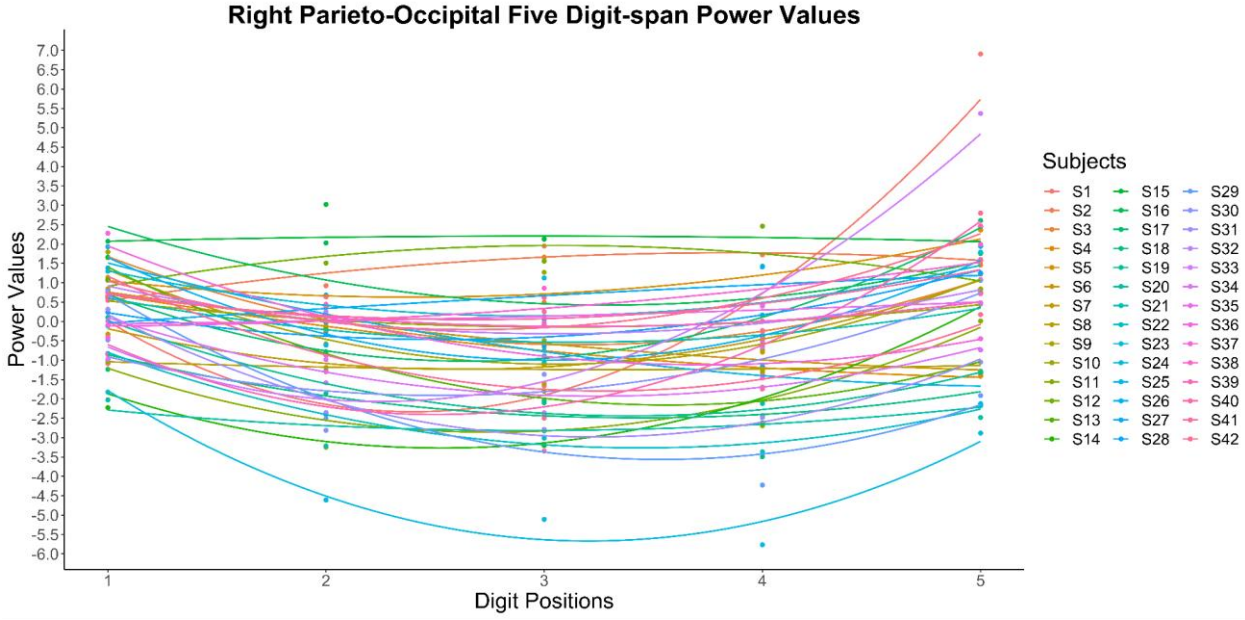

Supplementary Figure 13. Right Parieto-Occipital delta (1-3.5 Hz) responses power value distribution across the digit positions in the 5-ds backward task for each subject.

Examination of the summary output for the full model indicated that there is a quadratic relationship between *left parieto-occipital delta* power values and digit positions (β = 0.44, *SE* = 0.05, t = 8.90, $p < .0001$) (Supplementary Figure 14). A likelihood-ratio test indicated that the model for investigating the quadratic relationship provided a better fit for the data, $\chi 2$ (1) = 79.16, $p < .0001$.

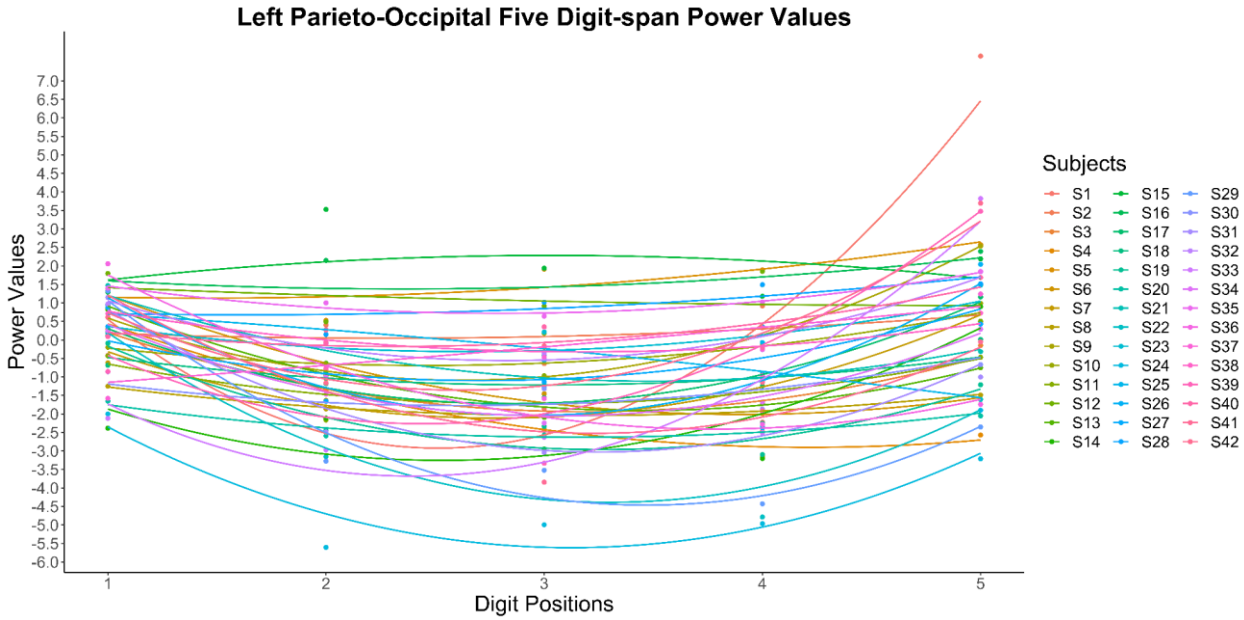

Supplementary Figure 14. Left Parieto-Occipital delta (1-3.5 Hz) responses power value distribution across the digit positions in the 5-ds backward task for each subject.

References

Bates D, Mächler M, Bolker B, Walker S (2015). “Fitting Linear Mixed-Effects Models Using lme4.” Journal of Statistical Software, 67(1), 1–48. doi:10.18637/jss.v067.i01.

Enhancing memory capacity by experimentally slowing theta frequency oscillations using combined EEG-tACS

Tuba Aktürk, Tom A. de Graaf, Bahar Güntekin, Lütfü Hanoğlu, Alexander T. Sack

Corresponding manuscript: Aktürk, T., de Graaf, T. A., Güntekin, B., Hanoğlu, L., & Sack, A. T. (2022). Enhancing memory capacity by experimentally slowing theta frequency oscillations using combined EEG-tACS. Scientific reports, 12(1), 1-14. https://doi.org/10.1038/s41598-022-18665-z

Abstract

The coupling of gamma oscillation (~40+ Hz) amplitude to the phase of ongoing theta (~6 Hz) oscillations has been proposed to be directly relevant for memory performance. Current theories suggest that memory capacity scales with number of gamma cycles that can be fitted into the preferred phase of a theta cycle. Following this logic, transcranial alternating current stimulation (tACS) may be used to adjust theta cycles (increasing/decreasing theta frequency) to decrease or increase memory performance during stimulation. Here, we used individualized EEG-informed theta tACS to i) experimentally "slow down" individual theta frequency (ITF), ii) evaluate cognitive *after effects* on a battery of memory and learning tasks, and iii) link the cognitive performance changes to tACS-induced effects on theta-band oscillations as measured by post EEG. We found frequency- and task-specific tACS after effects demonstrating a specific enhancement in memory capacity. This tACS-induced cognitive enhancement was specific to the visual memory task performed immediately after tACS offset, and specific to the ITF-1Hz (slowing) stimulation condition and thus following a protocol specifically designed to slow down theta frequency to enhance memory capacity. Follow-up correlation analyses in this group linked the enhanced memory performance to increased left frontal-parietal theta-band connectivity. Interestingly, resting-state theta power immediately after tACS offset revealed a theta power increase not for the ITF-1Hz group, but only for the ITF group where the tACS frequency was 'optimal' for entrainment. These results suggest that while individually calibrated tACS at peak frequency maximally modulates resting-state oscillatory power, tACS stimulation slightly below this optimal peak theta frequency is better suited to enhance memory capacity performance. Importantly, our results further suggest that such cognitive enhancement effects can last beyond the period of stimulation and are linked to increased network connectivity, opening the door towards more clinical and applied relevance of using tACS in cognitive rehabilitation and/or neurocognitive enhancement.

Key Words: memory encoding, learning, tACS, individual theta frequency, EEG, Brain oscillation

1. Introduction

Brain oscillations contribute to different cognitive functions according to different characteristics of the oscillatory signal itself (amplitude, frequency, phase, coherence, power, cross-frequency couplings) as well as their specific topologies[1–4]. For instance, theta oscillations (~ 6 Hz) measured from fronto-parietal network regions have been associated with memory processes. It is known that cortical theta oscillations reflect communication with the hippocampus, which has been proposed as a driver of memory functions[4–13]. Gamma oscillations (~40+ Hz), depending on the cortical region, have also been associated with several (sub) cognitive processes that contribute to memory, such as conscious perception[14], selective processing of information[15,16], and active preservation of memory content[17].

Memory processes are part of the foundation of human cognition, being closely related to other core functions such as attention or executive control[18–20]. Therefore, it is unsurprising to see interaction of theta oscillatory characteristics with oscillations in other frequency bands, associated with other high-level cognitive functions. In this sense, theta-gamma coupling appears to be an ideal mechanism for linking representations or operations from different neurocognitive sources into a cohesive mental representation. Lisman and Idiart (1995), for example, proposed that the number of gamma cycles that fit into one theta cycle determines the limits of memory capacity[21,22]. In other words, a longer theta cycle implies higher memory capacity by accommodating more gamma cycles. Several correlational studies provided evidence to support this suggested relationship between memory performance and theta-gamma cross-frequency coupling[7,8,21–25].

Transcranial alternating current stimulation (tACS) has been used to modulate and entrain endogenous brain oscillations, allowing causal investigation of hypothesized roles of oscillations in human cognition. TACS delivers low-intensity electrical current between two electrodes, alternating in polarity at predetermined frequencies associated with targeted cognitive processes. Since a slow oscillating theta can accommodate more cycles of fast gamma, previous studies evaluated whether tACS can be used to increase memory capacity by decreasing the frequency of theta[26–28].

In most of these studies, tACS was used to entrain brain oscillations and enhance/modulate cognitive functions *during* the tACS application (i.e., online effects). Although interesting and promising, such online tACS effects are potentially confounded by sensory entrainment effects (indirect entrainment) caused by the sensation of the tACS application on the skin. In contrast,

a successful demonstration of modulatory effects beyond the period of stimulation (*after effects*) would not only be less confounded by these sensory stimulation side effects, but also paramount for gaining new insights into the oscillatory processes underpinning possible tACS-induced changes. Finally, offline tACS memory effects would also open the door towards a more clinical and applied relevance of using tACS in cognitive rehabilitation and/or neurocognitive enhancement.

The oscillations entrained during rhythmic stimulation have been shown to be sustained for only a few oscillatory cycles after the stimulation is turned off[29–32]. These so-called "entrainment-echoes" are short-lived post-rhythmic resonances that are locked to the entraining field[31]. Most of the offline effects on neural oscillations, on the other hand, can be seen over considerably longer time periods (e.g., [33–35]) and may thus not represent the continuance of online entrainment[32]. There are some promising studies on the after effects of "theta" tACS on both brain activity and behavior[36–39], although most of these studies did not show direct evidence of the behavioral after effect of theta tACS[26,40]. These findings regarding the after effects of tACS are mostly discussed in the context of the "spike timing dependent plasticity" mechanism[32]. Theta-frequency after effects on EEG-correlates of tACS-induced behavioral changes are less established in the literature, except for some inconsistent evidence (for review, see Veniero et al., 2015). Therefore, investigating the behavioral and physiological after effects of theta tACS as presented here can also be considered important to start better understanding possible plasticity-related changes of tACS that go beyond the short-lived entrainment effects.

In the current study, we assessed potential after effects of a tACS protocol aiming to "slow down" the individual theta frequency (ITF), with the goal of enhancing memory performance capacity beyond the period of stimulation. Furthermore, we evaluated after effects on resting state EEG and memory task related EEG, with a focus on theta-band oscillations. To this end, we administered tACS at 1 Hz slower than ITF (ITF-1), to experimentally slow down theta frequency and thereby enhance memory performance[26,28,41]. In a between-subject design, participants were randomly assigned to three stimulation conditions: i) tACS at ITF (no frequency change, but stimulating at individually calibrated optimal peak frequency for most effective theta entrainment), ii) tACS at ITF-1 (for slowing down ITF, changing frequency but no or less entrainment), and SHAM tACS (no frequency change, no entrainment). TACS was applied over left frontoparietal network, as part of the neural networks underlying memory and learning functions[6,27,39,42–45].

In light of the inconsistent behavioral findings of studies using theta tACS across different task types[32,40,46,47], it is often assumed that the theta tACS effect may vary for different tasks and/or task modalities. Therefore, here, different tasks/tests (e.g., both visual and auditory memory tasks) were applied as an exploratory approach to test task-specificity of tACS after effects on behavioral performance. Based on our a priori hypothesis-driven main research question, tACS-related behavioral after effects were expected especially in memory-related tasks and for the ITF-1 group, due to the here induced "theta slowing" as compared to the ITF and sham conditions. In contrast, and in accordance with previous findings, EEG power spectrum changes were expected exclusively in the ITF group (entrainment) since only in this condition, tACS was administered at the individual peak frequency (e.g. [33,35,48,49]). Since we aimed to study after effects of theta tACS, stimulation was applied at rest (for 20 minutes), and memory/learning tasks and EEG measurements were obtained both before and after the tACS interventions.

2. Results

In this between-subject tACS-EEG experiment, different groups of participants performed various memory tasks before and after individual theta-frequency tACS (ITF), slowed theta tACS (ITF-1 Hz), and SHAM tACS. Here, after an analysis of participants' reports on side effects and blinding success, we evaluate tACS after effects on memory performance and on EEG (time)-frequency activity respectively.

2.1 Blinding Success and Side Effects

Before the experiment, participants were asked to rate their belief in the general effectiveness of the tACS application (between 0 to 10); greater values indicate greater belief in the efficacy of tACS. The belief in the effect of the tACS application didn't differ across groups ($X^2(2)=1.45$, $p=0.484$) (ITF group: mean/sd: 5.20 ± 1.42, ITF-1 group: mean/sd: 5.62 ± 1.63, Sham group: mean/sd: 5.40 ± 2.41). At the end of their session, participants were asked whether they thought the tACS they received was real or placebo. There were descriptive, but not statistically significant, differences between groups ($X^2(4, N=46)=6.33$, $p=0.176$) (ITF group: Real/Placebo/Don't Know: 9/1/5, ITF-1 group: Real/Placebo/Don't Know: 10/0/6, Sham group: Real/Placebo/Don't Know: 6/4/5). After the (sham) tACS session, participants filled out a side effect questionnaire including 7 items (e.g., itching, fatigue, etc.) (See Methods). Scores were summed to yield an individual 'side effect score' that did significantly differ between

groups ($X^2(2)=7.02$, p=0.030) (ITF group: mean/sd: 5.73 ± 2.83, ITF-1 group: mean/sd: 4.56 ± 2.90, Sham group: mean/sd: 2.80 ± 2.43), with fewer side effects reported by the sham group as compared to the ITF group (pairwise comparison, p=0.033). In sum, all groups were essentially identical in a priori 'belief' about tACS efficacy, not significantly different in their estimations of real vs placebo treatment, somewhat different in terms of reported side effects. We conclude that, in combination with the fact that we only measured behavior and EEG before and after tACS and not during tACS, these results raise no concerns about the validity of our between-subject model.

2.2 Behavioral Results

Participants performed two memory tasks before, and again after, their 20-minute (sham) tACS protocol; a visual memory task (VM), an auditory memory task (AM) during the EEG recording. The tasks were always administered in that order, which means that the visual memory task was always started approximately 6 minutes after offset of tACS (after the resting state EEG), and the auditory memory task always started approximately 14 minutes after offset of tACS (after the visual memory task). We performed mixed analyses of variance (ANOVA) with factors time (pre-tACS and post-tACS) and group (ITF tACS, ITF-1Hz tACS, sham tACS) separately per task.

The time*group interaction was significant for the VM task (F(2, 43) = 4.54, p = 0.016, and η_p^2 = 0.174) but not for the AM task (F(2, 43) = 1.26, p = 0.293, and η_p^2 = 0.055). Follow-up pairwise comparisons showed that specifically in the ITF-1 group, where the protocol aimed to slow the theta frequency in order to enhance memory capacity, VM performance was enhanced after tACS (mean VM score pre-tACS: 16.1 ± 3.9 and post-tACS: 17.9 ± 3.4,) (uncorrected t(43.0)=-2.306, p=0.026, d=0.48), with no significant change in the ITF (pre-tACS: 15.4 ± 3.9, post-tACS: 13.9 ± 5.6) (uncorrected t(43.0)= 1.871, p=0.068, d=-0.31) and Sham (pre-tACS: 15.1 ± 4.5, post-tACS: 14.7 ± 4.7) (uncorrected t(43.0)=0.510, p=0.612, d=-0.09) groups (Figure 1a). See Supplementary Table 1 for means and SDs of all task scores across the groups and times (pre-post).

Participants were evaluated with the neuropsychological battery before, and after, their tACS protocol; an Oktem verbal memory test (OVMT), Rey complex figure test (RCFT), digit span test, and letter-number sequencing test. We performed mixed ANOVA with factors time (pre-tACS and post-tACS) and group (ITF tACS, ITF-1Hz tACS, sham tACS) separately per

outcome measure. In the analyses of the OVMT, one subject was removed since the subject was familiar with the test.

The time*group interaction was significant only for the OVMT learning sub-score (F(2, 42) = 5.02, p = 0.011, and η_p^2 = 0.193). Post hoc pairwise comparisons show that ITF-1 group had an increased learning score after the tACS (mean learning score of the pre-tACS: 124 ± 12.2 and post-tACS: 133 ± 9.79) (uncorrected t(42.0)=-3.343, p=0.002, d=0.81) while there was no change in the ITF (mean learning score of the pre-tACS: 125 ± 11.8 and post-tACS: 126 ± 10.9) (uncorrected t(42.0)=-0.099, p=0.922, d=0.09) and Sham (mean learning score of the pre-tACS: 129 ± 9.65 and post-tACS: 127 ± 12.2) (uncorrected t(42.0)=-3.343, p=0.313, d=-0.18) groups (Figure 1b). Short-term memory (F(2, 42) = 0.76, p = 0.472, and η_p^2 = 0.032) and long-term memory (F(2, 42) = 2.92, p = 0.065, and η_p^2 = 0.122) sub-scores of the OVMT were not different between tACS groups. There were no time*group interactions for the other measures: short-term memory (F(2, 43) = 0.63, p = 0.539, and η_p^2 = 0.028) or long-term memory (F(2, 43) = 0.79, p = 0.458, and η_p^2 = 0.036) sub-scores of the RCFT, or digit span forward (F(2, 43) = 0.55, p = 0.581, and η_p^2 = 0.025) and letter-number sequencing (F(2, 43) = 0.212, p = 0.626, and η_p^2 = 0.022) tests. See Supplementary Table 2 for means and SDs of all test scores across the groups and times (pre-post).

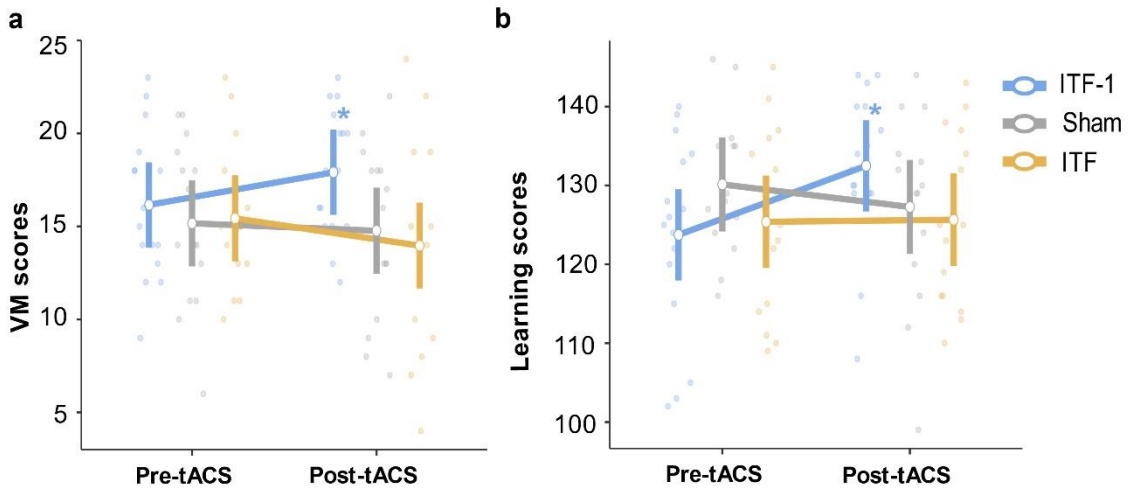

Figure 1. The significant behavioral results. a The mean values of the VM scores at pre- and post-tACS across the groups. The time*group interaction was significant (p = 0.016). The ITF-1 group had an increased VM score after the tACS. **b** The mean values of the Learning scores

at pre- and post-tACS across the groups. The time*group interaction was significant (p = 0.011). ITF-1 group had an increased learning score after the tACS. See Supplementary Fig. 1 for all behavioral time*group interaction graphs. VM: visual memory, tACS: transcranial alternating current stimulation, ITF: individual theta frequency. The vertical bars denote 0.95 confidence intervals. Dots represent the observed scores. Asterisks indicate line reflects a significant change over time.

2.3 EEG Results

We measured EEG at rest, before tACS and immediately following tACS, as well as during the various behavioral tasks. Of those, we here focused on and report EEG time-frequency activity in the theta range during the visual and auditory memory tasks that immediately followed the tACS and subsequent resting state EEG.

2.3.1 Resting EEG

In the analyses, we only used the 3-minutes eyes-open resting EEG recording since we anticipated less obscured theta activation by strong alpha activation. We performed Fast Fourier Transform to create power spectra that allowed us to extract 1) peak frequency in the theta range, and 2) power in a theta window +/- 1.5 Hz around that individual stimulation frequency.

Please, see supplementary material for the results of the first set ANOVAs which were included location and hemispheres as the within-subjects factors.

In a second ANOVA, more focused set of statistical analyses, we removed location and hemisphere factors to analyze specifically the left frontocentral EEG around the site of tACS stimulation. Here, four outlier subjects (see Methods) were removed (two from sham, one from the ITF, and one from the ITF-1 group). Now the ANOVA revealed that resting-state theta-band power values increased from pre-tACS to post-tACS (main effect of 'time': $F(1, 39) = 7.74$, $p = 0.008$, and $\eta_p^2 = 0.166$), and that this effect depended on group (time*group interaction: $F(2, 39) = 4.62$, $p = 0.016$, and $\eta_p^2 = 0.192$). Follow-up pairwise comparisons showed that specifically the ITF group had increased theta power after tACS ($p<0.001$) while we saw no tACS ('time') effects for the other groups (for ITF-1 $p=0.816$, for sham $p=0.288$) (Figure 2a). There were no aftereffects of tACS on the maximum peak frequency (time*group interaction: $F(2, 43) = 1.38$, $p = 0.263$, and $\eta_p^2 = 0.06$). It is interesting that, when it comes to finding a local increase in resting state theta power, this was specifically (and highly significantly) obtained in the group where tACS explicitly targeted the individual peak frequency. At the same time, note in Figure 2a the substantial inter-individual variability.

We performed resting coherence analysis over the FFT in the theta frequency range between F3 and P3 electrodes where we positioned the tACS electrodes. We again employed a mixed time (pre-tACS, post-tACS) by group (ITF, ITF-1, Sham) ANOVA, removing two outlier participants (one from the ITF and one from the ITF-1 group). While this analysis revealed a strong main effect of time ($F(1, 41) = 17.59$, $p = 0.0001$, and $\eta_p^2 = 0.300$), with higher resting theta coherence after tACS, there was no interaction with group ($F(2, 41) = 1.13$, $p = 0.333$, and $\eta_p^2 = 0.052$).

2.3.2 Event-Related EEG

We used complex Morlet Wavelet Transform (WT) to extract event-related theta band (4-7 Hz) activity in the time-frequency domain, time-locked to presentation of visual/auditory items in the visual/auditory memory tasks.

As in the resting EEG, the results of the first set of ANOVAs which include location and hemispheres as within-subjects factors were presented in the supplementary material of the current paper.

In the second set of statistical analyses, we removed factors location and hemisphere and focused on left frontocentral EEG, around the site of tACS stimulation. The auditory task ANOVA revealed no after effects of tACS on event-related theta power (time*group interaction: $F(2, 29) = 0.25$, $p = 0.781$, and $\eta_p^2 = 0.017$). However, in the analogous ANOVA on event-related theta-band power during the visual memory task, where we reported a behavioral time*group interaction, we found a significant time*group interaction ($F(2, 35) = 5.32$, $p = 0.01$, and $\eta_p^2 = 0.233$). Follow-up pairwise comparisons showed that both tACS groups had decreased event-related theta power after theta-frequency tACS (for ITF-1; $p=0.045$, for ITF; $p=0.011$), not observed in the sham group ($p=0.145$) (Figure 2b-c).

The event-related power-based connectivity analysis in the time-frequency domain used in the current study measures similarity between F3 and P3 electrodes where tACS stimulation electrodes were placed on. The Phase Locking Value (PLV) used in the current study is a phase-based connectivity metric in the time-frequency domain, and it indicates phase-lag consistency of specified channels (F3 and P3). We performed mixed-design ANOVAs with factors of time (pre-tACS and post-tACS), item encoding (remembered, forgotten), and group (ITF tACS, ITF-1 Hz tACS, sham tACS).

In the statistical analyses of event-related power-based connectivity, two outlier subjects were removed (one subject from the VM task and one from the AM task). There were no significant after effects of tACS on VM (time*group interaction: $F(2, 34) = 1.17$, $p = 0.322$, and $\eta_p^2 = 0.065$) and AM (time*group interaction: $F(2, 28) = 0.075$, $p = 0.928$, and $\eta_p^2 = 0.005$) tasks.

In the statistical analyses of PLV, no significant after effects of tACS on VM (time*group interaction: $F(2, 35) = 2.19$, $p = 0.127$, and $\eta_p^2 = 0.111$) or AM (time*group interaction: $F(2, 29) = 0.308$, $p = 0.738$, and $\eta_p^2 = 0.021$) tasks were shown.

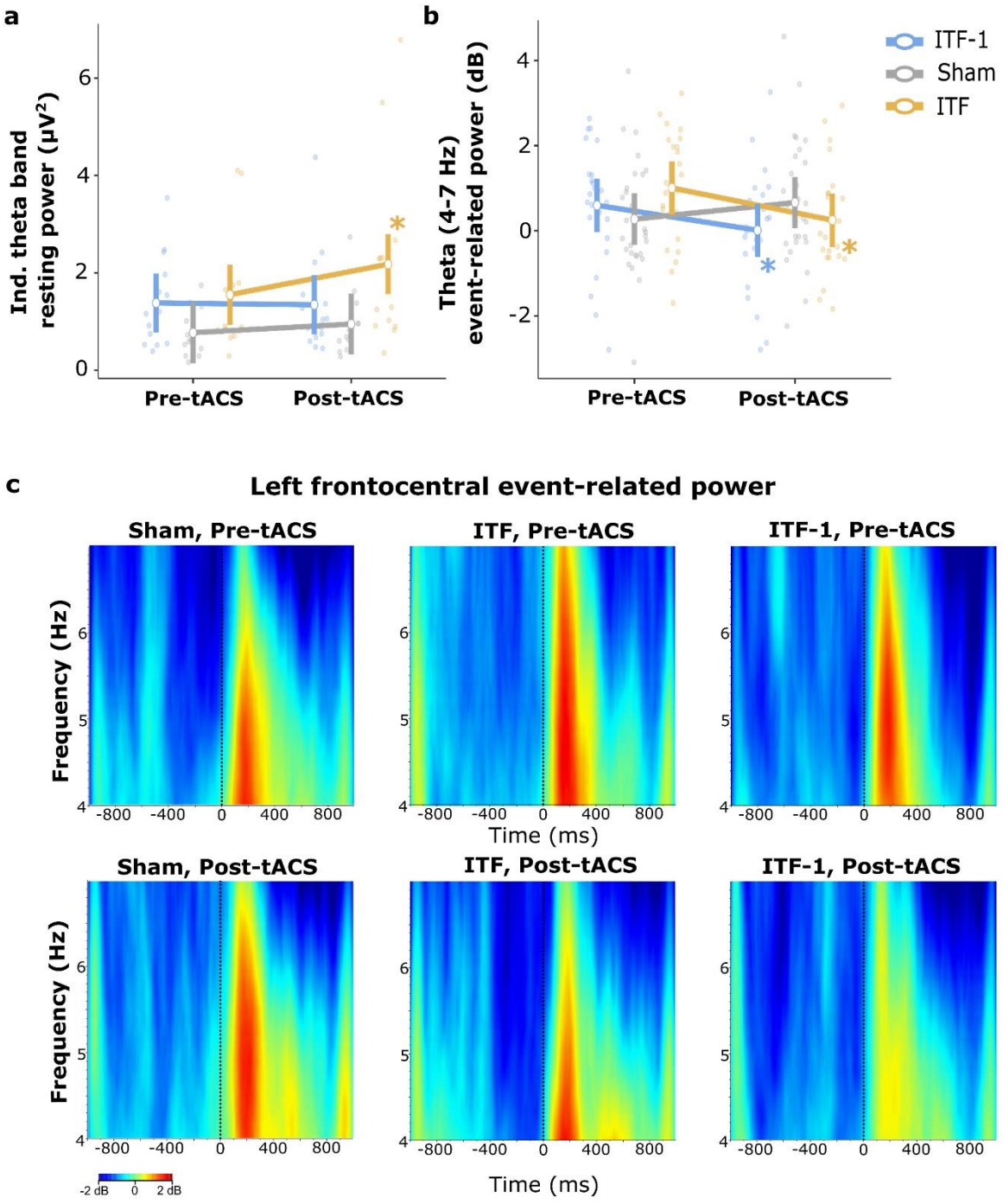

Figure 2. The significant results of the after effect of the tACS on EEG data. a The time*group interaction was significant (p = 0.016): ITF group had increased resting theta power after tACS while there were no tACS effects on the other groups. See Supplementary Fig. 2 for additional representation. **b** The time*group interaction was significant (p = 0.01) for VM task.

The tACS groups had decreased event-related theta power after tACS while no such difference was observed in the sham group. See Supplementary Fig. 3 for additional representation. **c** The grand average figures of event-related power analysis (4-7 Hz) in time-frequency domain in response to items in the VM task. The left frontocentral area was presented for each group in the figure. tACS groups had decreased event-related theta power after theta-frequency tACS (for ITF-1 p=0.045, for ITF p=0.011), not observed in the sham group (p=0.145). The X-axis represents time, and the Y-axis represents frequency; the point at which the stimulus arrives is marked as a zero point on the X-axis. tACS: transcranial alternating current stimulation, ITF: individual theta frequency. The vertical bars denote 0.95 confidence intervals. Dots represent the observed scores. Asterisks indicate line reflects a significant change over time.

2.4 EEG-Behavior Correlations

Since we observed tACS after effects specifically in the visual memory (VM) task both in behavioral and EEG data, we focused on the VM task in statistical follow-up analyses of EEG-behavior interactions. Here, we removed the same outliers as in the EEG analyses above.

There were no significant correlations between changes in behavioral data (difference scores for learning and VM: post tACS minus pre tACS values) and changes in left frontocentral event-related theta power, resting-state theta power, or resting state maximum peak frequency analysis (difference score: post tACS minus pre tACS values) for any group ($p>0.05$ for all). However, there was a positive correlation between tACS effects on left frontal-parietal *resting-state* theta coherence, and tACS effects on the VM task, specifically in the ITF-1 group ($r=0.544$, $p=0.036$; ITF group $p=0.559$; Sham group $p=0.303$) (Figure 3a). There was no such correlation with learning difference scores ($p>0.05$ for all). Instead, we observed a strong negative correlation between tACS effects on left frontal-parietal *event-related* power-based theta connectivity and learning scores ($r=-0.614$, $p=0.011$) (Figure 3b), again specifically for the ITF-1 group (ITF group $p=0.667$; Sham group $p=0.431$). This time, no such correlation with VM scores. Finally, there was also a negative correlation in specifically the ITF-1 group between tACS effects on specifically learning scores (not VM) and left frontal-parietal PLV (ITF-1 group $r=-0.539$, $p=0.031$; ITF group $p=0.897$; Sham group $p=0.737$) (Figure 3c).

In sum, in the search for EEG-correlates of tACS induced behavioral changes (after effects), coherence measures (between left frontal and left parietal electrodes) were found significant in the current dataset. Future studies might further explore these correlations between tACS effects

on visual memory scores and on resting-state theta coherence, as well as tACS effects on learning scores in relation to event-related coherence (power-based and PLV). We consider these results exploratory, to be interpreted only with caution, given the number of statistical tests and lack of corresponding correction of statistical threshold.

Additionally, to control whether pre-tACS EEG activity affected the after effect of the tACS on behavior, ANCOVAs for repeated measures were performed for the VM and total learning scores, separately, with the between-subjects factor of the group (ITF, ITF-1, Sham), within-subjects factors of time (pre-tACS, post-tACS), and the "pre-tACS EEG data" as the covariate. As the "pre-tACS EEG data", the same EEG measures used in the correlation analysis were employed as covariates in the ANCOVAs, however, not the difference scores as in the correlations, but the pre-tACS EEG values. These covariates were: left frontocentral theta values of the event-related power, resting power, resting maximum peak frequency, F3-P3 theta connectivity values of the event-related power- and phase-based connectivity, as well as resting coherence. In the ANCOVA results, the behavioral after effect of the tACS on the learning and VM scores in the ITF-1 group remained significant, and the results showed pre-tACS EEG data have no influence on the behavioral after effect of tACS. See supplementary material for detailed results of ANCOVAs.

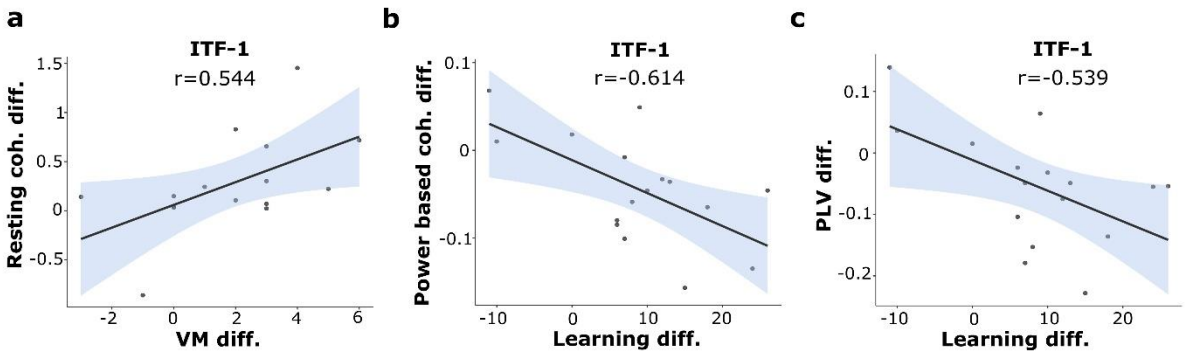

Figure 3. The scatter plots of the significant results in the EEG-behavior correlation analyses. a The subjects in the ITF-1 group with increased left frontal-parietal resting theta coherence after the tACS had the higher scores in the VM task (r=0.544, p=0.036) **b** The subjects in the ITF-1 group with decreased left frontal-parietal event-related power-based theta connectivity after the tACS had the higher learning scores (r=-0.614, p=0.011) **c** The subjects

in the ITF-1 group with decreased left frontal-parietal PLV after the tACS had the higher learning scores (r=-0.539, p=0.031). Other groups' scatter plots were presented in the Supplementary Fig. 4. Coh.: coherence, Diff.: difference score, PLV: phase locking value, VM: visual memory, ITF: individual theta frequency. The shaded area denotes the standard error. Dots represent the observed scores.

3. Discussion

Here we investigated cognitive and neurophysiological after effects of individualized EEG-informed theta-frequency tACS designed to either entrain or slow down the natural endogenous theta oscillations in order to enhance memory capacity. The goal was to experimentally 'slow' theta oscillations by tACS stimulation at 1 Hertz below the individual peak theta frequency (ITF-1, slowing), and to compare results to peak-theta-frequency tACS (ITF, entraining) and to placebo tACS (SHAM). Theoretical models[21,22] predict that lower-frequency theta oscillations would enable enhanced memory performance through the facilitation of more gamma-range activity at a preferred theta phase. Simply put, these theoretical concepts suggest that at slower theta frequencies more gamma cycles can be fitted into the preferred phase of a theta cycle, a form of theta-gamma cross frequency coupling that has been linked to memory capacity. Here, we tested for the first time whether i) such effects can be observed after the offset of tACS (i.e., in the form of after-effects), ii) such effects are indeed frequency specific, and iii) what neurophysiological correlates can be associated to such tACS induced cognitive enhancements. TACS was applied at rest, since we were explicitly interested in after-effects with EEG being recorded before and after tACS during resting-state, visual memory (VM), and auditory memory (AM) task execution (during the encoding phase). Additionally, before and after tACS, a battery of behavioral and neuropsychological tests was used to evaluate attention, learning, and memory performances.

The main results of the study can be summarized in three domains: behavior, EEG-brain oscillations, and behavior-EEG interactions. In terms of *behavior*, we found after-effects of tACS on memory performance in terms of enhanced visual memory capacity and higher learning scores in specifically the ITF-1 (slowing) condition. In the *EEG* data, we observed decreased frontocentral event-related theta power in both tACS conditions for the VM task, while frontocentral resting state theta power increased in the ITF group following the tACS session. *Behavior-EEG interaction* analyses suggested that subjects in the ITF-1 group with

enhanced left fronto-parietal resting theta connectivity after tACS performed better on the VM task, while subjects in the ITF-1 group with decreased event-related phase-and power-based connectivity had better learning scores.

Only a few previous studies have focused on theta tACS after effects on behavior[9,26,36–40]. Consistent with most of the previous theta tACS studies, we found a positive after effect of theta tACS on task performance. Furthermore, our study showed that behavioral after effects of theta tACS were prominent in the group that received slower theta stimulation than their theta peak frequency as we hypothesized based on the theta-gamma coupling theory[21,22]. Contrary to our findings, Polania et al. (2012) showed that fronto–parietal theta tACS delivered at anti-phase (180-degree phase difference) decreased working memory performance[46]. However, in contrast to Polania et al., we here focused on after effects (synaptic plasticity) of tACS rather than online effects (entrainment). In this sense, our approach is more similar to Pahor and Jaušovec (2018) who also investigated the effect of offline theta (and gamma) tACS on memory performance and on resting EEG and task-related EEG. Interestingly, Pahor and Jaušovec also reported no significant behavioral after effect of theta fronto-parietal tACS except for a tendency to a small improvement in certain working memory task types[40]. In contrast to all of this previous tACS memory research, however, we here employed an episodic memory task, and we aimed to slow down an individually calibrated theta frequency. This may be particularly relevant when comparing our results to previous findings considering that our behavioral positive after effect exclusively occurred in the ITF-1 tACS stimulation group. Wolinski et al. (2018) studied the online effects of theta tACS as well and showed increased working memory performance with 4 Hz tACS, and decreased performance in the 7 Hz tACS, both as compared to sham tACS. In the current study, even after tACS offset, we observed better behavioral performance in the slowing theta tACS group for VM and learning. Given a large number of behavior and EEG measures in this study, we should consider these findings encouraging but also in need of future replication. At the same time, the VM task was the first task applied immediately after the tACS session, making it the most likely to reveal behavioral tACS after-effects if after-effects were short-lived. Moreover, as expected based on the underlying theoretical models according to which memory capacity can be increased by lengthening theta cycles (i.e., decreasing theta frequency), we found memory improvement specifically and exclusively in the ITF-1 Hz group. On the other hand, a positive effect was seen also in "learning" scores, which were obtained from the applied neuropsychological battery that was administered quite some time after tACS offset. Intervening tasks, including

the auditory memory task (applied during the EEG recording) and other neuropsychological tests (digit span-forward, letter-number sequencing test, Rey complex figure) did not show any tACS effects.

The most consistent finding in previous EEG studies of tACS after effects is an increased amplitude in resting state EEG in the stimulation frequency range[32–35,40,50–52]. In accordance with these previous studies, we here also found increased fronto-central power in the targeted frequency range. Intriguingly, this tACs-induced frequency-specific entrainment effects was only observed in the ITF group, i.e., in the condition where tACS was applied based on the individual theta peak frequency. When applying tACS at ITF-1 (slowing), in contrast led to no significant increases in theta power and thus no entrainment effects. At first glance, this might seem in conflict with the cognitive after-effects we seclusively observed for the ITF-1 condition with the reported memory enhancement and associated EEG effects being induced specifically by tACS at 1 Hz slower than ITF. However, as explicitly hypothesized, this is what we expected as tACS consistently has shown to have the most pronounced effect on the EEG power spectrum when it is administered at the individual peak frequency (see also [33,35,48,49]), not when tACS is administered at a flanking frequency deviating from individual peak. In contrast, when it comes to the aim of enhancing memory performance, based on a very different mechanism related to theta-gamma coupling, we should in contrast expect cognitive enhancement in memory capacity specifically in the ITF-1 condition where tACS is designed to shift, i.e., slow, individual theta frequency, but not to affect theta power.

Several studies have shown that tACS applied to change the frequency of oscillations could have an impact on cognitive functions such as working memory and perception[26,28,53]. Vosskuhl et al. (2015) applied tACS at a frequency below ITF and stated that a frequency shift in post-tACS EEG data was not to be expected due to the disappearance of the behavioral after effect immediately following tACS offset; although a frequency shift was not directly assessed in their study. Here, we also did not find a significant "peak frequency" change, despite the revealed behavioral after effects of tACS at ITF-1. This could mean that 1) our behavioral results were false positives, 2) our EEG peak frequency results were false negatives (e.g., underpowered analysis), or 3) the behavioral effects do not require a change in peak frequency. We propose the latter option as our data also indicate that the behavioral after effects arise from a different mechanism than hypothesized, as reflected in the here observed changes in frontoparietal coherence at ITF-1 tACS.

Our EEG results revealed interesting differences between resting-state and task-state (event-related) after effects. We observed increased fronto-central resting theta power in specifically the ITF group as discussed above, but decreased event-related fronto-central theta power in both conditions, tACS at ITF and at ITF-1. Several studies showed that frontal theta increases with increased task demand[54–56]. Therefore, decreased event-related frontal theta after tACS might indicate that tACS at either ITF or ITF-1 showed the same effect, i.e., higher memory performance with lower effort, especially in the ITF-1 group. The observed decreased event-related theta responses for the VM task, not for the AM task, are consistent with this idea of changes in cognitive demand, since behavioral effects of tACS were also observed specifically in the VM task.

A similar opposite pattern between resting-state and event-related data was also observed in coherence analyses when correlating the EEG effects with the behavioral data. Subjects in the ITF-1 group who showed increased resting-state left frontal-parietal theta connectivity after tACS also showed higher scores in the VM task. On the other hand, subjects in the ITF-1 group with decreased event-related phase- and power-based connectivity after tACS showed higher learning scores. This negative correlation seems counter intuitive. However, Berger et al. (2019) showed that dynamic regulation of task difficulty is adjusted through fronto-parietal interaction indicating easier tasks induce fronto-parietal de-coupling between theta and gamma oscillations. In this context, this negative correlation in event-related connectivity may be due to the change in the perceived task difficulty in the ITF-1 tACS group. If so, we should expect an increase in behavioral scores as perceived task difficulty decreases, and this situation manifests itself with a decrease in fronto-parietal theta connectivity. The importance of connectivity between these two regions has been shown in many studies[57–59], in addition to studies showing the importance of frontal and parietal regions in memory functions. In accordance with these studies, our results showed correlations between the behavioral changes in memory tasks and theta left fronto-parietal connectivity only in the ITF-1 group, and thus again in line with our hypothesis. Even if a direct change or shift in the theta peak frequency following IFT-1 tACS was not shown as the neural mechanism underlying the enhanced memory performance in this condition, it appears that fronto-parietal theta connectivity may be a possible neural substrate of longer-lasting behavioral changes induced by optimal, in our case slowing, tÀCS at ITF-1. Reinhart & Nguyen (2019) also emphasized that tACS- enhanced memory performance may be related to neuroplastic changes in functional connectivity induced by exogenous modulation of theta-gamma characteristics. As such, this may represent a general

principle by which EEG-informed fronto-parietal tACS at individually calibrated frequency can exert lasting cognitive changes, namely by systematically stimulating slightly below (or above, depending on neural network and task demand) the individual peak frequency in each participant.

Overall, our findings suggest that left fronto-parietal tACS applied based on the individualized theta frequency may have potentially beneficial impacts on memory and theta brain oscillations, and that these effects of stimulation may continue beyond the duration of the stimulation. However, we should also acknowledge the limitations of this study. We here determined ITF based on a global (whole-head) EEG power spectrum. The literature shows no clear consensus or optimal way on how to estimate ITF: Jaušovec & Jaušovec (2014) found individual alpha frequency in the power spectrum according to the model proposed by Klimesch (1999) and calculated individual theta based on individual alpha frequency[39]. In a few papers, the theta frequency with the strongest coupling to gamma activity in the pre-stimulus state[26] or in the resting state[8,40] was accepted as the individual theta of the participant. Reinhart and Nguyen (2019) used PLV synchronization metrics between left temporal and left prefrontal areas during memory maintenance to determine ITF[9]. The enhanced power we found in the resting state specifically in the ITF tACS group is encouraging, suggesting that our approach might have successfully revealed ITF. On the other hand, it is also possible that the theta-range in the global power spectrum is predominantly driven by fronto-central theta oscillations, and that the more optimal procedure to estimate ITF is to only include activity over task-relevant areas (in this case fronto-central). Another limitation of the current study was the ceiling effect in behavioral tasks/tests. Since our participants were healthy, young-adult, and educated, they already achieved very high scores (close to the upper limit) on many of the tests, in the pre-application. Therefore, detection of actual tACS-related score changes in many of the tests may have been difficult to reveal. That is a limitation of our null findings, not our positive results.

All in all, our results provide new insights into oscillatory mechanisms underlying tACS-induced behavioral enhancements that outlast stimulation and may open the door to real-world applications of using NIBS in cognitive rehabilitation and/or neurocognitive enhancement. Reliable after effects of tACS would substantially broaden the range of applications of this technology.

4. Methods

4.1 Participants

Although no statistical methods were utilized to calculate sample sizes, our sample sizes are comparable to those published in earlier publications[33,35,52]. The study was designed as a single-blind, between-subject, randomized controlled study. A total of 46 right-handed, educated, healthy young-adult participants were included and randomly assigned to one of three groups: ITF group (N=15, 13 females, mean years of education (SD): 14.4 (± 1.76), mean age (SD): 20.87 (± 1.99)), ITF-1 group (N=16, 12 females, mean years of education (SD): 17.63 (± 2.9), mean age (SD): 27.13 (± 5.57)) or sham group (N=15, 10 females, mean years of education (SD): 17.13 (± 2.2), mean age (SD): 25.27 (± 3.41)). All participants had normal or corrected-to-normal vision and no specified hearing impairment. Participants with symptoms or history of psychiatric or neurological disorders and psychiatric or neurological medication usage were not included in the study. All participants were naive regarding the electrical stimulations, conditions, and tasks.

The study conformed to the principles of the Declaration of Helsinki. Participants provided written informed consent, and there was no compensation for participation as indicated in the written informed consent. The study was approved by the Istanbul Medipol University Ethics Committee (No: 10840098-604.01.01-E.18575).

4.2 Tasks and Design

The three groups were 1) ITF (tACS applied at individual theta frequency), 2) ITF-1 (tACS applied at ITF – 1 Hertz), or sham (placebo tACS). Each participant was measured in a single session. The procedure for each session consisted of 5 parts as can be seen in Figure 4a. First, a battery of behavioral and neuropsychological tests evaluated attention, learning, and memory processes. Second, pre-tACS EEG was recorded in 3 different sections. i) resting-state EEG was recorded for approximately 6 minutes (3 minutes eyes closed, 3 minutes eyes open), ii) EEG during a visual short term memory task (see below), iii) EEG during an auditory short term memory task. We determined individual theta frequencies (ITFs) of participants from the eyes open resting-state EEG (see "tACS" section for details). Third, we applied tACS/sham for 20 minutes. No tasks were performed during the tACS, participants were asked to relax and instructed to keep their eyes open. Fourth, we repeated the EEG recordings ('post-EEG'). And finally, fifth, we repeated the battery of behavioral and neuropsychological tests, identical to

the pre-tACS tasks/recordings, albeit with new stimuli (e.g., not repeating memory items from the early visual/auditory memory tasks). To avoid potential order effects, the pre and post versions of the performed tasks and neuropsychological battery were counterbalanced across the participants. Note that the visual memory task was the first task after tACS for all participants.

4.2.1 Behavioral and Neuropsychological Evaluation

Two subtests of the Wechsler Adult Intelligence Scale; digit span forward and letter-number sequencing tests [60], Oktem verbal memory test (OVMT) [61], and the Rey complex figure test (RCFT) [62,63] were administered. The digit span forward test is mainly used for the evaluation of verbal attention while the letter-number sequencing test measures the working memory. OVMT is a commonly used test to measure the verbal memory processes of individuals. The test offers the opportunity to evaluate many components related to verbal memory processes such as verbal short-term memory (max score: 15), long-term memory (max score: 15), and learning (max score: 150). RCFT is used to measure individuals' visual-spatial structuring skills and visual memory processes. The test consists of copying, immediate recall, and delayed recall sections (max score: 36 for all sections).

Additionally, before starting the experiment, participants were asked to rate their belief in the effect of the tACS application (between 0 to 10). Scores close to 0 indicate lower belief, while values close to 10 indicate greater belief in the efficacy of tACS. In this way we measured participants' general opinion/skepticism about tACS efficacy. After the experiment, they were asked whether they thought the tACS they had just received was real or placebo (or “do not know”). Side effects (e.g., itching) were assessed with a 7-item 4-point Likert scale side effects questionnaire. 7 items were as follows: itching, pain, burning, warmth/heat, metallic/iron taste, fatigue, alertness. Each item was rated between 1 to 4, indicating “none” to “strong”. For the statistical group comparison, scores of items were aggregated to a single ‘side effect score’ by summing each response.

4.2.2 Task Procedure

Our visual and auditory memory tasks were ‘subsequent memory paradigms’ (SMP), prepared and presented using E-prime software (Psychology Software Tools Inc., Pittsburgh, PA). The SMP is used for assessing brain activity generated during episodic learning/encoding that is associated with the later successful recall [11,64,65]. The pictures (black and white drawings) from the Boston Naming Test [66] were used as the stimuli for the visual memory task. In the visual memory task, during encoding, a selection of object images was shown. In the auditory memory

task, we presented audio recordings of items' names taken from the Oktem Verbal Memory Test (a different form relative to the neuropsychological battery), recorded in an isolated room and balanced by decibel and time using Audacity software (Audacity(R)).

In each task, the encoding phase was followed by the retrieval phase. EEG was recorded only during the encoding phase. The stimulus duration of visual images was 1 second, and as much as possible the audio stimulus durations approximated one second as well. The time between stimuli (interstimulus interval) varied randomly between 3 to 5 seconds (see Figure 4b). Per task, we presented 25 different stimuli with 3 repetitions, leading to 75 trials in total. The whole sequence of 25 items was presented and then re-randomized for each repetition, but with fixed order of items across participants (pseudo randomization). The visual stimuli were shown in full-screen mode on a 47.5 x 26.8 cm size monitor with a refresh rate of 60 Hz that was placed at a viewing distance of 90 cm. The visual angle for the stimuli measured approximately 19 degrees horizontally and 16 degrees vertically.

Before each task, participants were asked to pay attention to, and remember for later recall, the upcoming set of stimuli (encoding). Immediately after each task, participants were asked to say which items they remembered, and auditory and visual memory free-recall scores were obtained (numbers of items successfully recalled). To ensure that participants understood the tasks, a short practice preceded each memory task presenting 3 different stimuli (non-overlapping with main task stimuli) with 2 repetitions in pseudorandom order. This was only in the ‘pre-tACS’ task blocks where the tasks were introduced to participants for the first time.

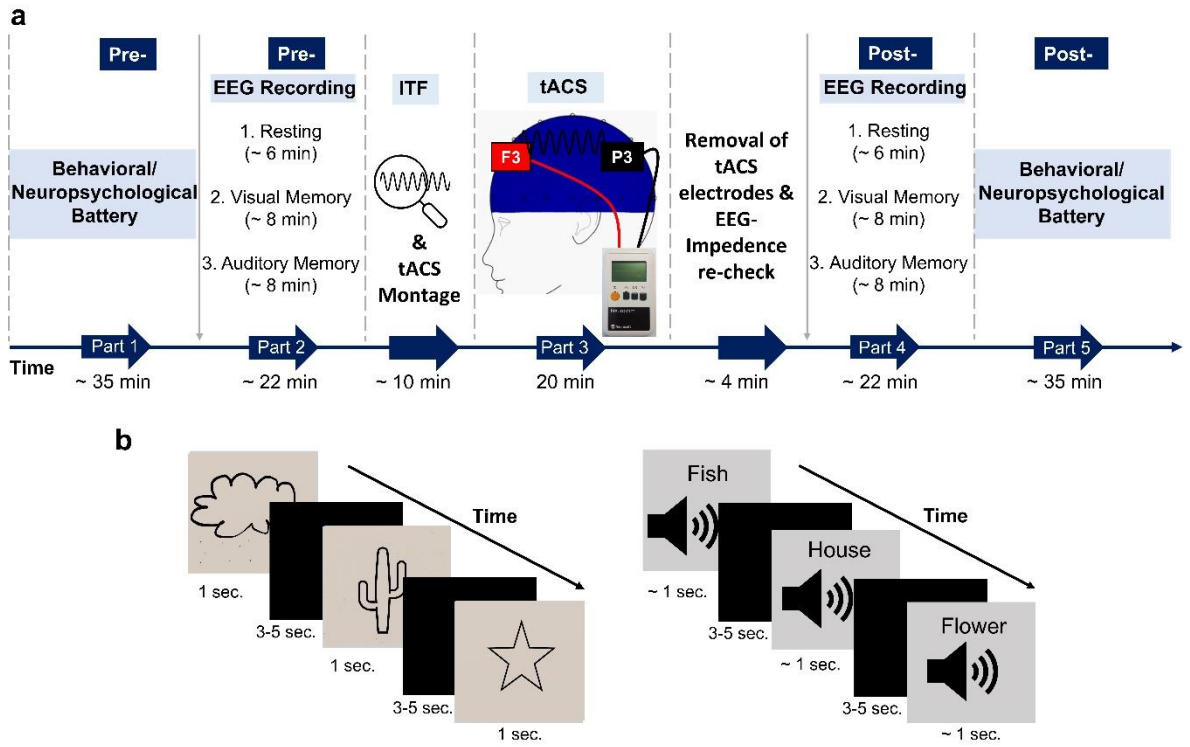

Figure 4. Experimental design and task procedure. a Design of the experiment. The "part" states each experimental phase. The horizontal dark blue arrow shows the time-course and application order of the parts with durations of them in minutes. The vertical grey arrows show the application order of the numbered measurements stated in the part. **b** The representations of the applied visual* (on the left) and auditory (on the right) memory tasks during the EEG recordings. * Given schematic images in Figure 4b are not actual exemplars from the Boston naming test set; drawn by TA as an example. tACS: transcranial alternating current stimulation, ITF: individual theta frequency, min: minute, sec.: second.

4.3 EEG Recording

EEG was recorded from Fp1, Fp2, F7 F3, Fz, F4, F8, Ft7, Fc3, Fcz, Fc4, Ft8, Cz, C3, C4, T7, T8, Tp7, Cp3, Cpz, Cp4, Tp8, P3, Pz, P4, P7, P8, O1, Oz and O2 electrodes with "BrainCap with Multitrodes" model cap (EasyCap GmbH, Germany) with 32 electrodes placements based on the international 10–20 system. Two linked electrodes (A1 + A2) were placed to the earlobes as references. The electrooculogram (EOG) was recorded at the medial upper and lateral orbital rim of the left eye. The impedance of electrodes was kept below approximately 10 kΩ. The EEG was amplified by means of a Brain Amp MR plus 32-channel DC system machine (Brain Product GmbH, Germany) with band limits of 0.01–250 Hz and digitized online with a

sampling rate of 500 Hz. The participants sat in a dimly lit and shielded room during EEG recordings.

4.4 Data Analysis

4.4.1 Resting EEG

The preprocessing steps of resting EEG data were performed in Brain Vision Analyzer. The preprocessing steps were as follows; I) 3 minutes continuous resting EEG data in eyes-open condition were filtered between 0.1 Hz to 60 Hz, II) data were segmented to 1-second length epochs, III) manual artifact rejection was performed over the segmented data.

The preprocessed (cleaned and segmented) data were imported to the FieldTrip Toolbox [67] for the resting EEG power analysis. Frequency domain power spectrum analysis of resting EEG data at the individual theta frequency range (calculated over the participants' stimulation frequencies) was performed with FFT by using Hanning tapers. To achieve the 0.1 Hz frequency resolution, epochs were zero-padded. For each participant, power was summed in a 3 Hz window around their tACS stimulation frequency (stimulation frequency +/- 1.5 Hz), and values were exported for statistical analysis. In addition to summed power values, the maximum peak frequencies in the same frequency range were also exported for use in the statistical analysis.

The theta (4-7 Hz) resting coherence analysis between the F3 and P3 electrodes where stimulation electrodes of the tACS were placed were performed over the FFT (Hanning window, zero-padded, 0.1 Hz frequency resolution) in the frequency domain using BVA. Current source density (CSD) was applied on the FFT, before calculating the coherence analysis to attenuate the possible volume conduction effect (CSD parameters: Order of Splines: 4, Maximal Degree of Legendre Polynomials: 10, Default Lambda was used: 1E-05). The mean coherence values between the F3 and P3 electrodes at the specified frequency band (4-7 Hz) were used in the statistical analysis.

4.4.2 Event-Related EEG

The preprocessing steps and further analyses of the event-related EEG data were performed in BVA. For the event-related EEG data preprocessing steps were as follows; I) EEG data were downsampled to the 256 Hz, II) data were filtered between 0.1 Hz to 60 Hz, III) independent component analysis was applied to remove eye-movement related artifacts, IV) data were segmented into 6-second epochs (3 seconds before and 3 seconds after the stimulus) for

remembered and forgotten items separately, V) manual artifact rejection was performed over the segmented data, VI) data were sub-segmented into 2-second epochs (1 second before and 1 second after the stimulus) for the time-frequency analyses.

All event-related analyses were performed for both remembered and forgotten items separately, to compare the after effect of theta tACS on associated event-related EEG activity. Event-related analyses in the time-frequency domain were completed by the Gabor normalized complex Morlet Wavelet Transform (WT) with 3 cycle wavelet widths for theta (4-7 Hz) frequency range. The determined frequency range (4-7 Hz) was subdivided into 60 bins ("frequency steps" parameter was set as "60"), scaled logarithmically (“Logarithmic Steps” option was selected). The WT was calculated in each frequency bin.

In the event-related power analysis, post-stimulus responses were normalized to the pre-stimulus baseline (-500 ms to -300 ms) and converted to decibels (dB). The event-related power was calculated by averaging single trials to which WT was applied to reach total power (evoked+induced power).

Current Source Density (CSD) processing was applied on the segmented data, before the WT to attenuate the possible volume conduction effect for the below-mentioned event-related connectivity analyses (CSD parameters: Order of Splines: 4, Maximal Degree of Legendre Polynomials: 10, Default Lambda was used: 1E-05). After CSD, WT was applied for the event-related connectivity analyses.

The event-related power-based connectivity analysis in the time-frequency domain used in the current study measures the similarity between specified channels across trials. In this method, the sources/channels with high similarity approach values of magnitude 1, whereas low similarity approaches 0. For the event-related power-based based connectivity analysis, WT output values were chosen as “Wavelet Coefficients - Complex Values [μV]”, then magnitude-squared coherence was applied. The event-related power-based connectivity analysis was calculated between F3 and P3 electrodes where the tACS stimulation electrodes were placed on.

The Phase Locking Value (PLV) used in the current study is a phase-based connectivity metric in the time-frequency domain based on the study of Lachaux et al. (1999), and it indicates the phase-lag consistency of two channels by computing the correlation between complex wavelets phases across trials. In this method, if the phase difference between the two channels is constant throughout time, one can conclude that the two channels are well synchronized, causing the

PLV to approach 1. If the phase difference is inconsistent, it can be interpreted as the two channels having low synchronization, and the PLV approaches 0. For the PLV analysis, WT output values were chosen as “Wavelet Phase - Complex Values”, then normalized correlation measures were applied, and results were rectified. The PLV was calculated between F3 and P3 electrodes where the tACS stimulation electrodes were placed on.

The sum values of the time window between 50 ms to 300 ms were divided by the total number of data points in the determined time (50-300 ms) and frequency (4-7 Hz) interval, producing average values (point mean normalization). These mean values were used in the statistical analyses of the event-related EEG.

Outliers were identified and removed from the dataset based on the interquartile range (IQR). Only extreme outliers were removed from the dataset, defined as data points below Q1-3*IQR or above Q3+3*IQR. Participant's difference score (post tACS minus pre tACS values) for both EEG measures and behavioral measures was checked for outliers separately for each measure, and if an extreme outlier was detected, they were removed from the dataset before the statistical analyses of the corresponding measure. The removed extreme outliers, if any, were reported in the results section for each analysis.

4.5 TACS

The tACS with maximum 1.5 mA (peak-to-peak) stimulation intensity was applied for 20 minutes during the rest condition, including 3 seconds fade-in and 3 seconds fade-out periods with a Neurostim device (Neurosoft, Ivanovo, Russia). If participants reported that they saw phosphenes or felt uncomfortable with 1.5 mA stimulation, the intensity of stimulation was decreased to the highest stimulation intensity that the participant did not see phosphenes and felt comfortable. Stimulation intensity did not significantly differ between the active tACS groups (ITF: min/max/mean/sd: 1.2/1.5/1.45/0.1, ITF-1: min/max/mean/sd: 0.85/1.5/1.38/0.19). In the sham group, tACS application was also 20 minutes, at the ITF frequency, but with ineffective 0.2 mA intensity, which has no influence on the neural activity but may deliver a skin sensation similar to active tACS [27,69]. Two pure water soaked-simple sponge electrodes (7x5 cm) were placed at the F3 and P3 locations to modulate the left frontoparietal network, globally, which has an important role in memory abilities [6,27,42–45]. Electrode locations were marked using an EEG cap, and stimulation electrodes were placed right under the cap to the marked area after the before-EEG recording and carefully removed

after the 20 minutes stimulation. After removing tACS electrodes, EEG electrodes were re-checked if there were electrodes with increased impedance and corrected accordingly. This procedure took ca. 4 minutes. The impedance values of the tACS electrodes were kept below 10 kOm. Please note, however, that the conductivity of the pure water-soaked tACS stimulation electrodes may have also been aided by EEG preparation processes we applied earlier. Concretely, prior to tACS, the scalp was already prepared for the pre-tACS EEG recording session with alcohol (%70) (first), followed by the application of EEG preparation gel (abrasive electroconductive gel) for placing the electrodes on the cap. This resulted in an impedance below ~<10 kOhm for all EEG electrodes. After the pre-tACS EEG recording, tACS electrodes were placed under the cap on the already cleaned and prepared scalp areas. Although here we have not experienced any difficulties considering electrode impedance or additional side effects when using pure water-soaked stimulation electrode (likely related to the above-mentioned preceding EEG preparation), saline-soaked electrode usage is currently the gold standard for sponge electrodes and we also recommend to rather use saline in any future studies. This may be relevant when aiming to replicate our behavioral tACS findings using our identical tACS procedure as we cannot rule out potential (conductivity) problems with using pure water on the sponges as we did here unless one also follows the exact same EEG preparation methods we applied during the preceding EEG measurements.

The application frequency was set to ITF, which we approximated based on a global power spectrum from eyes open resting-state EEG using Brain Vision Analyzer software (BVA) (BrainVision LLC, Morrisville, North Carolina, United States). The global power spectrum was used to determine the ITF considering that in addition to epicenters in the brain for specific cognitive functions, also a network activity spread over the scalp may have a decisive effect on the cognitive abilities[70]. The steps used to determine ITF were as follows; power spectra were obtained with Fast Fourier Transform (FFT) (Hanning window, zero-padded, 0.1 Hz frequency resolution) for each epoch over the preprocessed data (cleaned and segmented; see "Resting EEG" section for details) and then averaged. ITF was the frequency with maximum power in the theta range (4 to 7 Hz) from all EEG electrodes (excluding Fp1 and Fp2 since they are sensitive to eye movements.). The maximum theta was always chosen as ITF. The ITF did not differ between groups (ITF group: mean/sd: 5.03 ± 1.01 Hz, ITF-1 group: mean/sd: 4.97 ± 1.02 Hz, Sham group: mean/sd: 5 ± 0.99 Hz).

4.6 Statistical Analysis

Statistical analysis was performed with IBM SPSS Statistic 22 (IBM Corp., Armonk, N.Y., USA) and Jamovi (The jamovi project, 2021) software[71].

Chi-Square and Kruskal Wallis tests were used in the statistical analyses of the scores of the tACS-related questionaries.

For the statistical analysis of the behavioral data, Repeated Measures ANOVAs were performed with the 3-by-2 mixed design for each applied test/task. Time (pre-tACS, post-tACS) was the within-subject factor, and Group (ITF, ITF-1, Sham) was the between-subjects factor in the design.

For the statistical analysis of the resting EEG and Event-related power analysis, two sets of analyses were run. In the first set, "location" was added as the within-subjects factor to the ANOVA design to see the possible tACS effect on the main recorded cortical areas. Accordingly, for the resting EEG, mixed-design Repeated Measures ANOVA with the between-subjects factor of group (ITF, ITF-1, Sham) and within-subjects factors of time (pre-tACS, post-tACS), location (7 electrode clusters; Frontal, central, temporal, temporoparietal, parietal-1, parietal-2, occipital), and hemisphere (left, right) was performed. For the event-related power analysis, mixed-design Repeated Measures ANOVA with the between-subjects factor of group (ITF, ITF-1, Sham) and within-subjects factors of time (pre-tACS, post-tACS), location (7 electrode clusters; Frontal, central, temporal, temporoparietal, parietal-1, parietal-2, occipital), hemisphere (left, right), and item encoding (remembered, forgotten) was performed. After the first set of ANOVAs, the factor of location was removed, and analyses were repeated to focus only on the location around the site of tACS stimulation (left frontocentral location).

For the statistical analyses of the EEG connectivity analyses, theta frequency connectivity values between F3 and P3 electrodes were used in the ANOVAs. For the resting EEG coherence analysis, 3-by-2 mixed-design ANOVA was used. Time (pre-tACS, post-tACS) was the within-subjects factor, and group (ITF, ITF-1, Sham) was the between-subjects factor in the design. For the event-related power- and phase-based connectivity analyses, ANOVAs with the between-subjects factor of group (ITF, ITF-1, Sham) and within-subjects factors of time (pre-tACS, post-tACS) and item encoding (remembered, forgotten) were performed.

In order to reveal possible EEG-behavior interaction regarding after effect of theta tACS, correlation analysis and analysis of covariance (ANCOVA) for the repeated measures were conducted.

For the correlation analysis, bivariate linear correlation (Pearson correlation, 2-tailed) analysis was used between behavioral scores and EEG data. As behavioral data, the scores that were significantly affected by tACS according to the results of the ANOVAs were used in the correlation analysis (namely, VM and OVMT total learning scores). As the EEG data, left frontocentral theta values of the event-related power, resting power, and resting maximum peak frequency, and F3-P3 theta connectivity values of the event-related power-and phase-based connectivity, and resting coherence were used. Only the VM task was included in the correlation analysis for the event-related EEG data since there were no shown after effects of tACS on AM task. The difference scores were calculated for both behavioral and EEG data by subtracting the pre-values from the post-values (post minus pre values), and difference scores were used in the correlation analyses.

In order to check whether pre-tACS EEG activity had an effect on the after effect of the tACS on behavior, ANCOVAs for repeated measures were performed for the VM and total learning scores, separately, with the between-subjects factor of the group (ITF, ITF-1, Sham), within-subjects factors of time (pre-tACS, post-tACS), and the "pre-tACS EEG data" as the covariate. Pre-tACS EEG values of the 6 different EEG variables, which were also used in the correlation analysis, were used as the covariates. These covariates were: left frontocentral theta values of the event-related power, resting power, and resting maximum peak frequency, and F3-P3 theta connectivity values of the event-related power- and phase-based connectivity, and resting coherence.

The significance threshold was set at $p < 0.05$. Greenhouse Geisser corrected p values are reported for the ANOVA and ANCOVA analyses.

References

1. Başar, E. *Brain Function and Oscillations - Volume I: Brain Oscillations. Springer* (1998).

2. Başar, E., Schürmann, M., Demiralp, T., Başar-Eroglu, C. & Ademoglu, A. Event-related oscillations are 'real brain responses' — wavelet analysis and new strategies. *Int. J. Psychophysiol.* **39**, 91–127 (2001).

3. Başar, E. & Güntekin, B. Darwin's evolution theory, brain oscillations, and complex brain function in a new 'Cartesian view'. *Int. J. Psychophysiol.* **71**, 2–8 (2009).

4. Herrmann, C. S., Strüber, D., Helfrich, R. F. & Engel, A. K. EEG oscillations: From correlation to causality. *Int. J. Psychophysiol.* **103**, 12–21 (2016).

5. Başar, E., Başar-Eroglu, C., Karakaş, S. & Schürmann, M. Gamma, alpha, delta, and theta oscillations govern cognitive processes. *Int. J. Psychophysiol.* **39**, 241–248 (2000).

6. Sauseng, P., Griesmayr, B., Freunberger, R. & Klimesch, W. Control mechanisms in working memory: A possible function of EEG theta oscillations. *Neurosci. Biobehav. Rev.* **34**, 1015–1022 (2010).

7. Wulff, P. *et al.* Hippocampal theta rhythm and its coupling with gamma oscillations require fast inhibition onto parvalbumin-positive interneurons. *Proc. Natl. Acad. Sci. U. S. A.* **106**, 3561–3566 (2009).

8. Kamiński, J., Brzezicka, A. & Wróbel, A. Short-term memory capacity (7±2) predicted by theta to gamma cycle length ratio. *Neurobiol. Learn. Mem.* **95**, 19–23 (2011).

9. Reinhart, R. M. G. & Nguyen, J. A. Working memory revived in older adults by synchronizing rhythmic brain circuits. *Nat. Neurosci.* **22**, (2019).

10. Herweg, N. A., Solomon, E. A. & Kahana, M. J. Theta Oscillations in Human Memory. *Trends Cogn. Sci.* **24**, 208–227 (2020).

11. Fell, J. *et al.* Medial Temporal Theta/Alpha Power Enhancement Precedes Successful Memory Encoding: Evidence Based on Intracranial EEG. *J. Neurosci.* **31**, 5392–5397

(2011).

12. Dippel, G., Mückschel, M., Ziemssen, T. & Beste, C. Demands on response inhibition processes determine modulations of theta band activity in superior frontal areas and correlations with pupillometry – Implications for the norepinephrine system during inhibitory control. *Neuroimage* **157**, 575–585 (2017).

13. Mückschel, M., Dippel, G. & Beste, C. Distinguishing stimulus and response codes in theta oscillations in prefrontal areas during inhibitory control of automated responses. *Hum. Brain Mapp.* **38**, 5681–5690 (2017).

14. Engel, A. K. & Singer, W. Temporal binding and the neural correlates of sensory awareness. *Trends Cogn. Sci.* **5**, 16–25 (2001).

15. Fries, P. Neuronal Gamma-Band Synchronization as a Fundamental Process in Cortical Computation. *http://dx.doi.org/10.1146/annurev.neuro.051508.135603* **32**, 209–224 (2009).

16. Womelsdorf, T. & Fries, P. The role of neuronal synchronization in selective attention. *Curr. Opin. Neurobiol.* **17**, 154–160 (2007).

17. Herrmann, C. S., Munk, M. H. J. & Engel, A. K. Cognitive functions of gamma-band activity: memory match and utilization. *Trends Cogn. Sci.* **8**, 347–355 (2004).

18. Baddeley, A. *Human Memory: Theory and Practice*. (Psychology Press, 1997).

19. Weintraub, S. Neuropsychological Assessment of Mental State. in *Principles of Behavioral and Cognitive Neurology* (ed. Mesulam, M. M.) 121–174 (Oxford University Press, 2000).

20. Yıldırım, E. & Hanoğlu, L. Psikiyatride nöropsikolojik değerlendirme. *Psikiyatr. Güncel* (2016).

21. Lisman, J. & Idiart, M. Storage of 7 +/- 2 short-term memories in oscillatory subcycles. *Science (80-.).* **267**, 1512–1515 (1995).

22. Lisman, J. & Spruston, N. Postsynaptic depolarization requirements for LTP and LTD: a critique of spike timing-dependent plasticity. *Nat. Neurosci. 2005 87* **8**, 839–841

(2005).

23. Bayraktaroglu, Z. *et al.* Interactions of Gamma and Theta Oscillations in the Electroencephalogram (EEG) during Memory Processes. 1–4 (2006) doi:10.1109/siu.2006.1659833.

24. Demiralp, T. *et al.* Gamma amplitudes are coupled to theta phase in human EEG during visual perception. *Int. J. Psychophysiol.* **64**, 24–30 (2007).

25. Fell, J. *et al.* Human memory formation is accompanied by rhinal–hippocampal coupling and decoupling. *Nat. Neurosci. 2001 412* **4**, 1259–1264 (2001).

26. Vosskuhl, J., Huster, R. J. & Herrmann, C. S. Increase in short-term memory capacity induced by down-regulating individual theta frequency via transcranial alternating current stimulation. *Front. Hum. Neurosci.* **9**, 1–10 (2015).

27. Alekseichuk, I., Turi, Z., Amador de Lara, G., Antal, A. & Paulus, W. Spatial Working Memory in Humans Depends on Theta and High Gamma Synchronization in the Prefrontal Cortex. *Curr. Biol.* **26**, 1513–1521 (2016).

28. Wolinski, N., Cooper, N. R., Sauseng, P. & Romei, V. The speed of parietal theta frequency drives visuospatial working memory capacity. *PLoS Biol.* **16**, 1–17 (2018).

29. Marshall, L., Helgadóttir, H., Mölle, M. & Born, J. Boosting slow oscillations during sleep potentiates memory. *Nature* **444**, 610–613 (2006).

30. Reato, D. *et al.* Transcranial Electrical Stimulation Accelerates Human Sleep Homeostasis. *PLoS Comput. Biol.* **9**, (2013).

31. Hanslmayr, S., Matuschek, J. & Fellner, M. C. Entrainment of prefrontal beta oscillations induces an endogenous echo and impairs memory formation. *Curr. Biol.* **24**, 904–909 (2014).

32. Veniero, D., Vossen, A., Gross, J. & Thut, G. Lasting EEG/MEG aftereffects of rhythmic transcranial brain stimulation: Level of control over oscillatory network activity. *Frontiers in Cellular Neuroscience* vol. 9 (2015).

33. Zaehle, T., Rach, S. & Herrmann, C. S. Transcranial Alternating Current Stimulation

Enhances Individual Alpha Activity in Human EEG. *PLoS One* **5**, 1–7 (2010).

34. Vossen, A., Gross, J. & Thut, G. Alpha power increase after transcranial alternating current stimulation at alpha frequency (a-tACS) reflects plastic changes rather than entrainment. *Brain Stimul.* **8**, 499–508 (2015).

35. Kasten, F. H., Dowsett, J. & Herrmann, C. S. Sustained Aftereffect of α-tACS Lasts Up to 70 min after Stimulation. *Front. Hum. Neurosci.* **10**, (2016).

36. Hsu, W. Y., Zanto, T. P. & Gazzaley, A. Parametric effects of transcranial alternating current stimulation on multitasking performance. *Brain Stimul.* **12**, (2019).

37. Zanto, T. P. *et al.* Individual differences in neuroanatomy and neurophysiology predict effects of transcranial alternating current stimulation. *Brain Stimul. Basic, Transl. Clin. Res. Neuromodulation* **14**, 1317–1329 (2021).

38. Meiron, O. & Lavidor, M. Prefrontal oscillatory stimulation modulates access to cognitive control references in retrospective metacognitive commentary. *Clin. Neurophysiol.* **125**, 77–82 (2014).

39. Jaušovec, N. & Jaušovec, K. Increasing working memory capacity with theta transcranial alternating current stimulation (tACS). *Biol. Psychol.* **96**, 42–47 (2014).

40. Pahor, A. & Jaušovec, N. The Effects of Theta and Gamma tACS on Working Memory and Electrophysiology. *Front. Hum. Neurosci.* **11**, (2018).

41. Bender, M., Romei, V. & Sauseng, P. Slow Theta tACS of the Right Parietal Cortex Enhances Contralateral Visual Working Memory Capacity. *Brain Topogr.* **32**, (2019).

42. Meng, A. *et al.* Transcranial alternating current stimulation at theta frequency to left parietal cortex impairs associative, but not perceptual, memory encoding. *Neurobiol. Learn. Mem.* **182**, 1–20 (2021).

43. Barbey, A. K., Colom, R., Paul, E. J. & Grafman, J. Architecture of fluid intelligence and working memory revealed by lesion mapping. *Brain Struct. Funct. 2013 2192* **219**, 485–494 (2013).

44. Cabeza, R. & Nyberg, L. Neural bases of learning and memory: functional

neuroimaging evidence. *Curr. Opin. Neurol.* **13**, 415–421 (2000).

45. Klimesch, W., Freunberger, R., Sauseng, P. & Gruber, W. A short review of slow phase synchronization and memory: Evidence for control processes in different memory systems? *Brain Res.* **1235**, 31–44 (2008).

46. Polanía, R., Nitsche, M. A., Korman, C., Batsikadze, G. & Paulus, W. The Importance of Timing in Segregated Theta Phase-Coupling for Cognitive Performance. *Curr. Biol.* **22**, 1314–1318 (2012).

47. Jaušovec, N., Jaušovec, K. & Pahor, A. The influence of theta transcranial alternating current stimulation (tACS) on working memory storage and processing functions. *Acta Psychol. (Amst).* **146**, 1–6 (2014).

48. Kemmerer, S. K. *et al.* Frequency-specific transcranial neuromodulation of alpha power alters visuospatial attention performance. *Brain Res.* **1782**, 147834 (2022).

49. Ali, M. M., Sellers, K. K. & Frohlich, F. Transcranial Alternating Current Stimulation Modulates Large-Scale Cortical Network Activity by Network Resonance. *J. Neurosci.* **33**, 11262–11275 (2013).

50. Moliadze, V. *et al.* After-effects of 10 Hz tACS over the prefrontal cortex on phonological word decisions. *Brain Stimul.* **12**, 1464–1474 (2019).

51. Neuling, T., Rach, S. & Herrmann, C. S. Orchestrating neuronal networks: sustained after-effects of transcranial alternating current stimulation depend upon brain states. *Front. Hum. Neurosci.* **7**, 1–12 (2013).

52. Kasten, F. H. & Herrmann, C. S. Transcranial alternating current stimulation (tACS) enhances mental rotation performance during and after stimulation. *Front. Hum. Neurosci.* **11**, (2017).

53. Cecere, R., Rees, G. & Romei, V. Individual Differences in Alpha Frequency Drive Crossmodal Illusory Perception. *Curr. Biol.* **25**, 231–235 (2015).

54. McFerren, A., Riddle, J., Walker, C., Buse, J. & Frohlich, F. Causal role of frontal-midline theta in cognitive effort: a pilot study. (2021).

55. Meltzer, J. A. *et al.* Effects of Working Memory Load on Oscillatory Power in Human Intracranial EEG. *Cereb. Cortex* **18**, 1843–1855 (2008).

56. Jensen, O. & Tesche, C. D. Frontal theta activity in humans increases with memory load in a working memory task. *Eur. J. Neurosci.* **15**, 1395–1399 (2002).

57. Babiloni, C. *et al.* Human cortical rhythms during visual delayed choice reaction time tasks: A high-resolution EEG study on normal aging. *Behav. Brain Res.* **153**, 261–271 (2004).

58. Babiloni, C. *et al.* Functional frontoparietal connectivity during short-term memory as revealed by high-resolution EEG coherence analysis. *Behav. Neurosci.* **118**, 687–697 (2004).

59. Berger, B. *et al.* Dynamic regulation of interregional cortical communication by slow brain oscillations during working memory. *Nat. Commun.* **10**, 1–11 (2019).

60. Wechsler, D. Wechsler adult intelligence scale. *Arch. Clin. Neuropsychol.* (1995).

61. Tanör, Ö. Öktem sözel bellek süreçleri testi.(Öktem-SBST) el kitabı. (2011).

62. Meyers, J. E. & Meyers, K. R. Rey Complex Figure Test under Four Different Administration Procedures. *Clin. Neuropsychol.* **9**, 63–67 (1995).

63. Varan, E., Tanör, Ö. & Gürvit, H. Rey Complex Figure Test and Recognition Trial (RCFT): Norm Determination Study on Turkish Adult Sample. *Turk J Neurol* **13**, 387–394 (2007).

64. Kim, H. Neural activity that predicts subsequent memory and forgetting: A meta-analysis of 74 fMRI studies. *Neuroimage* **54**, 2446–2461 (2011).

65. Long, N. M., Burke, J. F. & Kahana, M. J. Subsequent memory effect in intracranial and scalp EEG. *Neuroimage* **84**, 488–494 (2014).

66. Kaplan, E., Goodglass, H. & Weintraub, S. Boston naming test. (2001).

67. Oostenveld, R., Fries, P., Maris, E. & Schoffelen, J. M. FieldTrip: Open source software for advanced analysis of MEG, EEG, and invasive electrophysiological data. *Comput. Intell. Neurosci.* **2011**, (2011).

68. Lachaux, J.-P., Rodriguez, E., Martinerie, J. & Varela, F. J. Measuring Phase Synchrony in Brain Signals. *Hum Brain Mapp.* **8**, 194–208 (1999).

69. Antal, A. & Paulus, W. Transcranial alternating current stimulation (tACS). *Front. Hum. Neurosci.* **7**, 1–4 (2013).

70. Mesulam, M. -M. Large-scale neurocognitive networks and distributed processing for attention, language, and memory. *Ann. Neurol.* **28**, 597–613 (1990).

71. The jamovi project. jamovi (Version 1.6) [Computer Software]. Retrieved from https://www.jamovi.org. (2021).

Supplementary Materials: Enhancing memory capacity by experimentally slowing theta frequency oscillations using combined EEG-tACS

Full Model ANOVA Results:

Resting State EEG Results

In a first set of ANOVA, we included the between-subjects factor of group (ITF, ITF-1, Sham) and within-subjects factor of time (pre-tACS, post-tACS), location (7 electrode clusters; Frontal, central, temporal, temporoparietal, parietal-1, parietal-2, occipital), and hemisphere (left, right). This analysis revealed no after effects of tACS on the resting EEG power (time*group interaction: $F(2, 43) = 0.71$, $p = 0.932$, and $\eta_p^2 = 0.003$) or the maximum peak frequency (time*group interaction: $F(2, 43) = 0.02$, $p = 0.243$, and $\eta_p^2 = 0.064$) in the individualized theta frequency range (no higher-order interactions; all p's>0.05). The location effect was significant in the power analysis ($F(1.72, 73.93) = 9$, $p = 0.001$, and $\eta_p^2 = 0.174$), and the highest theta power values were observed at the frontocentral locations (pairwise comparisons: frontal vs other 5 locations $p<0.003$, central vs temporo-parietal locations $p<0.01$).

Event-Related EEG

The first set of ANOVAs included group (ITF, ITF-1, Sham), time (pre-tACS, post-tACS), location (7 electrode clusters; Frontal, central, temporal, temporoparietal, parietal-1, parietal-2, occipital), hemisphere (left, right), and now additionally item encoding success (remembered, forgotten, post-hoc labeled based on later (un)successful recall). Despite the complexity of this 5-factor model, the ANOVA revealed several interesting effects.

In the auditory memory task ANOVA, there were no after effects of tACS on event-related power for the AM task in the theta band (time*group interaction: $F(2, 29) = 0.76$, $p = 0.474$, and $\eta_p^2 = 0.05$). The location effect was significant ($F(2.6, 77) = 42.53$, $p = 0.0001$, and $\eta_p^2 = 0.595$), with the highest event-related theta power at frontocentral locations (pairwise comparisons: frontal vs. other 5 locations $p<0.007$, central vs. other 5 locations $p<0.001$). The item encoding*hemisphere*group interaction was also significant ($F(2, 29) = 4.9$, $p = 0.015$, and $\eta_p^2 = 0.253$). Accordingly, sham group had higher left theta power during the encoding of remembered items (pairwise comparison, $p=0.018$), with no such difference for the tACS groups (ITF-1; $p=0.350$, ITF; $p=0.440$). Since there were no other indications of any tACS after

effects on the auditory memory task, and since we were mostly interested in differences between the ITF-1 and ITF groups, we did not explore these results further.

In the ANOVA on event-related theta-band power during the visual memory task, we found a significant time*location*group interaction ($F(4.4, 76.5) = 2.63$, $p = 0.036$, and $\eta_p^2 = 0.131$). Following up: decreased event-related frontocentral theta power after tACS was observed in the tACS groups especially in the ITF group (pairwise comparisons: for ITF group, pre-tACS vs. post-tACS for frontal location p=0.014 and central location p=0.035, for ITF-1 group, pre-tACS vs. post-tACS for frontal location p=0.057 and central location p=0.014) compared to the sham group (pairwise comparisons: pre-tACS vs. post-tACS for frontal location p=0.153 and central location p=0.116). The item encoding success*location*hemisphere*group interaction was found significant ($F(13.1, 89.4) = 2.55$, $p = 0.013$, and $\eta_p^2 = 0.127$): Post hoc analyses on item encoding success conditions showed no difference for location*hemisphere*group interaction (for remembered p=0.439, for forgotten p=0.110). We did not pursue this interaction further because there were no additional signs of tACS after effects on the visual memory task. The location*hemisphere interaction was significant ($F(31, 216.8) = 5.01$, $p = 0.003$, and $\eta_p^2 = 0.125$): the highest event-related theta power values were observed at the right parieto-occipital locations (for all pairwise comparisons, $p<0.001$). Accordingly, there were significant main effects of location ($F(2.1, 72.1) = 21.94$, $p = 0.0001$, and $\eta_p^2 = 0.385$) and hemisphere ($F(1, 35) = 4.98$, $p = 0.032$, and $\eta_p^2 = 0.125$). Follow-up pairwise comparisons revealed that the parieto-occipital locations had higher theta power compared to the other locations (for all pairwise comparisons, $p<0.006$), and the right hemisphere had higher theta power compared to the left hemisphere (p=0.032).

Analysis of Covariance

The result of the ANCOVA in which maximum peak frequency of the pre-left frontocentral resting added as a covariate showed only significant covariate effect, suggesting that pre-left frontocentral resting maximum peak frequency significantly related to the after effect of the tACS on the VM scores ($F(1, 42) = 8.37$, $p = 0.006$, and $\eta_p^2 = 0.166$). There was a negative relation between the pre-resting maximum peak frequency and VM scores: The subjects with lower pre-theta frequency had a higher VM score (for pre-VM scores: r=-0.449, p=0.002, post-VM scores: r=-0.404, p=0.005) (Supplementary Fig. 5). For the remaining ANCOVAs, the behavioral after effect of the tACS on the learning and VM scores in the ITF-1 group remained significant, and the results showed pre-EEG data have no influence on the behavioral after effect of tACS.

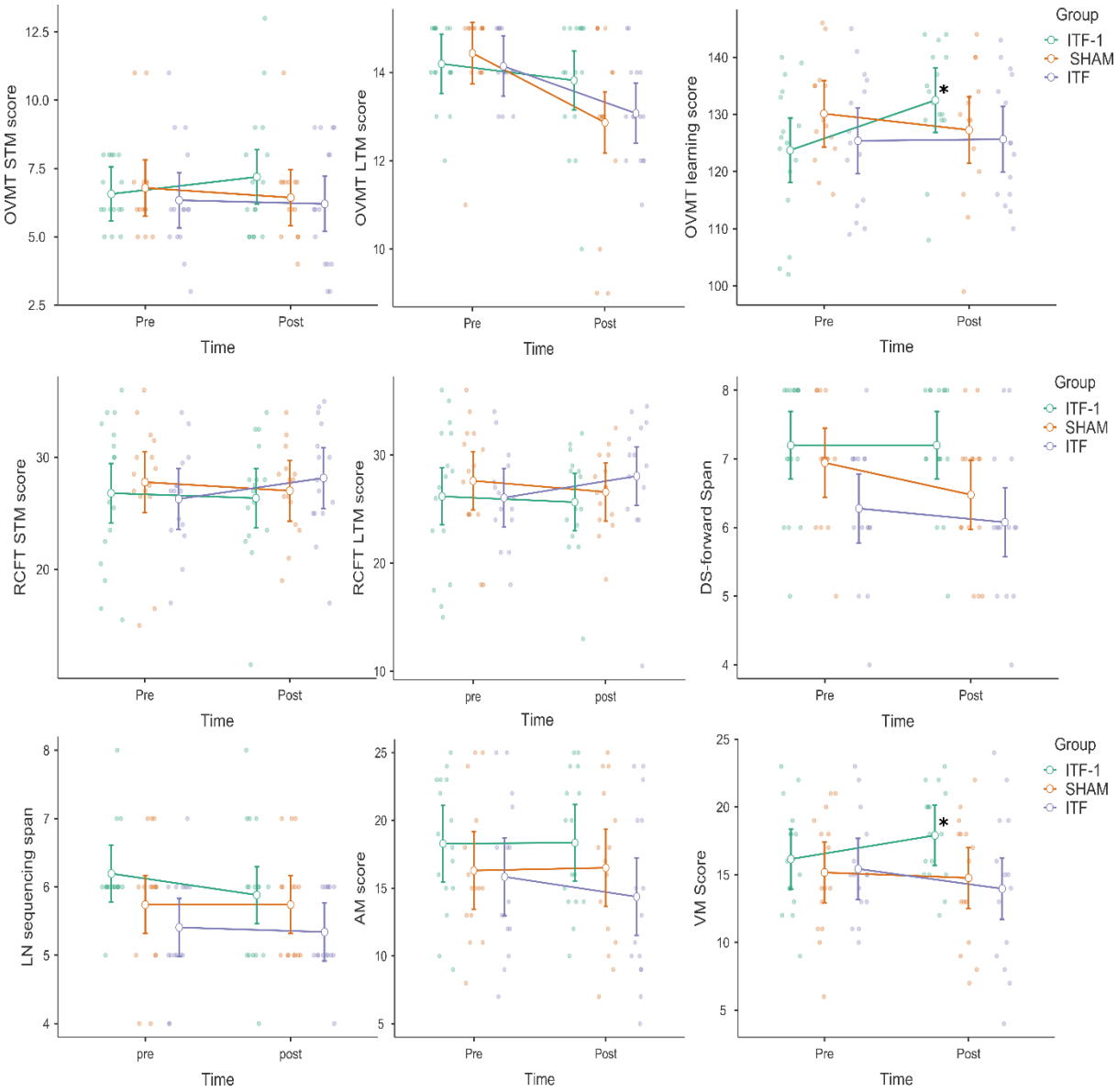

Supplementary Figure 1: The mean values of the behavioral test scores at pre- and post-tACS across the different groups. The ITF-1 group had an increased learning and VM scores after the tACS while there was no time*group interaction for other behavioral measures. OVMT: Oktem verbal memory test, STM: short-term memory, LTM: long-term memory, RCFT: Rey complex figure test, DS: digit span, LN: letter-number, AM: auditory memory, VM: visual memory, tACS: transcranial alternating current stimulation, ITF: individual theta frequency. The vertical bars denote 0.95 confidence intervals. Dots represent the observed scores. Asterisks (*) represent $p<.05$.

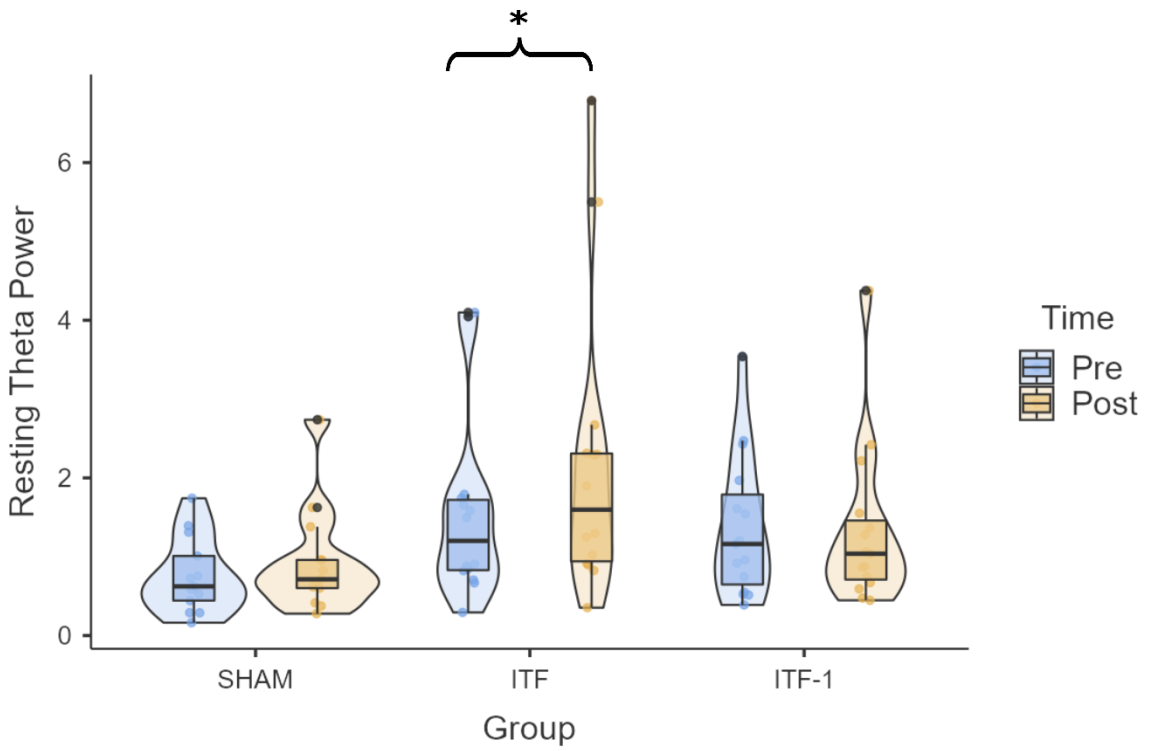

Supplementary Figure 2: The time*group interaction was significant (p = 0.016): ITF group had increased theta power after tACS while there were no tACS effects on the other groups. ITF: individual theta frequency. The vertical bars denote 0.95 confidence intervals. Dots represent the observed scores. Asterisks (*) represents p<.05.

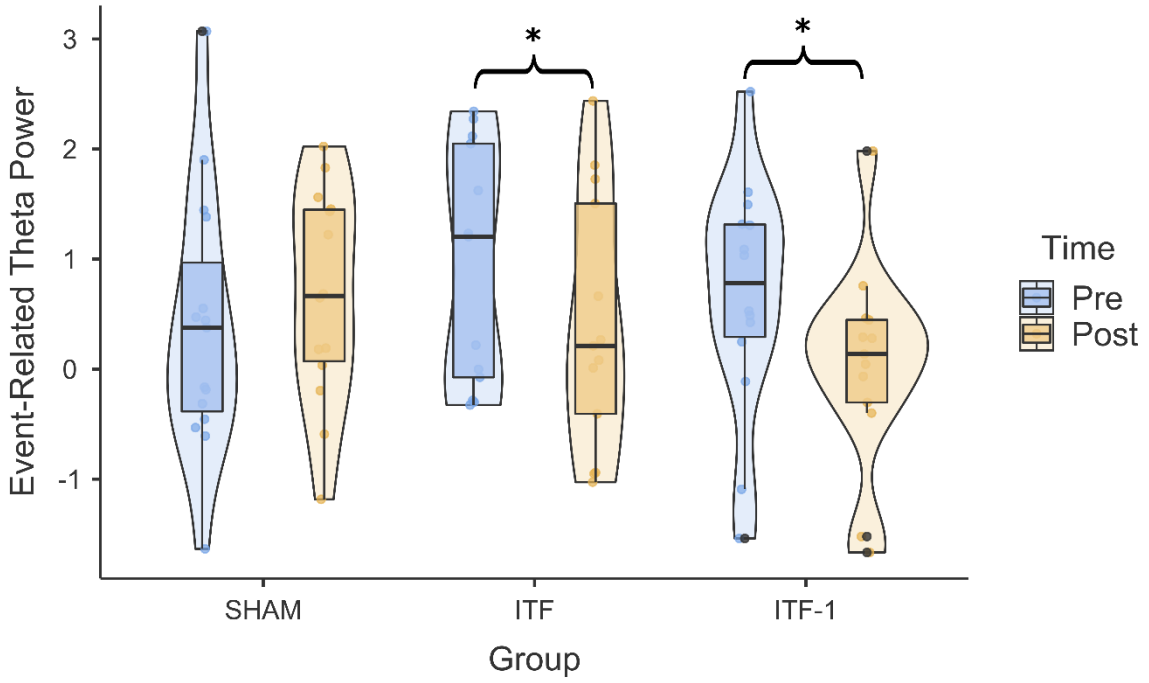

Supplementary Figure 3: The time*group interaction was significant (p = 0.01) for VM task. The tACS groups had decreased event-related theta power after tACS (post) (for ITF-1 p=0.045, for ITF P=0.011) while no such difference was observed in the sham group (p=0.145). ITF: individual theta frequency. The vertical bars denote 0.95 confidence intervals. Dots represent the observed scores. Asterisks (*) represents p<.05.

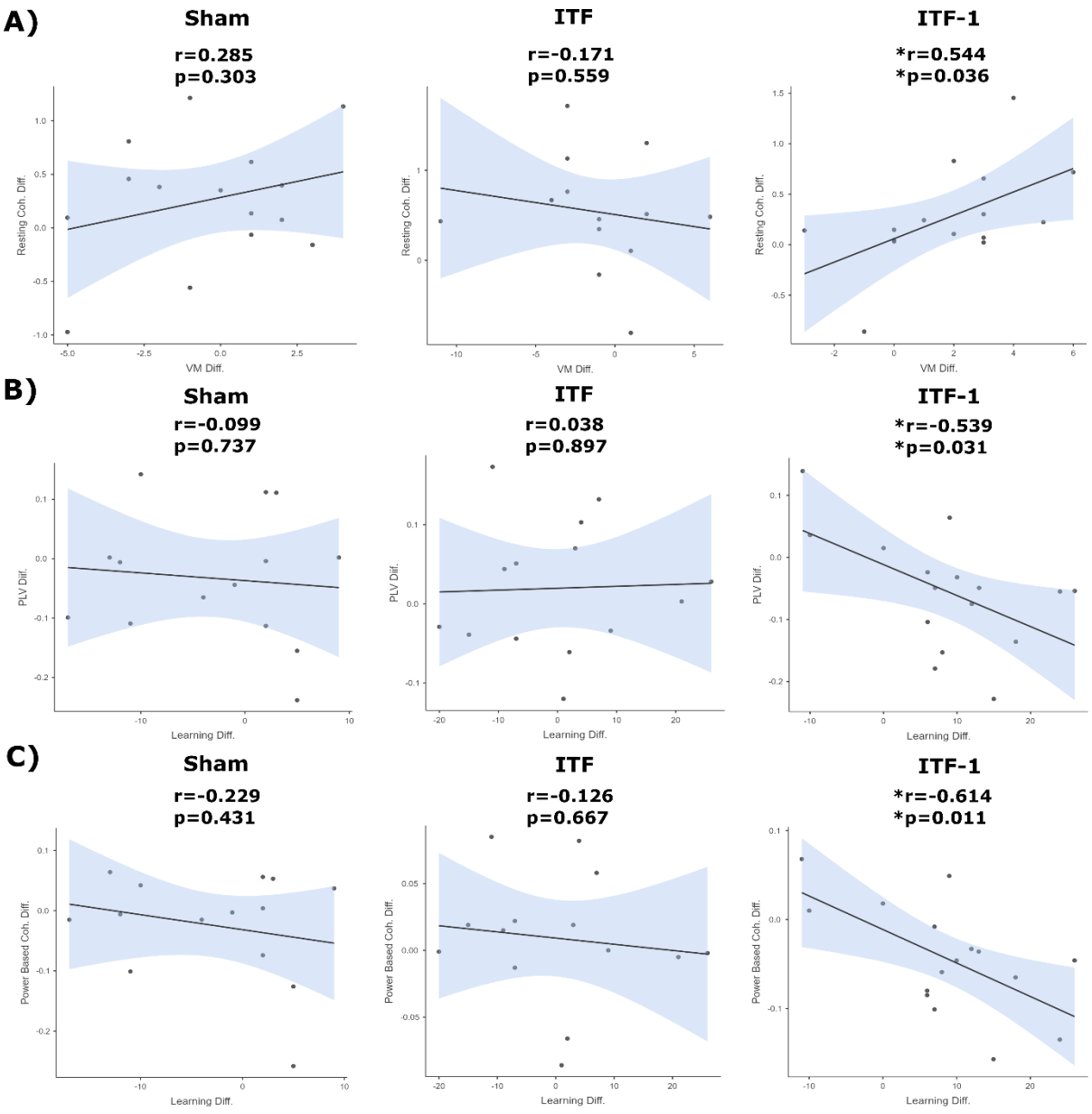

Supplementary Figure 4: A) There was a positive correlation between tACS effects (pre-/post tACS difference score) on left frontal-parietal resting-state theta coherence and the VM task, specifically in the ITF-1 group (r=0.544, p=0.036 ; ITF group p=0.559; Sham group p=0.303) **B)** There was also a negative correlation in specifically the ITF-1 group between tACS effects on specifically learning scores (not VM) and left frontal-parietal PLV (ITF-1 group r=-0.539, p=0.031; ITF group p=0.897; Sham group p=0.737) **C)** We observed a strong negative correlation between tACS effects on left frontal-parietal event-related power-based theta connectivity and learning scores (r=-0.614, p=0.011), again specifically for the ITF-1 group (ITF group p=0.667; Sham group p=0.431). Coh.: coherence, Diff.: difference score, PLV: phase locking value, Max.: maximum, Freq.: frequency, VM: visual memory, ITF: individual theta frequency. The shaded area denotes the standard error. Dots represent the observed scores. Asterisks (*) represents p<.05.

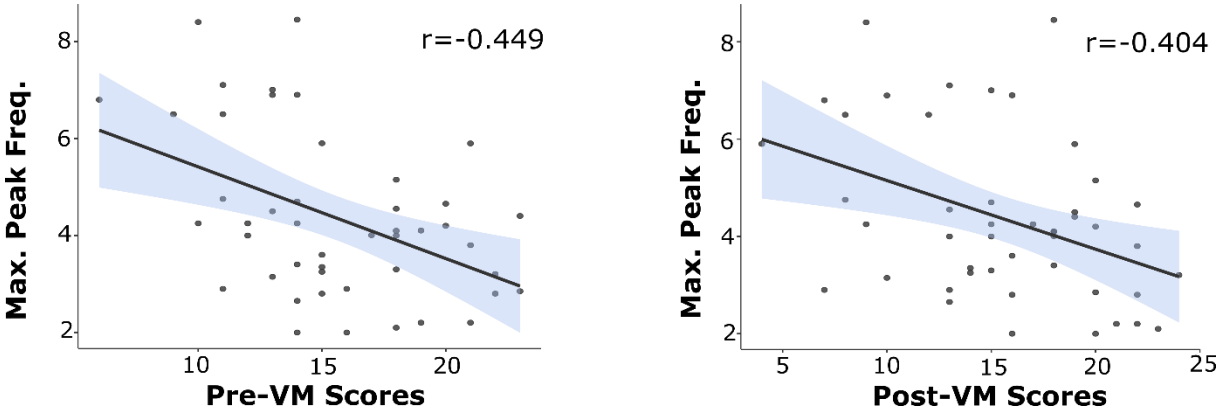

Supplementary Figure 5: The pre-left frontocentral resting maximum peak frequency significantly related to the after effect of the tACS on the VM scores (p = 0.006). There was a negative relation between the pre-resting maximum peak frequency and VM scores: The subjects with lower pre-theta frequency had a higher VM score (for pre-VM scores: r=-0.449, p=0.002, post-VM scores: r=-0.404, p=0.005). Max.: maximum, Freq.: frequency, VM: visual memory. The shaded area denotes the standard error. Dots represent the observed scores.

Supplementary Table 1: Behavioral Results for Tasks

Tasks (During the EEG recording)	**ITF-1 (N=16)**		**ITF (N=15)**		**Sham (N=15)**		***P***
	Pre Mean SD	**Post** Mean SD	**Pre** Mean SD	**Post** Mean SD	**Pre** Mean SD	**Post** Mean SD	
Auditory Memory: Free-recall Scores	18,2 ± 5	18,3 ± 5	15,8 ± 5,7	14,3 ± 6,4	16,3 ± 5,2	16,5 ± 5,8	0.400
Visual Memory: Free-recall Scores	16.1 ± 3.9	17.9 ± 3.4	15.4 ± 3.9	13.9 ± 5.6	15.1 ± 4.5	14.7 ± 4.7	0.016*****
	pre < post		-		-		0.026

SD: standard deviation. ITF: individual theta frequency. P values belong to the results of Group X Time interaction. Asterisks (*) represents p<.05.

Supplementary Table 2: Behavioral Results for Neuropsychological Tests

Neuropsychological Tests	**ITF-1 (N=16)**		**ITF (N=15)**		**Sham (N=15)**		***P***
	Pre Mean SD	**Post** Mean SD	**Pre** Mean SD	**Post** Mean SD	**Pre** Mean SD	**Post** Mean SD	
Oktem Verbal Memory Test:							
Short-term Memory	6.6 ± 1.2	7.2 ± 2.4	6.3 ± 2.1	6.2 ± 2.3	6.7 ± 1.9	6.4 ± 1.6	0.472
Long-term Memory	14.2 ± 0.9	13.8 ± 1.5	14.1 ± 0.7	13.1 ± 1.2	14.2 ± 1.1	12.9 ± 2.1	0.065
Total Learning	124 ± 12.2	133 ± 9.8	125 ± 11.8	126 ± 10.9	129 ± 9.7	127 ± 12.2	0.011*****
	pre < post		-		-		0.002
Rey Complex Figure Test:							
Short-term Memory	26.8 ± 6.6	26.4 ± 5.4	26.3 ± 4.5	28.2 ± 5.1	27.8 ± 5.6	27 ± 4	0.539
Long-term Memory	26.2 ± 6.8	25.7 ± 4.8	26.1 ± 4.4	25.7 ± 4.8	28.1 ± 6	26.6 ± 3.7	0.458
Digit Span Forward	7.2 ± 1	7.2 ± 0.9	6.3 ± 1	6.1 ± 1.1	6.9 ± 0.9	6.5 ± 1	0.581
Letter-Number Sequencing Test	6.2 ± 0.7	5.9 ± 1	5.4 ± 0.8	5.3 ± 0.6	5.7 ± 1	5.7 ± 0.8	0.626

SD: standard deviation. ITF: individual theta frequency. P values belong to the results of Group X Time interaction. Asterisks (*) represents p<.05.

Abnormal Cross Frequency Coupling of Brain Electroencephalographic Oscillations related to Visual Oddball Task in Parkinson's Disease with Mild Cognitive Impairment

Zübeyir Bayraktaroğlu, Tuba Aktürk, Görsev Yener, Tom A. de Graaf, Lütfü Hanoğlu, Ebru Yıldırım, Duygu Hünerli Gündüz, İlayda Kıyı, Alexander T. Sack, Claudio Babiloni, Bahar Güntekin

Corresponding manuscript: Bayraktaroğlu, Z., Aktürk, T., Yener, G., de Graaf, T. A., Hanoğlu, L., Yıldırım, E., Hünerli Gündüz, D., Kıyı, İ., Sack, A. T., Güntekin, B. (2022). Abnormal Cross Frequency Coupling of Brain Electroencephalographic Oscillations related to Visual Oddball Task in Parkinson's Disease with Mild Cognitive Impairment. Clinical EEG and Neuroscience. doi:10.1177/15500594221128713

Abstract

Parkinson's disease (PD) is a movement disorder caused by degeneration in dopaminergic neurons. During the disease course, most of PD patients develop mild cognitive impairment (PDMCI) and dementia, especially affecting frontal executive functions. In this study, we tested the hypothesis that PDMCI patients may be characterized by abnormal neurophysiological oscillatory mechanisms coupling frontal and posterior cortical areas during cognitive information processing. To test this hypothesis, event-related EEG oscillations (EROs) during counting visual target (rare) stimuli in an oddball task were recorded in healthy controls (HC; N=51), cognitively unimpaired PD patients (N=48), and PDMCI patients (N=53). Hilbert transform served to estimate instantaneous phase and amplitude of EROs from delta to gamma frequency bands, while modulation index computed ERO phase-amplitude coupling (PAC) at electrode pairs.

As compared to the HC and PD groups, the PDMCI group was characterized by (1) more posterior topography of the delta-theta PAC and (2) reversed delta-low frequency alpha PAC direction, i.e., posterior-to-anterior rather than anterior-to-posterior.

These results suggest that during cognitive demands, PDMCI patients are characterized by abnormal neurophysiological oscillatory mechanisms mainly led by delta frequencies underpinning functional connectivity from frontal to parietal cortical areas.

Keywords: Parkinson's Disease (PD), Parkinson's Disease with Mild Cognitive Impairment (PDMCI), Brain Event-Related Oscillations (EROs), Cross-frequency Coupling, Phase-Amplitude Coupling, Oddball Paradigm.

1. Introduction

Parkinson's disease (PD) is a movement disorder, mainly caused by degeneration in dopaminergic neurons of substantia nigra affecting basal ganglia circuits and cognitive motor functions. Notably, those circuits modulate several cognitive functions including frontal executive functions (i.e., attention and working memory, decision-making, etc.), learning, and episodic memory[1]. During the disease course, those dysfunctions in these circuits are associated to a clinical syndrome progressing from mild cognitive impairment (MCI) to dementia in most PD patients[2–6].

In the framework of a Precision Medicine approach, PD patients should be periodically assessed according to their (1) cognitive status by neuropsychological "paper and pencil" tests and (2) brain neurophysiological functioning by adequate biomarkers. Informative biomarkers of brain neurophysiological functioning may derive from the analysis of electroencephalographic (EEG) oscillatory activity recorded during cognitive demands. This activity reflects event-related oscillations (EROs) in cortical neural excitability during sensory information processing and can provide useful information on the derangement of brain cognitive systems in patients with PD or other neurodegenerative disorders[7,8].

In previous studies, topographically widespread EROs during auditory and visual cognitive tasks were lower in magnitude at delta (<4 Hz) and theta (4-7 Hz) frequencies in PDMCI patients when compared to PD patients without cognitive deficits and healthy cognitively unimpaired control (HC) persons[9–14]. Notably, similar abnormalities in EROs were found in patients with cognitive deficits due to Alzheimer's disease, so these biomarkers may be not specific for PD effects on brain cognitive systems[15]. Nevertheless, EROs may be useful to appreciate the extent to which brain cognitive systems at work are disrupted in PD patients with the same medical diagnosis.

A new frontier in the study of EROs during cognitive tasks is the computation of the statistical interdependence (coupling) of those oscillations at different frequency bands and scalp electrodes, as a reflection of multi-scale integration of neural activity in cortical cognitive networks at work[16]. This statistical interdependence is generally referred to as cross-frequency coupling (CFC) of resting state EEG activity or EROs during cognitive tasks at a given scalp electrode (cortical source) or scalp electrode (cortical source) pair. Notably, CFCs from those EEG signals can be observed at different scales in the brain, from invasive intracerebral to scalp-recorded EEG or ERO signals[7,17–20]. While the statistical interdependence (coupling)

between high-frequency EEG oscillations (>30 Hz within beta and gamma frequency bands) at an electrode pair is usually significant only in close proximity to their cortical EEG sources, that between EROs slower on frequency (<8 Hz within delta and theta frequency bands) is significant for more widespread ranges in the cortical source space[21]. This typical observation suggests that EROs at delta and theta frequencies may integrate cognitive information processing over larger spatial scales, while EROs at beta and gamma frequencies may play a role in local cognitive information processing[21,22].

Several variants of CFC of EEG or ERO activity have been defined, such as frequency-frequency amplitude-amplitude coupling, and phase-amplitude-coupling (PAC), both at a given scalp electrode (cortical source) or electrode pair[23]. Among them, the CFC based on PAC quantifies the modulation of the EEG or ERO amplitude at a given frequency and electrode (source) by the phase of another frequency band. The same concept has been applied to the CFC based on PAC computed at a given frequency and electrode pair[23].

In physiological conditions[24–26], the phase of EEG oscillations at theta frequencies (~6 Hz) in the hippocampus was shown to modulate the amplitude of local gamma EEG oscillations (~40 Hz) as a neurophysiological underpinning of the ability to hold a (limited) number of items available for cognitive processing, namely the short-term memory capacity. Several studies extended these CFC based on PAC findings on the electrophysiological data recorded at multiple spatial scales in several brain regions for investigating other cognitive functions such as attention[27], decision making[27,28], and sensory detection[29]. In parallel to this prominent theta-gamma PAC, a large number of EEG studies reported other CFC based on PACs (in the related-brain regions), such as delta-beta coupling as an indicator of cortical-subcortical control of motivational and emotional processes[30], temporal prediction, and prediction accuracy[31], and social anxiety[32].

In pathophysiological conditions, abnormal CFC from EEG activity was associated with cognitive impairment[33]. Specifically, it happened in patients with schizophrenia[34], epilepsy[35], and Alzheimer's disease[36,37]. Furthermore, power-to-power and phase-to-amplitude CFCs from EEG activity were also abnormal in PD patients in relation to motor symptoms[19,20]. Notably, no previous study investigated the CFC based on PAC from cognitive EROs in PD patients with cognitive deficits, typically involving frontal executive functions.

The importance of anterior-posterior connectivity in cognition (and impairment in some pathologies) is the point on which the study's central hypothesis is based [38–41]. Therefore, in this

study, we tested the hypothesis that PDMCI patients may be characterized by abnormal neurophysiological oscillatory mechanisms coupling specifically between frontal and posterior cortical areas during cognitive information processing as revealed by the CFC based on cognitive EROs. To test this hypothesis, EROs during counting visual target (rare) stimuli in a standard oddball task intermingling those stimuli with frequent ones were recorded in healthy controls (HC), cognitively unimpaired PD patients, and PDMCI patients. Furthermore, that CFC from EROs at electrode pairs was used as a measure of underlying cortical functional connectivity between frontal and posterior areas during cognitive information processing.

2. Method

2.1 Participants

The participants were recruited into three study groups: PD (N=48) only with motor symptoms, PDMCI (N=53), and healthy controls (HC, N=51). The demographics of the participants are given in Table 1. All participants had normal or corrected-to-normal vision.

Table 1. Demographic data and MMSE, Stroop, Oddball error and UPDRS (motor) scores.

	HC (N=51) M ± SD	PD (N=48) M ± SD	PDMCI (N=53) M ± SD	*P*
Age	66.7 ± 9.9	65.3 ± 7.7	66.9 ± 8.4	.124[a]
Education	10.1 ± 4.9	9.5 ± 4.7	7.9 ± 4.8	.065[a]
Gender	♀ 28 ♂ 23	♀ 15 ♂ 33	♀ 12 ♂ 41	**.002[b]**
MMSE	28.3 ± 1.7	27.8 ± 2.0	24.6 ± 4.6	0.200 (HC vs. PD)[c] **<0.05 (HC vs. PDMCI)[c]** **< 0.05 (PD vs. PDMCI)[c]**
Stroop	51.9 ± 16.5	52.2 ± 17.6	82.7 ± 25.5	0.935 (HC vs. PD)[c] **<0.001 (HC vs. PDMCI)[c]** **< 0.001 (PD vs. PDMCI)[c]**
Oddball error score	0.51 ± 0.88	2.29 ± 2.74	4.17 ± 5.31	**<0.001 (HC vs. PD)[c]** **<0.001 (HC vs. PDMCI)[c]** **< 0.05 (PD vs. PDMCI)[c]**
UPDRS	-	19.7 ± 7.6	20.6 ± 8.5	.425[c]
Disease Duration	-	4.0 ± 3.5	4.5 ± 4.0	.570[c]

♀**:** Female; ♂**:** Male; M: Mean; SD: Standard Deviation; HC: Healthy Controls; PD: Parkinson's Disease; PDMCI: Parkinson's Disease with mild cognitive impairment; MMSE: Mini-Mental State Examination Test; UPDRS: Unified Parkinson's Disease Rating Scale; [a] One-way ANOVA; [b] Chi-square test; [c] Two-sample *t*-test

The patients with PD were diagnosed by the neurology specialists according to the "United Kingdom Parkinson's Disease Society Brain Bank" criteria[42]. Litvan's criteria were used for the diagnosis of PDMCI[43]. The participants were assessed extensively with neuropsychological tests in several cognitive domains including memory processes, language abilities, executive functions, attention, and visuospatial skills (see supplementary for details of the neuropsychological assessment). Additionally, the Turkish version of the standardized Mini-Mental State Examination (MMSE)[44,45] was employed to assess the general cognitive states. The dementia stage was determined by the Clinical Dementia Rating scale (CDR)[46]. The

Unified Parkinson's Disease Rating Scale (UPDRS)[47] was applied to evaluate the severity of PD. UPDRS scores of the patient groups were given in Table 1. To establish the stage of the disease, the Hoehn-Yahr scale[48] was used. All participants in PD and PDMCI groups were on stage 3 or below.

The history of severe head trauma, drug abuse or chronic alcoholism, and any other neurological or psychiatric disease (e.g., mood disorders and schizophrenia) or Parkinson plus syndromes were exclusion criteria for the PD and the PDMCI group. In addition to these, any cognitive impairment according to the neuropsychological assessments were exclusion criteria for the HC group. All patients with PD were included in the assessments after taking their daily levodopa (equivalent) dose (On period).

The study was approved by the local ethics committee (no. 10840098-51). Oral and written informed consents was obtained from all participants and/or their caregivers who approved their participation in the study.

2.2 Experimental Design

The visual oddball paradigm was the cognitive task during the EEG recordings. A total of 120 stimuli that consisted of 40 targets and 80 non-targets were presented. Before the experiment began, a short version of the paradigm was presented for practice. Two different diffuse screen luminance levels were defined as target (10 cd/cm^2) and non-target (40 cd/cm^2) stimuli. The participants were asked to mentally count the number of target stimuli while ignoring the non-targets. At the end of the experiment, they were asked for the total number of target stimuli to assess their task performance. Based on these self-reported behavioral outputs, oddball task scores of the participants were calculated. In the calculations of the oddball task scores, deviated numbers from the correct target number (40 targets) were considered as participants' error scores.

The stimulus duration was 1000 ms and the interstimulus interval was randomly varied between 3 to 7 s. The stimuli were displayed on a 19" square screen (refresh rate 60 Hz) which was located 120 cm away from the participants.

2.3 EEG Recordings

EEG was recorded from 30 Ag/AgCl scalp electrodes with EasyCap (EasyCap GmbH, Germany) according to the extended 10-20 electrode placement system. Two physically linked electrodes placed on the right and the left earlobes served as references. The ground electrode was placed behind the right earlobe. The electrooculogram was recorded from the electrodes

on the nasion and outer canthus of the right eye and referenced to each other. BrainAmp DC amplifier (Brain Product GmbH, Germany) was used for EEG recordings with 0.01-250 Hz analog input filter and the sampling rate of 500 samples/s. Impedances for all recording electrodes were kept below 10 KOhm, and below 5 KOhm for the reference and ground electrodes. The participants were seated in a dimly lit, soundproof, and electromagnetically shielded room for EEG recordings.

2.4 EEG Analysis

All EEG preprocessing and statistical analysis steps were performed in MATLAB (ver. 2019b) environment using the BBCI Toolbox[49] developed in MATLAB along with the MATLAB core functions and Statistical Analysis Toolbox (Mathworks Inc, USA). The head-in-head plots produced with the showcs.m function from the METH toolbox by Guido Nolte[50].

2.4.1 EEG Preprocessing

Continuous EEG signals bandpass filtered between 0.01 and 45 Hz with Butterworth 2nd order filter with zero phase distortion only to mark the segments with artifacts. The filtered EEG signals were split into epochs spanning the time 500 ms before and 1000 ms after the stimulus for modulating delta frequency, for higher modulating frequencies epoch limits were 500 ms before and 500 ms after stimulus. The epochs were baseline corrected for the mean EEG amplitude of 200 ms before each stimulus. Artifact rejection was done semi-automatically on the epoched EEG data. The automatic rejection criteria were 150 μV amplitude differences between the minimum and the maximum samples or absolute amplitude larger than 80 μV in the epoch of interest, and differences larger than 50 μV between two consecutive samples in an epoch. The amplitudes lower than 0.1 μV for more than 20 ms were marked as low activity. Additionally, automatically marked artifacts and the epochs with low EEG amplitude were inspected visually by an expert, and muscle, eye or movement artifacts not detected by the algorithm were also marked. The epochs with artifacts marked on the raw EEG data were removed from further analysis.

2.4.2 Calculation of Cross-Frequency Coupling based on Phase Amplitude Coupling (PAC)

The CFC based on PAC was computed from the artifact-free EROs associated with the visual rare (target) stimuli. Specifically, it was calculated between the phase of a lower frequency and the amplitude of a higher frequency signal in target epochs between electrode pairs. The CFC based on PAC analysis was constrained to 18 electrodes representative of frontal, central,

parietal, and occipital scalp regions of interest (F3, Fz, F4, FC3, FCz, FC4, C3, Cz, C4, CP3, CPz, CP4, P3, Pz, P4, O1, Oz, O2). The remaining electrodes, mostly located in the border of the scalp were more prone to residual muscular and ocular artifacts and would have possibly inflated computational solutions and statistical comparisons.

The CFC based on PAC was calculated between canonical EEG frequency bands strictly following the procedure described in the reference study by Tort et al. (2010)[51]. The EEG frequency bands were defined as follows: delta (0.5-3.5 Hz), theta (4-7 Hz), low-frequency alpha (7-11 Hz), high-frequency alpha (9-13 Hz), beta (15-25 Hz), and gamma (35-45 Hz).

The continuous raw EEG data of the EROs were band-pass filtered in the modulating (delta, theta) and modulated (theta, low-frequency alpha, high-frequency alpha, beta, gamma) frequency bands. Specifically, the EROs were filtered around a center frequency at the described frequency bands with a fourth order, zero phase-shift Butterworth filter. The bandwidth for the delta and theta bands were ± 1 Hz, for alpha was ± 2 Hz, and for the beta and gamma bands were ± 5 Hz. Instantaneous phase and amplitude values were calculated on the filtered EROs between electrode pairs by the Hilbert transform using the hilbert.m function in MATLAB. The CFC based on PAC was calculated on the segmented data for 1000 ms and 500 ms time periods after the rare (target) stimulus presentation for the delta and theta modulating-frequencies, respectively. The amplitude of the modulated EEG signals was binned as a function of the phase of the modulating frequencies, and the normalized mean amplitude was calculated for bins by dividing each bin value by the sum over the bins at a single electrode level. Modulation index (MI) was calculated as a measure of the amount of PAC between EROs at a given electrode pair with 15-degree phase angle resolution[51]. The modulating (phase) and modulated (amplitude) frequency pairs over the CFC calculated are reported in Table 2. Mean CFC values for each group are visualized as head-in-head plots as introduced by Nolte et al. (2014)[50] for each frequency pair of CFC values (see Supplementary Fig. 1-3).

Table 2. The modulating (phase) and modulated (amplitude) frequency pairs for MI were calculated.

CFC Pairs		Modulated				
		theta	low alpha	high alpha	beta	gamma
Modulating	delta	x	x	x	x	x
	theta	-	x	x	x	x

2.4.3 Substantial CFC Testing

In the present study, we followed the common practice to compare the MI values computed from EROs for a given electrode pair and subject against the distribution of MI values computed from surrogate EEG time series mathematically generated to have statistical properties (e.g., EEG power density, signal-to-noise ratio, etc.) similar to EROs[51–54]. For this purpose, the amplitude of the modulated higher-frequency EEG segments was randomly shuffled concerning the phase of the modulating lower-frequency EEG segments. As a result, we generated 1000 surrogate MI values for each electrode and frequency pair (see Table 2) to establish the MI distribution computed at the chance level (alpha=0.05). Afterward, we defined significance thresholds individually as a MI value greater than 1.96 SD from the mean value. Furthermore, we transformed all measured MI values to z values by subtracting the mean and dividing them into the SD of the null distribution for each subject for given frequency pairs (see table 2). For practicality as in the common practice, we considered z transformed MI values $z \geq 2$ significant (determined according to the standard normal distribution), which approximately corresponds to $p<0.05$, namely 95% confidence level. In the procedure explained here, within-subject values were tested to assess substantial CFC values at the individual level compared to the CFC values from surrogated data. This procedure was used to determine the data which had the robust CFC to be used in between-subject statistical analysis (in ANOVAs).

The CFC based on PAC from EROs was calculated for all combinations of 18 electrodes and each frequency band, so producing 324 MI values for each subject. The topographical distribution of the mean MI values (z transformed) for all subjects and 3 groups (HC, PD, and PDMCI) is shown in Supplementary Fig. 1 for 3 different CFCs based on PAC electrode pairs.

Fig. 1, 2, and 3 show a matrix-wise representation of these values across all subjects and 3 groups.

2.5 Statistical Analysis

2.5.1 EEG

The electrode pairs of interest for the statistical analysis were selected with the guidance of the topographical distribution of the mean CFC based on PAC values in the head-in-head plots (Supplementary Fig. 1) and the CFC matrices (Fig. 1, 2, 3) for groups.

Fig. 1-3 illustrated the changes of the CFC based on PAC from EROs among the fronto-central and parieto-occipital sites for each group of persons. For data reduction purposes, we pooled electrodes in the following scalp regions of interest: fronto-central (F3, Fz, F4, FC3, FCz, FC4) and parieto-occipital (P3, Pz, P4, O1, Oz, O2), which were denoted as FC (anterior) and PO (posterior), respectively. Afterward, we calculated mean *z* values for each subject and electrode and moved to the statistical comparisons between the groups.

Due to head volume conduction effects, a certain amount of CFC based on PAC from EROs can be observed between all electrode pairs. Therefore, we create a null distribution to define a threshold to eliminate "fake" CFCs from EROs as mentioned above ($z \geq 2$).

The robustness of the CFC based on PAC values was controlled using the number of z values under 2 for each electrode pair per subject for a given frequency pair. If the number of CFC pairs (n=324) with low values was 3 SD away from the population mean, these subjects were removed from further evaluation of the frequency pair (delta-theta: 3 subjects (1 subject from each group); delta-low alpha: 4 subjects (1 from HC, 1 from PD, 2 from PDMCI); delta-high alpha: 1 subject from PDMCI group).

The mean *z* values pooled from the fronto-central (anterior) and parieto-occipital (posterior) electrodes formed 4 modulating and modulated electrodes for each frequency pair: Anterior-to-Anterior (AA), Anterior-to-Posterior (AP), Posterior-to-Anterior (PA), and Posterior-to-Posterior (PP). These four modulating and modulated electrode pairs were used in ANOVA design as the level of location within-subject factor.

The repeated measures ANOVA test with the 3-by-4 mixed design was performed for each CFC based on the PAC frequency pair where the 3 groups were defined as the between-subjects factor (Group: HC, PD, PDMCI) and 4 modulating-modulated electrode pairs (Location: AA, AP, PA, PP) as within-subject factors.

The raw MI values distributed exponentially, therefore, to make data more amenable for the F-test we used the z values for statistical analysis. Because the sphericity condition was not met as controlled with the Mauchly method[55], we reported the Greenhouse-Geisser corrected *p* values in the results section.

3. Results

3.1 Behavioral

MMSE was used to assess general cognitive functioning while the Stroop test more specifically targeted the frontal-executive functions. Therefore, these tests' scores and additionally visual oddball task performance were compared across the groups. Results showed that MMSE and Stroop scores were decreased in the PDMCI group compared to both PD and HC groups ($ps<0.05$) while there was no difference between PD and HC ($ps>0.05$) (Table 1). For the oddball task scores, PDMCI had lower scores than the PD and HC groups ($ps<0.05$), and HC group had better scores than both PD and PDMCI groups ($ps<0.05$) (Table 1).

Additionally, these task/test scores were used in the correlation analyses as cognitive measures (see supplementary).

3.2 EEG

Three out of 9 CFC based on PAC electrode pairs, as defined in Table 2, were statistically tested for between-group differences, namely, delta-theta, delta-low frequency alpha, and delta-beta coupling. The other CFC pairs were eliminated from further analysis because not enough subjects remained in the study groups with robust CFC, when the electrode pairs and the subjects with CFC under the threshold ($z<2$) were removed. In the following sections, we reported statistical results for delta-theta, delta-low frequency alpha, and delta-beta coupling, which showed statistically significant effects in the comparison among the groups ($p<0.05$).

The most significant CFC based on PAC difference between the groups was found in anterior-to-posterior coupling. In the post-hoc tests, significant differences were consistently observed between the HC and PD groups as well as between the HC and PDMCI ($p<0.05$). Therefore, here, in line with the hypothesis of the study, the results of the anterior-to-posterior CFC value, which is the electrode pair where significant differences between the groups are observed, will be reported in the following paragraphs.

The direction of the CFC based on PAC at delta-theta was prominent from the anterior to the posterior scalp regions in all groups. In relation to the HC and PD groups, the PDMCI group

was characterized by more posteriorly located CFC values (see Supplementary Fig. 1 and Fig. 1; Tables 3a, 3b).

For the CFC based on PAC at delta-low frequency alpha, the prominent direction was anterior-to-posterior in the HC group. In contrast, that prominent direction was posterior-to-anterior in the PD and PDMCI groups, with an emphasis on right frontal electrode pairs (see Supplementary Fig. 2 and Fig. 2; Tables 4a, 4b).

For the CFC based on PAC at delta-beta, the prominent direction was anterior-to-posterior in all groups. However, the CFC was lower especially at left electrode pairs in the PD and PDMCI groups as compared to the HC group (see Supplementary Fig. 3 and Fig. 3; Tables 5a, 5b).

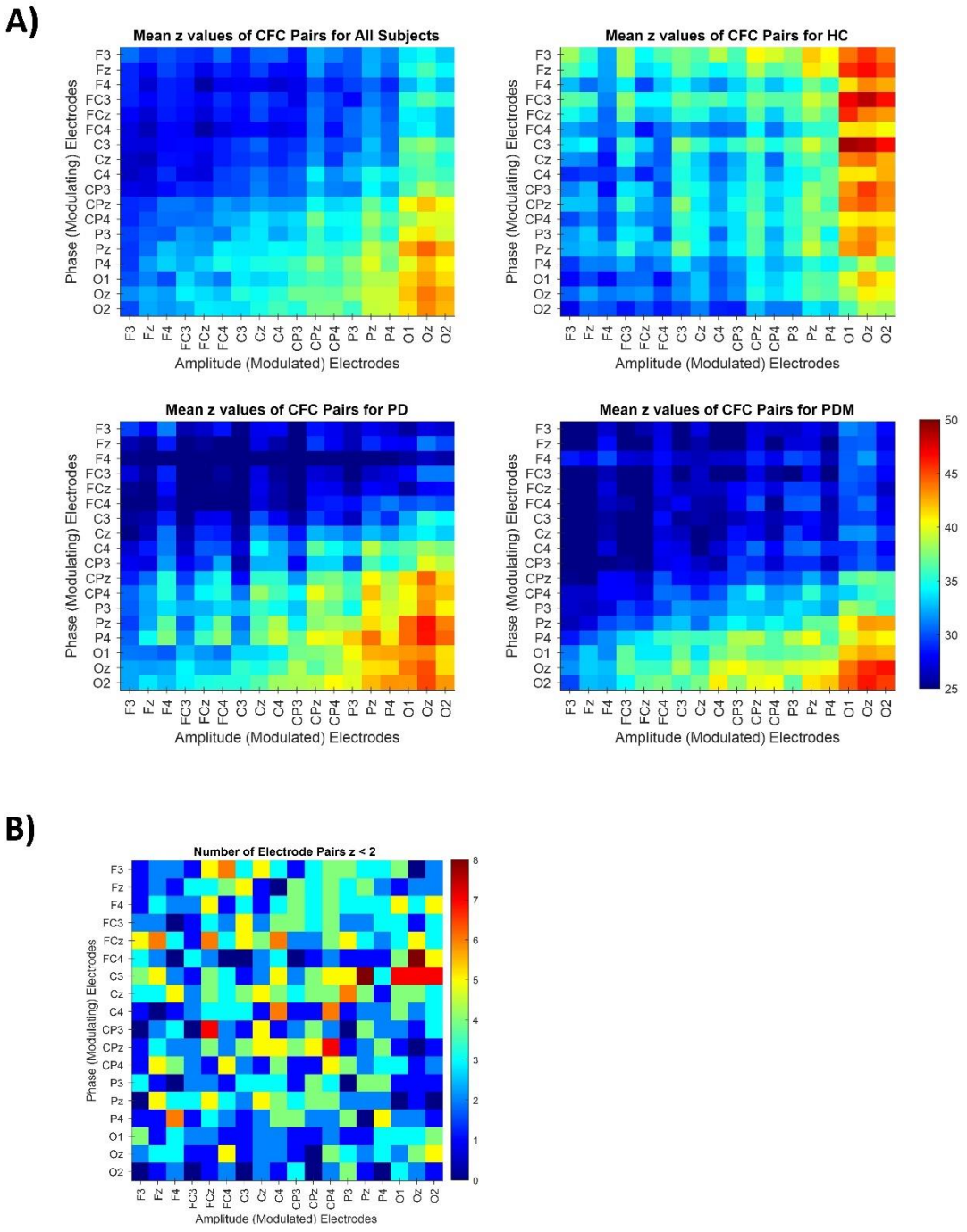

Fig. 1. A) Z values for delta - theta CFC between all electrode pairs. The mean z values for all subjects, healthy controls, Parkinson's Disease, Parkinson's Disease with MCI. HC: Healthy Controls; PD: Parkinson's Disease; PDM: PD with MCI. **B)** The number of subjects where z < 2 in a specific electrode pair.

Table 3a. Delta - Theta CFC. Repeated measures ANOVA results between groups for the within-subject factor of location.

	Sum Sq.	**DF**	**Mean Sq.**	**F**	***pGG***
Intercept	10521.0	3	3506.90	12.329	0.000
Group:Location	5901.5	6	983.58	3.458	***0.006***
Error	124590	438	284.45		

*p*GG: Greenhouse-Gaisser corrected *p* values for non-sphericity.

Table 3b. Significant group by location interactions for Delta-Theta CFC.

		Diff.	**SE**	***p***	**Lower**	**Upper**
AP	**HC vs. PD**	13.154	4.138	***0.004***	3.457	22.851
	HC vs. PDM	12.279	4.034	***0.007***	2.826	21.733
	PD vs. PDM	-0.875	4.099	ns	-10.481	8.732

Lower and Upper limits of simultaneous 95% confidence intervals for the true differences. AP: Anterior-to-Posterior, HC: Healthy Controls; PD: Parkinson's Disease; PDM: PD with MCI, Diff.: Difference, SE: Standard Error.

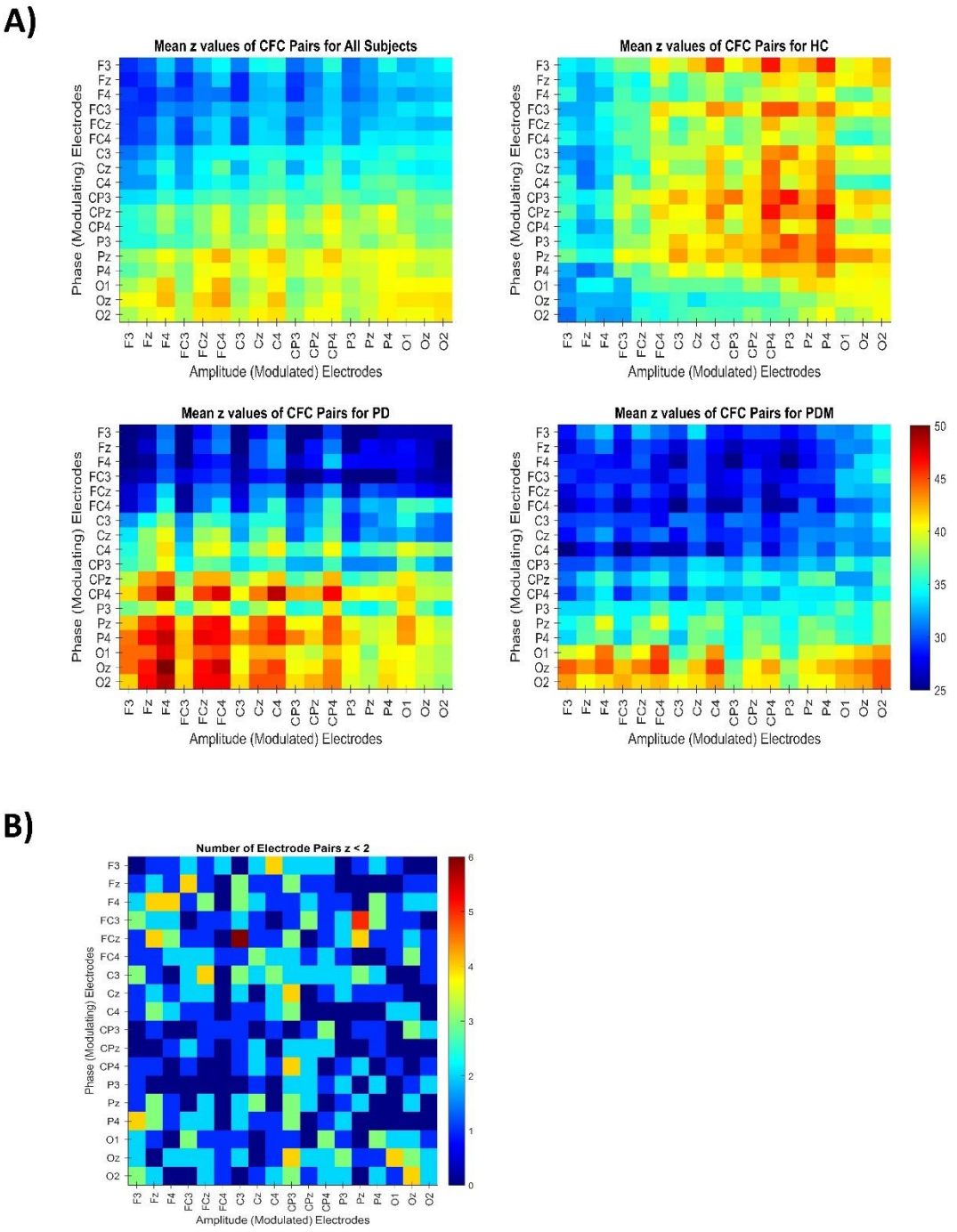

Fig. 2. A) Z values for delta - low frequency alpha CFC between all electrode pairs. The mean z values for all subjects, healthy controls, Parkinson's Disease, Parkinson's Disease with MCI. HC: Healthy Controls; PD: Parkinson's Disease; PDM: PD with MCI. **B)** The number of subjects where z < 2 in a specific electrode pair.

Table 4a. Delta - Low Frequency Alpha CFC. Repeated measures ANOVA results between groups for the within-subject factor of location.

	Sum Sq.	**DF**	**Mean Sq.**	**F**	***pGG***
Intercept	9007.5	3	3002.50	14.001	0.000
Group:Location	6543.4	6	1090.60	5.085	***0.000***
Error	93286.0	435	214.45		

*p*GG: Greenhouse-Geisser corrected *p* values for non-sphericity.

Table 4b. Significant group by location interactions for Delta-Low Frequency alpha CFC.

		Diff.	**SE**	***p***	**Lower**	**Upper**
AP	**HC vs. PD**	12.487	3.793	***0.003***	3.598	21.376
	HC vs. PDM	9.599	3.715	***0.026***	0.892	18.306
	PD vs. PDM	-2.888	3.775	ns	-11.734	5.959

Lower and Upper limits of simultaneous 95% confidence intervals for the true differences. AP: Anterior-to-Posterior, HC: Healthy Controls; PD: Parkinson's Disease; PDM: PD with MCI, Diff.: Difference, SE: Standard Error.

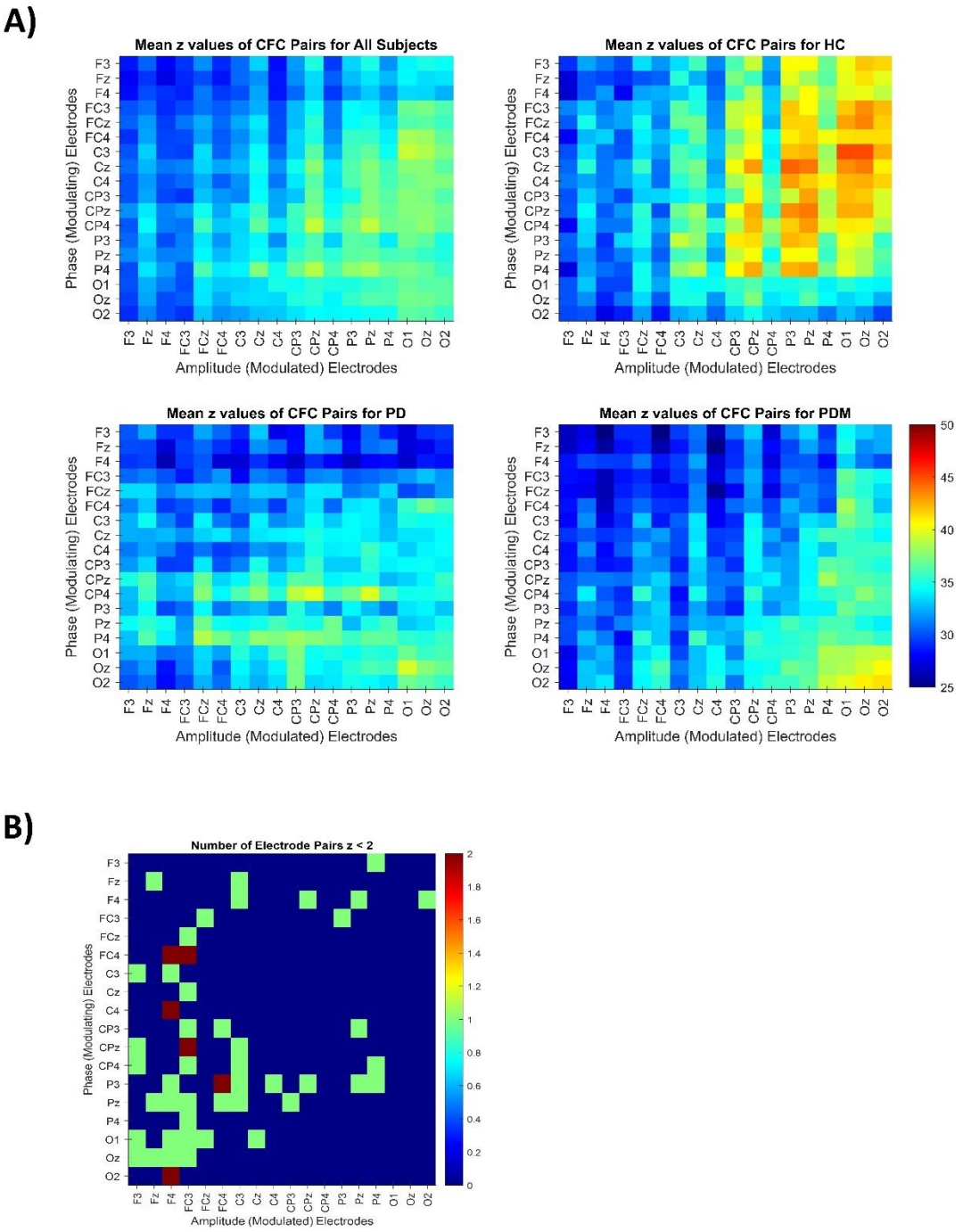

Fig. 3. **A)** Z values for delta - beta CFC between all electrode pairs. The mean z values for all subjects, healthy controls, Parkinson's Disease, Parkinson's Disease with MCI. HC: Healthy Controls; PD: Parkinson's Disease; PDM: PD with MCI. **B)** The number of subjects where z < 2 in a specific electrode pair.

Table 5a. Delta - Beta CFC. Repeated measures ANOVA results between groups for the within-subject factor of location.

	Sum Sq.	**DF**	**Mean Sq.**	**F**	***pGG***
Intercept	3467.3	3	1155.80	9.727	0.000
Group:Location	2332.7	6	388.78	3.272	***0.008***
Error	53113	447	118.82		

*p*GG: Greenhouse-Geisser corrected *p* values for non-sphericity.

Table 5b. Significant group by location interactions for Delta-Beta CFC.

		Diff.	**SE**	***p***	**Lower**	**Upper**
AP	**HC vs. PD**	9.893	3.188	**0.005**	2.422	17.364
	HC vs. PDM	8.091	3.109	**0.025**	0.803	15.378
	PD vs. PDM	-1.802	3.158	ns	-9.205	5.600

Lower and Upper limits of simultaneous 95% confidence intervals for the true differences. AP: Anterior-to-Posterior, HC: Healthy Controls; PD: Parkinson's Disease; PDM: PD with MCI, Diff.: Difference, SE: Standard Error.

4. Discussion

Here we tested the hypothesis that PDMCI patients may be characterized by abnormal CFC based on PAC from EROs recorded during counting visual target (rare) stimuli in an oddball task. A specific focus was on the CFC values at frontal and posterior electrode pairs in relation to typical impairment in frontal executive functions in PDMCI patients. The experimental design included HC and cognitively unimpaired PD patients as controls. Hilbert transform served to estimate instantaneous phase and amplitude of EROs from delta to gamma frequency bands, while modulation index computed CFC based on PAC from EROs at electrode pairs.

The main results showed significant CFC based on PAC at delta between the three groups. For the CFC based on PAC at delta-theta, the coupling direction was prominent from anterior to posterior scalp regions in all groups. However, the PDMCI group showed that delta PAC was more posteriorly located compared to the HC and PD groups. For the CFC based on PAC at

delta-low frequency alpha, the prominent coupling direction was anterior-to-posterior in the HC and posterior-to-anterior in the PD and PDMCI groups.

These findings complement previous results showing that EROs recorded during counting visual and auditory target (rare) stimuli in an oddball task presented main abnormalities at delta and theta frequency bands in PD patients with cognitive impairment when compared to HC persons[10,11].

These results suggest that PDMCI patients may be characterized by reduced and more posterior topography of delta-theta, delta-low frequency alpha, and delta-beta CFCs as a reflection of the impairment of brain cognitive systems. According to Lakatos et al. (2005), there may be a hierarchy in the EROs at different frequency bands during the cognitive information processing of external stimuli. In PDMCI patients, abnormal CFCs at the low frequencies might reflect a derangement in the "initial processes" in this hierarchical neurophysiological mechanisms occurring during the processing of rare (target) stimuli in a visual oddball paradigm[7]. In this line, the reduced CFC at low-to-low alpha frequency prominent in the frontal areas found in the PDMCI patients may reflect an impairment in the long-range cortical functional connectivity within frontal-parietal attention systems underpinning frontal executive functions, which may be a precursor to low-to-beta CFC that have decreased in patients. "In all group" correlation results (see supplementary) also may indicate that the Stroop test scores, which measure frontal-executive functions, as well as the general cognitive scores (MSSE), are deteriorating with the decrease of AP delta-beta CFC.

Another current finding in the PDMCI patients showed an altered direction in the CFC based on PAC at delta-low frequency alpha from EROs, especially the PDMCI patients. That direction reversed from the anterior-to-posterior in the HC persons to the posterior-to-anterior in the PDMCI patients. As the slow frequency oscillations are typically associated with functional inhibition mostly[56–58], PDMCI patients may suffer from impaired inhibitory control from frontal to posterior cortical regions during cognitive information processing[56–58].

In previous studies, frontal EROs at slow frequencies during cognitive tasks were supposed to be modulated by the dopaminergic system[59,60]. In that system, dopamine may cause neural inhibition or excitation according to its receptor[61]. Parker et al. (2014, 2015) showed the relationship between cortical EEG theta oscillations and the stimulation of D1 dopamine receptors which have inhibition effects[60,62]. Consistently, the present findings showed higher CFC based on PAC at delta-low frequency alpha from the anterior to the posterior direction in

the HC group but not in the PD patient groups, especially PDMCI patients. Impaired directionality in the slow oscillatory CFC based on PAC in the PDMCI patients may depend on the impaired dopaminergic mechanisms during the cognitive processes of target stimuli probed by the visual oddball task. Future studies in PDMCI patients will have to correlate the present abnormalities in the CFC based on PAC and the dopaminergic disruption as revealed by neuroimaging techniques.

5. Conclusions

To our knowledge, the present study is the first study presenting the altered CFC based on PAC from EROs in PDMCI patients. As compared to the HC and PD groups, the PDMCI group was characterized by (1) more posterior topography of the CFC based on PAC at delta-theta, (2) reversed CFC based on PAC at delta-low frequency alpha, namely from anterior-to-posterior to posterior-to-anterior, and (3) reduced anterior-to-posterior CFC based on PAC at delta-beta. These results suggest that during cognitive demands, PDMCI patients are characterized by abnormal neurophysiological oscillatory mechanisms mainly led by delta frequencies underpinning functional connectivity from frontal to posterior cortical areas.

References

1. Calabresi P, Picconi B, Tozzi A, Di Filippo M. Dopamine-mediated regulation of corticostriatal synaptic plasticity. *Trends Neurosci*. 2007;30(5):211-219. doi:10.1016/J.TINS.2007.03.001

2. Aarsland D, Brønnick K, Fladby T. Mild cognitive impairment in Parkinson's disease. *Curr Neurol Neurosci Rep*. 2011;11(4):371-378. doi:10.1007/s11910-011-0203-1

3. Aarsland D, Andersen K, Larsen JP, Lolk A, Nielsen H, Kragh-Sørensen P. Risk of dementia in Parkinson's disease. *Neurology*. 2001;56(6):730-736. doi:10.1212/WNL.56.6.730

4. Aarsland D, Andersen K, Larsen JP, Lolk A, Kragh-Sørensen P. Prevalence and Characteristics of Dementia in Parkinson Disease: An 8-Year Prospective Study. *Arch Neurol*. 2003;60(3):387-392. doi:10.1001/ARCHNEUR.60.3.387

5. Hughes TA, Ross HF, Musa S, et al. A 10-year study of the incidence of and factors predicting dementia in Parkinson's disease. *Neurology*. 2000;54(8):1596-1603. doi:10.1212/WNL.54.8.1596

6. Babiloni C, Pascarelli MT, Lizio R, et al. Abnormal cortical neural synchronization mechanisms in quiet wakefulness are related to motor deficits, cognitive symptoms, and visual hallucinations in Parkinson's disease patients: an electroencephalographic study. *Neurobiol Aging.* 2020;91:88-111. doi:10.1016/j.neurobiolaging.2020.02.029

7. Lakatos P, Shah AS, Knuth KH, Ulbert I, Karmos G, Schroeder CE. An oscillatory hierarchy controlling neuronal excitability and stimulus processing in the auditory cortex. *J Neurophysiol*. 2005;94(3):1904-1911. doi:10.1152/jn.00263.2005

8. Jensen O, Colgin LL. Cross-frequency coupling between neuronal oscillations. *Trends Cogn Sci*. 2007;11(7):267-269. doi:10.1016/j.tics.2007.05.003

9. Yener GG, Fide E, Özbek Y, et al. The difference of mild cognitive impairment in Parkinson's disease from amnestic mild cognitive impairment: Deeper power decrement and no phase-locking in visual event-related responses. *Int J Psychophysiol*. 2019;139. doi:10.1016/j.ijpsycho.2019.03.002

10. Güntekin B, Hanoglu L, Güner D, et al. Cognitive impairment in parkinson's disease is reflected with gradual decrease of EEG delta responses during auditory discrimination.

Front Psychol. 2018;9(FEB). doi:10.3389/fpsyg.2018.00170

11. Güntekin B, Aktürk T, Yıldırım E, Yılmaz NH, Hanoğlu L, Yener G. Abnormalities in auditory and visual cognitive processes are differentiated with theta responses in patients with Parkinson's disease with and without dementia. *Int J Psychophysiol*. 2020;153:65-79. doi:10.1016/j.ijpsycho.2020.04.016

12. Emek-Savaş DD, Özmüş G, Güntekin B, et al. Decrease of Delta Oscillatory Responses in Cognitively Normal Parkinson's Disease. *Clin EEG Neurosci*. 2017;48(5):355-364. doi:10.1177/1550059416666718

13. Schmiedt C, Meistrowitz A, Schwendemann G, Herrmann M, Basar-Eroglu C. Theta and alpha oscillations reflect differences in memory strategy and visual discrimination performance in patients with Parkinson's disease. *Neurosci Lett*. 2005;388(3):138-143. doi:10.1016/j.neulet.2005.06.049

14. Schmiedt-Fehr C, Schwendemann G, Herrmann M, Basar-Eroglu C. Parkinson's disease and age-related alterations in brain oscillations during a Simon task. *Neuroreport*. 2007;18(3):277-281. doi:10.1097/WNR.0b013e32801421e3

15. Güntekin B, Aktürk T, Arakaki X, et al. Are there consistent abnormalities in event-related EEG oscillations in patients with Alzheimer's disease compared to other diseases belonging to dementia? *Psychophysiology*. 2021;(July). doi:10.1111/psyp.13934

16. Fries P. A mechanism for cognitive dynamics: Neuronal communication through neuronal coherence. *Trends Cogn Sci*. 2005;9(10):474-480. doi:10.1016/j.tics.2005.08.011

17. Demiralp T, Bayraktaroglu Z, Lenz D, et al. Gamma amplitudes are coupled to theta phase in human EEG during visual perception. *Int J Psychophysiol*. 2007;64(1):24-30. doi:10.1016/j.ijpsycho.2006.07.005

18. Bragin A, Jand61vb G, Nddasdy Z, Hetke J, Wise K, Buzsirkil G. *Gamma Rat ,100 Hz) Oscillation Hippocampus Behaving*. Vol 15.; 1995. https://www.jneurosci.org/content/15/1/47.short. Accessed April 22, 2021.

19. Muthuraman M, Bange M, Koirala N, et al. Cross-frequency coupling between gamma oscillations and deep brain stimulation frequency in Parkinson's disease. *Brain*.

2020;143(11):3393-3407. doi:10.1093/BRAIN/AWAA297

20. De Hemptinne C, Ryapolova-Webb ES, Air EL, et al. Exaggerated phase-amplitude coupling in the primary motor cortex in Parkinson disease. *Proc Natl Acad Sci U S A*. 2013;110(12):4780-4785. doi:10.1073/pnas.1214546110

21. Buzsáki G, Draguhn A. Neuronal olscillations in cortical networks. *Science (80-)*. 2004;304(5679):1926-1929. doi:10.1126/science.1099745

22. Weiss S, Mueller HM. "Too many betas do not spoil the broth": The role of beta brain oscillations in language processing. *Front Psychol*. 2012;3(JUN):1-15. doi:10.3389/fpsyg.2012.00201

23. Canolty RT, Knight RT. The functional role of cross-frequency coupling. *Trends Cogn Sci*. 2010;14(11):506-515. doi:10.1016/j.tics.2010.09.001

24. Lisman J, Idiart M. Storage of 7 +/- 2 short-term memories in oscillatory subcycles. *Science (80-).* 1995;267(5203):1512-1515. doi:10.1126/science.7878473

25. Axmacher N, Henseler MM, Jensen O, Weinreich I, Elger CE, Fell J. Cross-frequency coupling supports multi-item working memory in the human hippocampus. *Natl Acad Sci*. 2010;107(7). doi:10.1073/pnas.0911531107

26. Tort ABL, Komorowski RW, Manns JR, Kopell NJ, Eichenbaum H. Theta-gamma coupling increases during the learning of item-context associations. *Proc Natl Acad Sci U S A.* 2009;106(49):20942-20947. doi:10.1073/pnas.0911331106

27. Schroeder CE, Lakatos P. Low-frequency neuronal oscillations as instruments of sensory selection. *Trends Neurosci*. 2009;32(1):9-18. doi:10.1016/j.tins.2008.09.012

28. Cohen MX, Elger CE, Fell J. Oscillatory activity and phase-amplitude coupling in the human medial frontal cortex during decision making. *J Cogn Neurosci*. 2009;21(2):390-402. doi:10.1162/jocn.2008.21020

29. Händel B, Haarmeier T. Cross-frequency coupling of brain oscillations indicates the success in visual motion discrimination. *Neuroimage*. 2009;45(3):1040-1046. doi:10.1016/j.neuroimage.2008.12.013

30. Najjar R, Brooker RJ. Delta-beta coupling is associated with paternal caregiving behaviors during preschool. *Int J Psychophysiol*. 2017;112:31-39.

doi:10.1016/j.ijpsycho.2016.11.014

31. Arnal LH, Doelling KB, Poeppel D. Delta-beta coupled oscillations underlie temporal prediction accuracy. *Cereb Cortex*. 2015;25(9):3077-3085. doi:10.1093/cercor/bhu103

32. Poppelaars ES, Harrewijn A, Westenberg PM, van der Molen MJW. Frontal delta-beta cross-frequency coupling in high and low social anxiety: An index of stress regulation? *Cogn Affect Behav Neurosci*. 2018;18(4):764-777. doi:10.3758/s13415-018-0603-7

33. Salimpour Y, Anderson WS. Cross-Frequency Coupling Based Neuromodulation for Treating Neurological Disorders. *Front Neurosci*. 2019;0(FEB):125. doi:10.3389/FNINS.2019.00125

34. Allen EA, Liu J, Kiehl KA, et al. Components of cross-frequency modulation in health and disease. *Front Syst Neurosci*. 2011;0(JULY 2011):59. doi:10.3389/FNSYS.2011.00059/BIBTEX

35. Zhang R, Ren Y, Liu C, et al. Temporal-spatial characteristics of phase-amplitude coupling in electrocorticogram for human temporal lobe epilepsy. *Clin Neurophysiol*. 2017;128(9):1707-1718. doi:10.1016/J.CLINPH.2017.05.020

36. Mazaheri A, Segaert K, Olichney J, et al. EEG oscillations during word processing predict MCI conversion to Alzheimer's disease. *NeuroImage Clin*. 2018;17(September 2017):188-197. doi:10.1016/j.nicl.2017.10.009

37. Goodman MS, Kumar S, Zomorrodi R, et al. Theta-Gamma coupling and working memory in Alzheimer's dementia and mild cognitive impairment. *Front Aging Neurosci*. 2018;10(APR):1-10. doi:10.3389/fnagi.2018.00101

38. Babiloni C, Frisoni GB, Pievani M, et al. White matter vascular lesions are related to parietal-to-frontal coupling of EEG rhythms in mild cognitive impairment. *Hum Brain Mapp*. 2008;29(12):1355-1367. doi:10.1002/HBM.20467

39. Dauwan M, van Dellen E, van Boxtel L, et al. EEG-directed connectivity from posterior brain regions is decreased in dementia with Lewy bodies: a comparison with Alzheimer's disease and controls. *Neurobiol Aging*. 2016;41:122-129. doi:10.1016/J.NEUROBIOLAGING.2016.02.017

40. Teipel S, Grothe MJ, Zhou J, et al. Measuring Cortical Connectivity in Alzheimer's Disease as a Brain Neural Network Pathology: Toward Clinical Applications. *J Int*

Neuropsychol Soc. 2016;22(2):138-163. doi:10.1017/S1355617715000995

41. Muller AJ, Shine JM, Rolle CE, et al. Anterior-posterior electrophysiological activity characterizes Parkinsonian visual misperceptions. *Neurol Clin Neurosci*. 2021;9(4):312-318. doi:10.1111/NCN3.12508

42. Hughes AJ, Daniel SE, Kilford L, Lees AJ, Society Brain Bank D, WClN IPJ J Hughes S E Daniel L Kilford A J Lees LA. Accuracy of clinical diagnosis of idiopathic Parkinson's disease: a clinico-pathological study of 100 cases. *J Neurol Neurosurg Psychiatry*. 1992;55:181-184. doi:10.1136/jnnp.55.3.181

43. Litvan I, Goldman JG, Tröster AI, et al. Diagnostic criteria for mild cognitive impairment in Parkinson's disease: Movement Disorder Society Task Force guidelines. *Mov Disord*. 2012;27(3):349-356. doi:10.1002/mds.24893

44. Folstein MF, Folstein SE, McHugh PR. "Mini-mental state". A practical method for grading the cognitive state of patients for the clinician. *J Psychiatr Res*. 1975;12(3):189-198. doi:10.1016/0022-3956(75)90026-6

45. Güngen C, Ertan T, Eker E, Yaşar R, Engin F. [Reliability and validity of the standardized Mini Mental State Examination in the diagnosis of mild dementia in Turkish population]. *Turk Psikiyatri Derg*. 2002;13(4):273-281. http://www.ncbi.nlm.nih.gov/pubmed/12794644. Accessed April 24, 2021.

46. Morris JC. The clinical dementia rating (cdr): Current version and scoring rules. *Neurology*. 1993;43(11):2412-2414. doi:10.1212/wnl.43.11.2412-a

47. Lang AET, Fahn S, Munsat TL. Assessment of Parkinson's disease. In: Quantification of Neurologic Deficit. Boston, MA: Butterworth; 1989:285-309.

48. Hoehn MM, Yahr MD. Parkinsonism: onset, progression, and mortality. Neurology. 2001;57(10):11-26..

49. Blankertz B, Tangermann M, Vidaurre C, et al. The Berlin brain-computer interface: Non-medical uses of BCI technology. *Front Neurosci*. 2010;4(DEC). doi:10.3389/fnins.2010.00198

50. Nolte G, Bai O, Wheaton L, Mari Z, Vorbach S, Hallett M. Identifying true brain interaction from EEG data using the imaginary part of coherency. *Clin Neurophysiol*. 2004;115(10):2292-2307. doi:10.1016/j.clinph.2004.04.029

51. Tort ABL, Komorowski R, Eichenbaum H, Kopell N. Measuring phase-amplitude coupling between neuronal oscillations of different frequencies. *J Neurophysiol*. 2010;104(2):1195-1210. doi:10.1152/jn.00106.2010

52. Bayraktaroglu Z, von Carlowitz-Ghori K, Losch F, Nolte G, Curio G, Nikulin V V. Optimal imaging of cortico-muscular coherence through a novel regression technique based on multi-channel EEG and un-rectified EMG. *Neuroimage*. 2011;57(3):1059-1067. doi:10.1016/j.neuroimage.2011.04.071

53. Hurtado JM, Rubchinsky LL, Sigvardt KA. Statistical Method for Detection of Phase-Locking Episodes in Neural Oscillations. *J Neurophysiol*. 2004;91(4):1883-1898. doi:10.1152/jn.00853.2003

54. Hesterberg T, Monaghan S, Moore DS, Clipson A, Epstein R, Freeman WH. *Bootstrap Methods and Permutation Tests Companion Chapter 18 To the Practice of Business Statistics*. New York: W. H. Freeman and Company; 2003.

55. Mauchly JW. Significance Test for Sphericity of a Normal n-Variate Distribution. *Ann Math Stat.* 1940;11(2):204-209. doi:10.1214/aoms/1177731915

56. Chmielewski WX, Mückschel M, Dippel G, Beste C. Concurrent information affects response inhibition processes via the modulation of theta oscillations in cognitive control networks. *Brain Struct Funct*. 2016;221(8):3949-3961. doi:10.1007/s00429-015-1137-1

57. Dippel G, Mückschel M, Ziemssen T, Beste C. Demands on response inhibition processes determine modulations of theta band activity in superior frontal areas and correlations with pupillometry – Implications for the norepinephrine system during inhibitory control. *Neuroimage*. 2017;157:575-585. doi:10.1016/j.neuroimage.2017.06.037

58. Mückschel M, Dippel G, Beste C. Distinguishing stimulus and response codes in theta oscillations in prefrontal areas during inhibitory control of automated responses. *Hum Brain Mapp*. 2017;38(11):5681-5690. doi:10.1002/hbm.23757

59. Parker KL, Chen K-H, Kingyon JR, Cavanagh JF, Narayanan NS. Medial frontal ~4-Hz activity in humans and rodents is attenuated in PD patients and in rodents with cortical dopamine depletion. *https://doi.org/101152/jn004122015*. 2015;114(2):1310-1320. doi:10.1152/JN.00412.2015

60. Parker KL, Ruggiero RN, Narayanan NS. Infusion of D1 Dopamine Receptor Agonist into Medial Frontal Cortex Disrupts Neural Correlates of Interval Timing. *Front Behav Neurosci*. 2015;0(NOVEMBER):294. doi:10.3389/FNBEH.2015.00294

61. Śmiałowski A, Bijak M. Excitatory and inhibitory action of dopamine on hippocampal neurons in vitro. Involvement of D2 and D1 receptors. *Neuroscience*. 1987;23(1):95-101. doi:10.1016/0306-4522(87)90274-0

62. Parker KL, Chen K-H, Kingyon JR, Cavanagh JF, Narayanan NS. D1-Dependent 4 Hz Oscillations and Ramping Activity in Rodent Medial Frontal Cortex during Interval Timing. *J Neurosci*. 2014;34(50):16774-16783. doi:10.1523/JNEUROSCI.2772-14.2014

Supplementary Materials: Abnormal Cross Frequency Coupling of Brain Electroencephalographic Oscillations related to Visual Oddball Task in Parkinson's Disease with Mild Cognitive Impairment

Neuropsychological Evaluation

Neuropsychological evaluations were applied in five cognitive domains including memory processes, language abilities, executive functions, attention, and visuospatial functions. Standardized Mini-Mental Test for General Cognitive Assessment (MMSE) [1], Oktem verbal memory processes test (OVMT) [2] and visual subtest of Wechsler Memory Scale [3] for the evaluation of memory functions, Digit Span subtests of Wechsler Memory Scale for the evaluation of attention, Boston Naming Test [4] for the evaluation of language domain, Stroop Color-Word Test [5], Clock Drawing Test [6] and Categorical Verbal Fluency Test [7] for the evaluation of executive functions, Turkish versions of Benton's Face Recognition Test (BFR) and Benton Line Judgment Orientation Test (BLOT) [5] for the evaluation of visuospatial functions were used. Each applied test has its own normative data for a certain age and education level. Therefore, participants were evaluated according to their own age and educational norms (or correction scores were added for people with low education levels as indicated in the test instruction). These norms were used to decide impairment in that specific test and the cognitive domain measured by this test. According to the literature [8], the test scores that shifted greater than 1.5 SD from the age and education appropriate norms are considered as an "impairment" in that test and particular domain. For the healthy control group, all participants' scores for each test were within the "normal range".

Depending on the participant's cognitive state, applying a full neuropsychological test battery took approximately 2 hours for each participant.

EEG Results

The head-in-head plots produced with the showcs.m function from the METH toolbox by Guido Nolte [8]. In the head-in-head plots, the entire scalp is represented by a single big circle. Within the big circle, each electrode is presented with a little circle mapping the mean CFC values from that electrode with all the other electrodes.

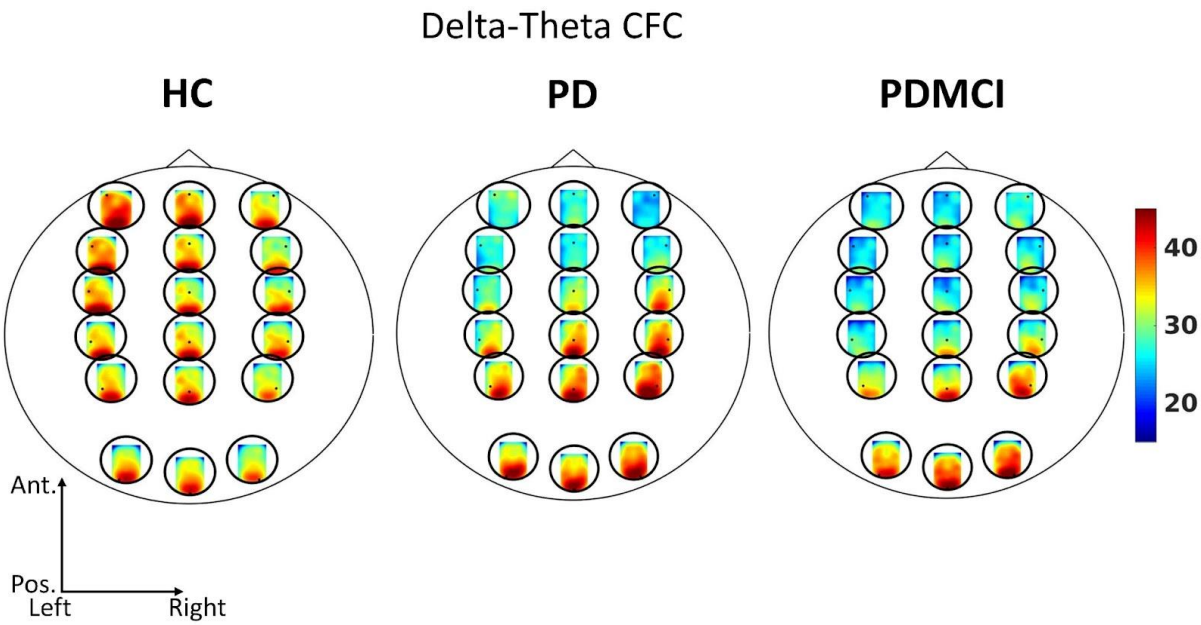

Supplementary Fig. 1. CFC between delta (0.5-3.5 Hz) and theta (4-7 Hz). In these plots, the single large circle represents the whole scalp. At each electrode position, a small circle was placed also representing the scalp and containing the CFC of that particular electrode with all other electrodes. Namely, each head topography on an electrode location represents the CFC distribution between that individual location and all other electrodes. Ant.: Anterior; Pos.: Posterior; HC: Healthy Controls; PD: Parkinson's Disease; PDMCI: PD with MCI. The values plotted are z-transformed.

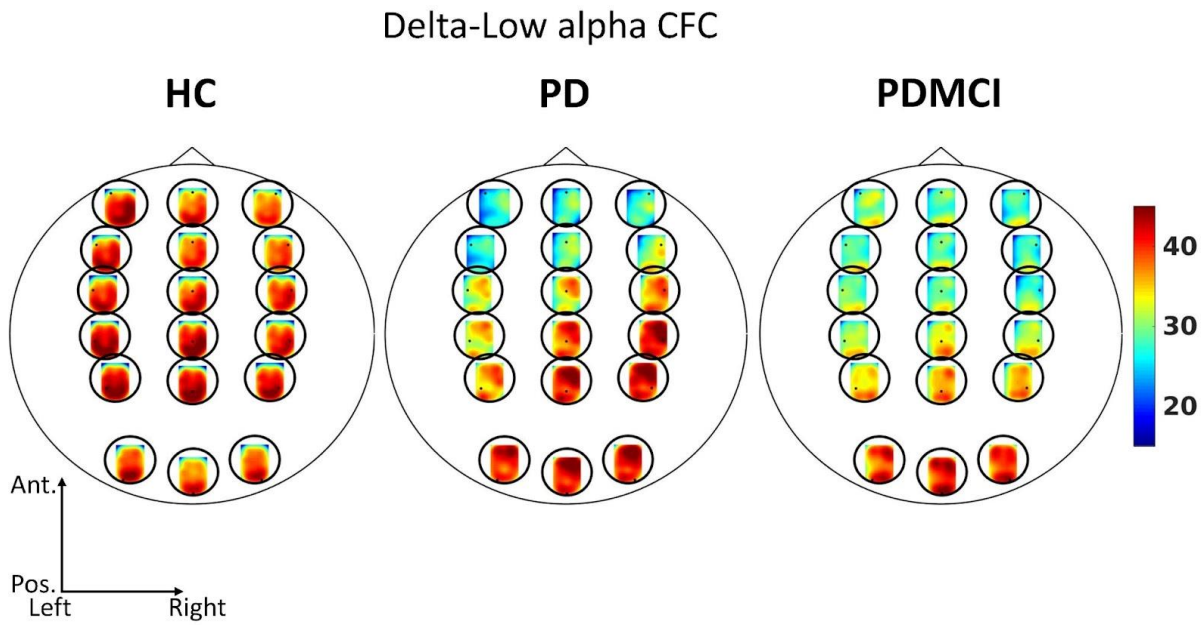

Supplementary Fig. 2. CFC between delta (0.5-3.5 Hz) and low frequency alpha (7-11 Hz). In these plots, the single large circle represents the whole scalp. At each electrode position, a small circle was placed also representing the scalp and containing the CFC of that particular electrode with all other electrodes. Namely, each head topography on an electrode location represents the CFC distribution between that individual location and all other electrodes. Ant.: Anterior; Pos.: Posterior; HC: Healthy Controls; PD: Parkinson's Disease; PDMCI: PD with MCI. The values plotted are z-transformed.

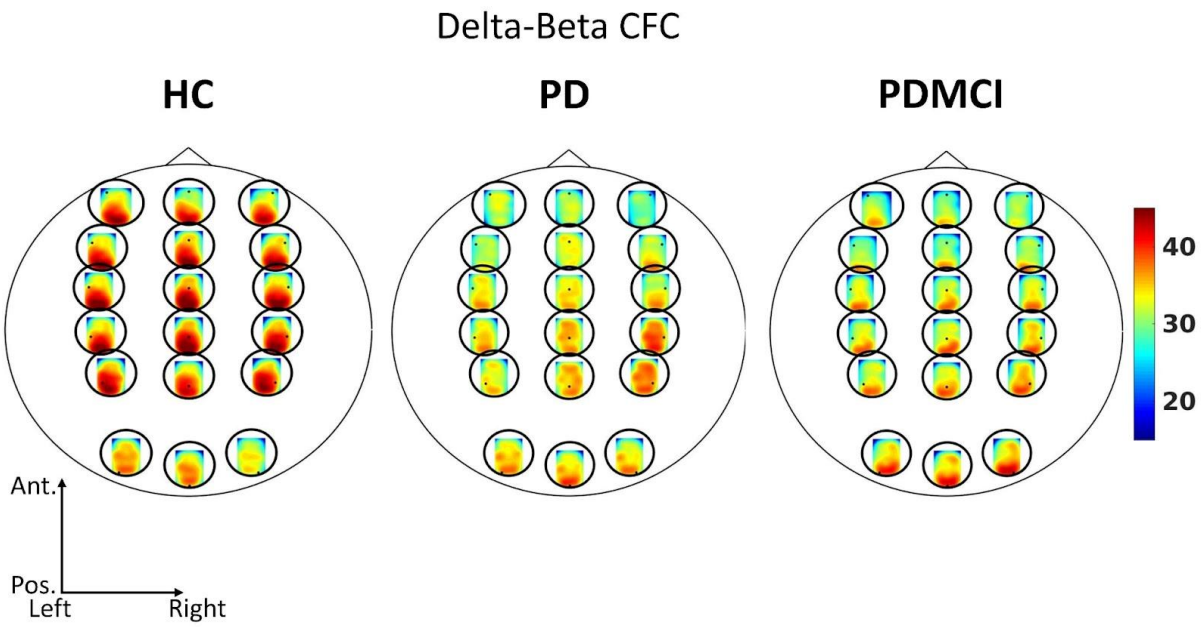

Supplementary Fig. 3. CFC between delta (0.5-3.5 Hz) and beta (15-25 Hz). In these plots, the single large circle represents the whole scalp. At each electrode position, a small circle was placed also representing the scalp and containing the CFC of that particular electrode with all other electrodes. Namely, each head topography on an electrode location represents the CFC distribution between that individual location and all other electrodes. Ant.: Anterior; Pos.: Posterior; HC: Healthy Controls; PD: Parkinson's Disease; PDMCI: PD with MCI. The values plotted are z-transformed.

Correlation of CFC with Cognitive Measures

MMSE was used to assess general cognitive functioning while the Stroop test more specifically targeted the frontal-executive functions. Therefore, these tests' scores were used as cognitive measures in the correlation analysis in addition to oddball task (error) scores. As the EEG measure in the correlation, the anterior-to-posterior (AP) CFCs based on PAC at delta-theta, delta-low frequency alpha, and delta-beta which showed significant group differences were

used. The correlation analyses were performed in 2 different ways. In one, correlation analyses were run between the above-mentioned CFC values and cognitive measures using subjects from all groups. The main reason for the "all groups" correlation analysis was to see the general relation pattern between CFC scores and behavioral scores across all subjects considering the PDMCI patients have reduced MMSE, Stroop, and oddball task (error) scores relative to the other groups. However, the calculation of a correlation across subjects (for all groups) may likely be capturing the group differences in these measures already shown in the ANOVA results. Therefore, the correlations were also calculated within each group if the Group×CFC measure interaction was significant in the regression model in which cognitive measure was regressed with the ANCOVA analysis (CFC measures were added as a predictor variable to the model).

Behavioral data were checked for outliers. Outliers were identified and removed from the dataset based on the interquartile range (IQR). Only extreme outliers were removed from the dataset, defined as data points below Q1-3*IQR or above Q3+3*IQR (for MMSE: 1 subject (1 from PDMCI); for Stroop: 2 subjects (1 from PD, 1 from PDMCI); for Oddball task score: 5 subjects (1 from HC, 2 from PD, 2 from PDMCI group). For the sake of standardization, z-transformed test scores were used in the correlations. Since the clinical scores were not normally distributed, Kendall's tau-b rank correlation was reported.

1. **In all groups**

There was no correlation detected between clinical measures and AP delta-theta and delta-low frequency alpha PAC values (p>0.05). The Stroop scores were found negatively correlated with AP delta-beta PAC values (p<0.05). Additionally, there was a positive correlation between MMSE scores and AP delta-beta PAC values (p<0.05) (Supplementary Table 1).

Supplementary Table 1. Correlation of CFC and Cognitive Measures

	CFC (Delta vs.)					
	Theta		**Low-alpha**		**Beta**	
	τb	***p***	**τb**	***p***	**τb**	***p***
Stroop	-0.08	ns	-0.05	ns	-0.16	***<0.01***
MMSE	0.06	ns	0	ns	0.12	***<0.05***
Oddball score*	0.05	ns	-0.04	ns	-0.05	ns

MMSE: Mini-Mental State Examination. *Error scores. ns: not significant. Significant p values were indicated in bold and italic.

2. **Within each group**

The only ANCOVA that we found a significant Group×CFC measure interaction was for the Stroop test scores and the predictor was the AP delta-theta CFC ($p<0.05$). There were no significant interactions for other conducted ANCOVAs ($ps>0.05$). Therefore, the correlation analyses were performed between AP delta-theta CFC and Stroop test scores for each group separately. The results of the correlation analyses showed that there is a negative correlation between AP delta-theta CFC and Stroop test scores only for the PD group ($p<0.05$) (Supplementary Fig. 4).

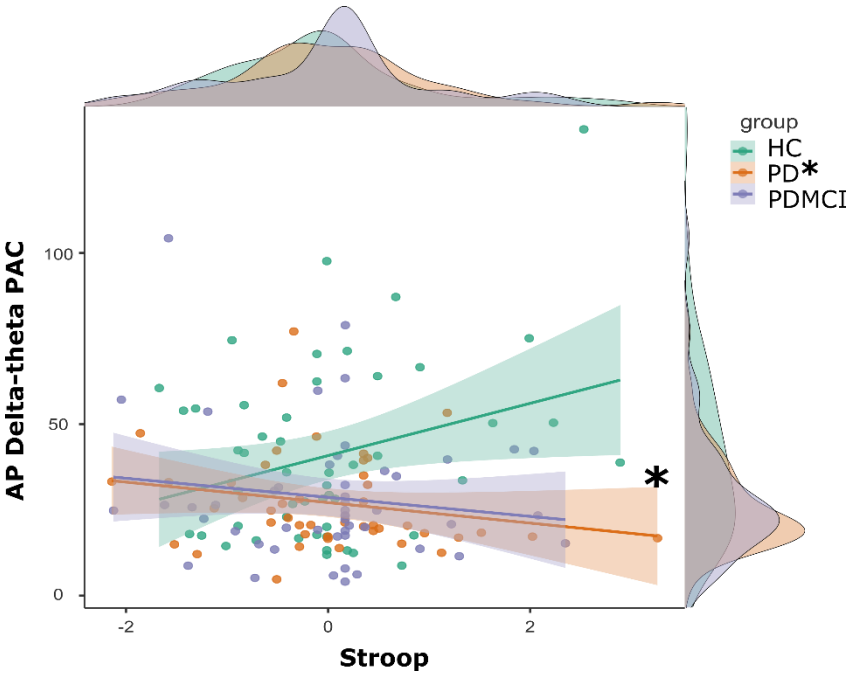

Supplementary Fig. 4. Scatter plots of the significant correlations between AP delta-theta CFC and Stroop test scores. The shaded area denotes the standard error. Density marginals for each group were presented at the outside of the plot. Dots represent the observed scores. Asterisks indicate statistical significance (*: $p \leq 0.05$)

Limitations

Although the results of the study suggest that the PDMCI patients may be characterized by CFC-related impairments in their anterior-posterior brain oscillatory networks, we should also acknowledge the limitations of this study. The higher number of male subjects in the PD groups

is a limitation of the current study. However, according to the literature, a 2:1 male/female ratio is expected in clinical diagnosis [9]. Nevertheless, since the brain oscillatory dynamics can be affected by gender [10], the gender ratio in the compared groups should consider in future studies. Another point that should be mentioned is that the education years of Parkinson's groups seem to be lower than the healthy elderly group, although it was not statistically significant. Related to this limitation, it should be noted that in the tests applied to the participants within the scope of the detailed neuropsychological test battery, which is also used in patients' cognitive impairment diagnosis or decision of "healthy elderly", the participants were evaluated according to their own age and educational norms (or correction scores were added for people with low education level). Therefore, naturally, we believe, it can be said that the difference in years of education, which is not reflected in the statistics between the groups, but can be distinguishable by the eye, does not cause a difference in the neuropsychological evaluation of the individuals in group comparison. However, indeed, it should be taken into account when interpreting the results. One point that also should be mentioned here is related to our paradigm design. In our visual oddball paradigm used in the current study to avoid motor-related EEG activity in the event-related responses, button press was not used for the target responses. Therefore, it was not possible to eliminate missed targets while performing CFC analysis for the target stimuli. It may serve as the confound in the EEG activity in response to the target stimuli.

In the current study, we were interested in robust CFC in order to eliminate randomly spurious activity with calculated surrogated data on randomly shuffled EEG segments. When we compared the real CFC values with the surrogated data, if the CFC values fall below the surrogated CFC (i.e., $z<2$) we concluded that these frequency pairs do not have reliable CFC any different than random correlation. This testing procedure was used by following the relevant literature[11–14]. Although this may seem to prevent us from seeing the results for frequency pairs that are not included in further statistical analyses, in fact, it permits us to avoid inflated significance. The determined frequency pairs (delta-theta, delta-low alpha, and delta-beta) according to this comparison, show substantial event-related CFC values while other frequency pairs failed to pass this test and therefore event-related CFC observed in those was considered to be random activity.

References

1. Güngen C, Ertan T, Eker E, Yaşar R, Engin F. [Reliability and validity of the standardized Mini Mental State Examination in the diagnosis of mild dementia in Turkish population]. *Turk Psikiyatri Derg*. 2002;13(4):273-281. http://www.ncbi.nlm.nih.gov/pubmed/12794644. Accessed April 24, 2021.

2. Tanör Ö. Öktem sözel bellek süreçleri testi.(Öktem-SBST) el kitabı. 2011. http://acikerisim.istanbulbilim.edu.tr:8080/xmlui/handle/11446/477. Accessed September 9, 2021.

3. Wechsler D. Wechsler adult intelligence scale. *Arch Clin Neuropsychol*. 1995. https://psycnet.apa.org/doiLanding?doi=10.1037/t15169-000. Accessed September 9, 2021.

4. Kaplan E, Goodglass H, Weintraub S. Boston naming test. 2001. https://osf.io/vy8gh/download. Accessed September 9, 2021.

5. Karakaş S. *Bilnot-Yetişkin (2 Cilt Takım)*. EĞİTİM YAYINEVİ; 2013. https://books.google.com/books?hl=tr&lr=&id=cMOiDwAAQBAJ&oi=fnd&pg=PA255&dq=karakaş+2006+bilnot&ots=dUivso0jND&sig=07XtgBiVI47U9WPpopByx2ku6Dc. Accessed May 26, 2022.

6. Brodaty H, Moore CM. The clock drawing test for dementia of the Alzheimer's type: A comparison of three scoring methods in a memory disorders clinic. *Int J Geriatr Psychiatry*. 1997;12(6):619-627. doi:10.1002/(SICI)1099-1166(199706)12:6<619::AID-GPS554>3.0.CO;2-H

7. Tombaugh TN, Kozak J, Rees L. Normative Data Stratified by Age and Education for Two Measures of Verbal Fluency: FAS and Animal Naming. *Arch Clin Neuropsychol*. 1999;14(2):167-177. doi:10.1016/S0887-6177(97)00095-4

8. Busse A, Hensel A, Gühne U, Angermeyer MC, Riedel-Heller SG. Mild cognitive impairment: Long-term course of four clinical subtypes. *Neurology*. 2006;67(12):2176-2185. doi:10.1212/01.WNL.0000249117.23318.E1

9. Miller IN, Cronin-Golomb A. GENDER DIFFERENCES IN PARKINSON'S DISEASE: CLINICAL CHARACTERISTICS AND COGNITION. *Mov Disord*. 2010;25(16):2695. doi:10.1002/MDS.23388

10. Güntekin B, Ba E. Brain oscillations are highly influenced by gender differences. 2007;65:294-299. doi:10.1016/j.ijpsycho.2007.03.009

11. Bayraktaroglu Z, von Carlowitz-Ghori K, Losch F, Nolte G, Curio G, Nikulin V V. Optimal imaging of cortico-muscular coherence through a novel regression technique based on multi-channel EEG and un-rectified EMG. *Neuroimage*. 2011;57(3):1059-1067. doi:10.1016/j.neuroimage.2011.04.071

12. Tort ABL, Komorowski R, Eichenbaum H, Kopell N. Measuring phase-amplitude coupling between neuronal oscillations of different frequencies. *J Neurophysiol*. 2010;104(2):1195-1210. doi:10.1152/jn.00106.2010

13. Hurtado JM, Rubchinsky LL, Sigvardt KA. Statistical Method for Detection of Phase-Locking Episodes in Neural Oscillations. *J Neurophysiol*. 2004;91(4):1883-1898. doi:10.1152/jn.00853.2003

14. Hesterberg T, Monaghan S, Moore DS, Clipson A, Epstein R, Freeman WH. *Bootstrap Methods and Permutation Tests Companion Chapter 18 To the Practice of Business Statistics*. New York: W. H. Freeman and Company; 2003.